RSC Advances

REVIEW

View Article Online
View Journal | View Issue

Open Access Article. Published on 11 September 2020. Downloaded on 10/25/2025 7:46:44 PM.
This article is licensed under a Creative Commons Attribution-NonCommercial 3.0 Unported Licence.

Check for updates

Cite this: *RSC Adv.*, 2020, **10**, 33782

Recent advances and future perspectives of sol–gel derived porous bioactive glasses: a review

Kalim Deshmukh, *[a] Tomáš Kovářík, [a] Tomáš Křenek, [a] Denitsa Docheva, [b] Theresia Stich[b] and Josef Pola[a]

The sol–gel derived porous bioactive glasses have drawn worldwide attention by virtue of the convenience and flexibility of this versatile synthesis method. In this review, the recent advances in sol–gel processed porous bioactive glasses in biomedical fields, especially for bone tissue regeneration applications have been comprehensively reviewed. Generally, it is envisaged that the morphology and chemical compositions of sol–gel derived porous bioactive glasses significantly affect their biological properties. Therefore, the controlled synthesis of these porous glasses is critical to their effective use in the biomedical fields. With this context, the first part of the review briefly describes the fundamentals of the sol–gel technique. In the subsequent section, different approaches frequently used for the sol–gel synthesis of porous glasses such as microemulsion and acid-catalyzed based synthesis have been reviewed. In the later part of the review, different types of sol–gel derived bioactive glasses namely silica, phosphate and silica–titania based glasses along with organic–inorganic hybrids materials have been discussed. The review also discusses the chemical, surface, mechanical and biological properties and further highlights the strategies to control the pore structure, shape, size and compositions of sol–gel derived bioactive glasses. Finally, the review provides a detailed discussion about the bone tissue regeneration application of different types of sol–gel derived bioactive glasses and presents future research perspectives.

Received 13th May 2020
Accepted 2nd September 2020

DOI: 10.1039/d0ra04287k

rsc.li/rsc-advances

1. Introduction

In recent years, the solution–gelation (sol–gel) processing technique has gained increasing attention across various scientific disciplines because of the wide range of potential applications of the resulting materials. Generally, it is recognized as a wet chemistry-based synthesis technique which offers promising and flexible approaches to obtain a varied type of novel and functionalized materials such as glasses, ceramics and organic/inorganic hybrids with different architectures at low temperatures and mild chemical conditions.[1,2] Sol–gel technique is the most dynamic, reliable and environmentally friendly bottom-up synthesis method which has received tremendous interest in diverse research fields such as nanotechnology, optoelectronics, semiconductors, medicines, biotechnology as well as separation science.[3] In particular, the sol–gel method is very useful, highly attractive and versatile because of its simplicity, low cost and the diversity of high purity materials of varied configurations such as monoliths, nanoparticles, thin films, foams, fibers *etc.*, that can be produced from the same composition directly from the solutions.[1] Furthermore, it is the most exploited technique used for the synthesis of metal oxides and metal oxides based nanocomposites.[4] By varying the synthesis parameters in the sol–gel process, homogenous materials with tailored properties such as good chemical and thermal stability, good mechanical strength, good optical transparency and controlled porosity can be obtained.[5] The final product obtained *via* sol–gel synthesis is explicated by the mesoporous texture which is inherent in sol–gel materials.[1] Moreover, this technique allows the direct synthesis of high purity multi-component materials without the use of powder intermediates or using high-cost vacuum-based processing techniques.[6,7] These advantages make the sol–gel method a promising synthesis route to prepare different types of functional materials with varied structures and porosity.[8]

A typical sol–gel synthesis method consists of two distinct phases; *i.e.* solution and gelation. In the first phase, small molecules (precursors) get converted into a colloidal solution (sol) which are generally obtained *via* controlled hydrolysis and condensation of metal alkoxide precursors or organic/inorganic salts within the solution.[8,9] In the second phase, the polycondensation reaction occurs which leads to the formation of a rigid and highly interconnected three dimensional (3D) network (gel) comprising discrete particles or polymer chains due to the addition of a catalyst (acid or base).[2,8,9] The structure

[a]*New Technologies – Research Center, University of West Bohemia, Plzeň, 30100, Czech Republic. E-mail: deshmukh@ntc.zcu.cz; Tel: +420-775942198*

[b]*Experimental Trauma Surgery, Department of Trauma Surgery, University Regensburg Medical Centre, 93042, Regensburg, Germany*

 This journal is © The Royal Society of Chemistry 2020

Open Access Article. Published on 11 September 2020. Downloaded on 10/25/2025 7:46:44 PM.
This article is licensed under a Creative Commons Attribution-NonCommercial 3.0 Unported Licence.

of the resulting gel depends on the catalyst and this is due to the relative rates of the hydrolysis and condensation reactions.[10] Hence, understanding the kinetics of hydrolysis and condensation reactions is the key to conquer the sol–gel synthesis method. In general, a clear and stable solution composed of hydrolyzed monomers having low condensation rates is required for the gelation process.[10] Thus, these processes are affected by the number of experimental parameters such as pH of the solution, temperature, reactants concentration and the presence of additives that could be controlled in the sol–gel synthesis.[9] The processing temperature in the sol–gel method is generally very low, more often very close to room temperature which further minimizes the thermal volatilization and deterioration of entrapped species and also allows control over the production of novel glass compositions.[11] Thus, the sol–gel method renders the possibility to control the physicochemical properties of the resulting material by carefully varying the experimental parameters affecting the various synthesis steps.[12] Furthermore, the sol–gel process exhibits several unique merits over other conventional synthesis methodologies. Among the key advantages of the sol–gel method is the ability to produce organic–inorganic hybrid materials in addition to the low production cost as compared with other vacuum-based synthesis methods which are comparatively expensive.[13] The other ascendancy of the sol–gel process includes the synthesis of highly pure and homogeneous multi-component systems with controllable kinetics of various chemical reactions namely hydrolysis, condensation, nucleation and the evolution of primary colloidal particles to achieve microstructure with special shape and size distribution.[12,14] Besides, the sol–gel method facilitates controlling all these parameters and results in the synthesis of tailor-made homogeneous materials with controlled homogeneity at the molecular scale.[14]

The adaptability of the sol–gel method allows to manipulate the material characteristics which are required for a particular application. In this context, this technique is a promising tool for obtaining bioactive materials (biomaterials) for numerous biomedical applications owing to its environmental friendliness, low-temperature processing and intrinsic biocompatibility of the synthesized materials.[1,15] During the last decade and a half, the demand for the biomaterials have grown significantly and the intense research interest is attributed to their wide range of applications in the healthcare and medical industries, for example; in regenerative medicines, implantable devices, wound healing therapies, tissue engineering, plastic surgeries, drug delivery systems and orthopedic disorders.[16–21] In particular, sol–gel derived biomaterials have been recently investigated for the prevention of prosthetic joint infections,[22,23] bone cements,[24,25] artificial tissue and ligaments,[26,27] dental implants,[28,29] tissue engineering[30–32] and drug delivery.[33,34] The biomaterials are anticipated to enhance the natural tissue regeneration, thereby stimulating the restoration of structural, functional, metabolic, biochemical and biomechanical properties.[35,36] The growing interest in sol–gel derived biomaterials is due to their potential to form excellent contact and strong chemical bonding with the surrounding tissues.[37,38] Furthermore, the sol–gel method was utilized to immobilize biologically active compounds or biomolecules *via* entrapment or encapsulation throughout the sol–gel derived matrix.[39–41] Hence, sol–gel derived materials with a high specific surface area provide good biocompatibility while their external surface enables them to be functionalized easily using suitable biomolecules.

Sol–gel based bioactive glasses have been extensively explored as a promising and highly porous scaffold material for bone tissue regeneration applications owing to their exceptional osteoconductivity, osteostimulation and degradation rate.[42–45] These bioactive glasses develop strong bonds with the bone through the formation of hydroxyapatite (HA) or hydroxycarbonate apatite (HCA) layer on the surface by releasing Si, Ca, P and Na ions and stimulate the formation of bone tissues when implanted in the living body.[46] Mesoporous bioactive glasses (MBGs) are the latest development of sol–gel derived glasses exhibiting large surface area and porosity with the capability of being functionalized with a broad spectrum of moieties.[47] The development of MBGs using the sol–gel method provides higher bonding rates and exceptional degradation or resorptive properties can be achieved.[47,48] Since their inception in 2004, the research on the MBGs for the bone tissue regeneration application has grown tremendously.[48] An ideal scaffold material for bone tissue regeneration should possess good osteoconductivity, biodegradability and good mechanical properties in addition to a highly porous structure.[49] Bioactive glasses with macroporous structures can promote cell infiltration, nutrient delivery, bone ingrowth and vascularization.[50] The surface roughness and the micro or mesoporosities were also proven equally important as they influence the ability of a material to stimulate apatite nucleation and cell attachment.[50–52] The most suitable materials for bone tissue regeneration/repair application are the one who mimics the natural bone structure and presents specific surface chemistry functions.[53] In that context, porous inorganic materials,[54,55] calcium phosphates (CAPs) and bioactive glass scaffolds have been developed.[56,57] Porous Si–Ti based materials are also fascinating materials for bone tissue regeneration because both Si–OH and Ti–OH surfaces were found to promote HA surface nucleation for *in vitro* bio-mineralization.[58]

Hence, this review briefly describes the basic chemistry involved in the sol–gel processing of porous bioactive glasses. Besides, different methods of sol–gel synthesis of porous glasses namely microemulsion and acid-catalyzed synthesis have also been discussed. Moreover, the main focus of this review is to give a comprehensive overview of recent advances in sol–gel derived porous bioactive glasses of different types and compositions for bone tissue regeneration applications. Finally, the preparation strategies of porous scaffolds from sol–gel derived glasses for bone grafting and tissue engineering applications have been discussed.

2. Sol–gel synthesis of porous glasses

The sol–gel process is a facile and highly efficient method for synthesizing porous bioactive glasses since it offers the possibility to tune their properties which can be influenced by some

Open Access Article. Published on 11 September 2020. Downloaded on 10/25/2025 7:46:44 PM.
This article is licensed under a Creative Commons Attribution-NonCommercial 3.0 Unported Licence.

parameters such as hydrolysis ratio, gelation time, aging, drying and calcination temperature *etc.* The density, pore-volume, specific surface area and porosity of glasses are influenced by the synthesis method employed. As compared with the conventional melt quench synthesis, the sol–gel synthesis method allows the production of glasses with higher purity, high specific surface area and intrinsic porous structure owing to the advantages of low-temperature processing.[59] High porosity and high specific surface area of sol–gel derived glasses is normally associated with enhanced degradability and bioactivity but lower mechanical stability. Glasses which possess suitable degradation rate, appropriate mechanical properties, the ability to promote the formation of HA layer, as well as the capability to stimulate biologically beneficial responses are desirable for bone grafting application.[60] The formation of the HA layer facilitates a strong bond between the living tissues and the implants.[61] Moreover, the formation of HA layers is the characteristic of all the inorganic materials used in the development of orthopedic implants, bone replacements and bone tissue engineering.[62] The glasses obtained using the sol–gel method have been utilized as bioactive materials in several applications such as for the encapsulation of proteins, enzymes and biomolecules for controlled drug delivery and bone tissue regeneration because these glasses are biocompatible and possess excellent bioactivity.[63] Moreover, it was realized that the molecular structure as well as the enhanced textural properties such as pore size which is associated with the high surface area, negative surface charge and higher dissolution rate are the real key for enhanced bioactivity of sol–gel glasses.[64] Thus, based on this technique, numerous strategies were developed for the synthesis of porous glasses. These strategies and synthesis methods are described in the following sections.

2.1 Microemulsion based sol–gel synthesis

Since their inception, the interest in the microemulsions has grown significantly in academic as well as industrial research due to their distinctive properties such as very low interfacial tension, large interfacial area, high thermodynamic stability and the ability to stabilize immiscible liquids.[65] Generally, microemulsions are known as an isotropic, homogeneous and thermodynamically stable liquid mixtures comprising of three phases namely oil, water and surfactant.[63,66] The oil phase generally consists of long-chain hydrocarbons whereas the surfactants can be defined as the long-chain organic molecules having a hydrophilic head and lipophilic tail.[67] At the microscopic level, the surfactant molecules form an interfacial film which separates the aqueous and oil phase. The main difference between the conventional emulsions and the microemulsions is that shear effects are required for the formation of conventional emulsions while microemulsions can be formed by directly adding the components which are further stabilized using surfactant.[66] There are three types of microemulsions, (i) oil dispersed in water (O/W), (ii) water dispersed in oil or reverse (W/O) and (iii) intermediate bicontinuous structure type microemulsions which can turn reversibly from one type to another.[66,68] Microemulsion technique is an ideal method for synthesizing inorganic nanoparticles with minimum agglomeration.[69,70] However, the key drawback associated with this technique is the low yield and the requirement of a large quantity of oil and surfactants.[63] For the synthesis of microemulsion based sol–gel glasses, the aqueous phase consists of silicate and metal ion precursors in addition to catalysts.[71] The silicate precursors undergo hydrolysis and condensation reaction within the water droplets serving as reactors.[66] The water droplets more often collide with each other *via* Brownian motion and unite together to form bigger droplets. The droplets interact with each other due to collision which is unfavorable for achieving homogenous glass composition.[68] The surfactant stabilizes the microemulsion droplets while the oil phase is served as a barrier thereby preventing the agglomeration of nanoparticles.[66] The synthesized glass thus exhibits homogeneous dispersions and compositions but they may not be uniform in size due to the breakage of microemulsion drop during their collision.[72] Moreover, vigorous washing is essential to get rid of the excessive surfactants and the oil phase before drying and calcination thereby avoiding the conversion of organic residues into nanoparticle aggregations.[66]

The microemulsion based sol–gel synthesis of MBGs has been demonstrated by several authors by employing hexadecyltrimethylammonium bromide (CTAB) as the surfactant.[73–76] In sol–gel processing, surfactants are typically used to reduce shrinkage, prevent cracking and to avoid supercritical drying.[77] Generally, CTAB surfactant is employed as a pore-forming agent in the sol–gel synthesis of MBGs.[78] The pore size, pore volume as well as the particle size of MBGs can be customized by using different solvents and by varying CTAB concentration.[73,74] Recently, Wang and Chen[76] reported a facile method for the synthesis of hollow mesoporous bioactive glasses (HMBGs) with controllable shell thickness and excellent monodispersity in the microemulsion system comprising cyclohexane, ethanol and water. CTAB was added to cyclohexane to form microemulsion droplets and also used as a surfactant as well as the template for mesoporous structure.[76] The author demonstrated the synthesis of HMBGs with different shell thicknesses as well as different cavity sizes simply by varying the CTAB concentration. Furthermore, the microemulsion technique also contributed to good monodispersibility of HMBGs. The mechanism of HMBGs formation is depicted in Fig. 1.[76] The droplets of oil in water microemulsions were formed when CTAB and cyclohexane were mixed with the solution containing water and ethanol which offered reaction vehicle for the synthesis of HMBGs. First, tetraethyl orthosilicate (TEOS) was dissolved in cyclohexane and later triethylphosphate (TEP) and calcium nitrate tetrahydrate (CN) were mixed with the microemulsion system. The hydrolysis and the condensation of the prepared sol were carried out at the oil–water interface using ammonia as a catalyst. The microstructure was formed due to the gathering of the sol particle in the CTAB micelle layer.[76] The HMBGs were formed once the organics and nitrates are removed *via* calcination. Fig. 2 depicts the microstructure of synthesized HMBGs showing good monodispersibility (Fig. 2a) as well as a rough surface (Fig. 2b). The rough surface of HMBGs is beneficial for

Open Access Article. Published on 11 September 2020. Downloaded on 10/25/2025 7:46:44 PM.
This article is licensed under a Creative Commons Attribution-NonCommercial 3.0 Unported Licence.

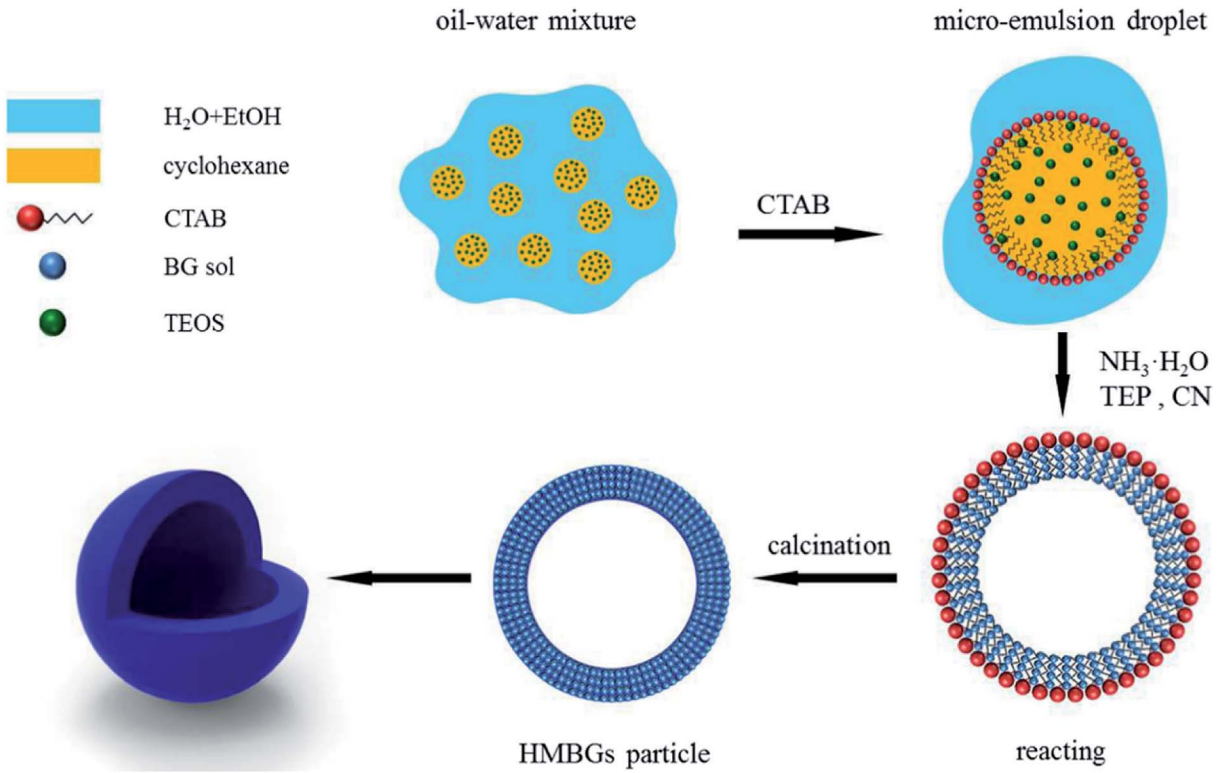

Fig. 1 Mechanism of HMBGs formation. Reproduced with permission from ref. 76. Copyright 2017, Elsevier.

drug loading. The TEM image depicted in Fig. 2c demonstrates the hollow microstructure of synthesized HMBGs with a large cavity of the particles which can be useful for the loading of bioactive molecules. Fig. 2d–f shows the magnified TEM images of HMBGs prepared using the different concentrations of CTAB.[76] From TEM images it was observed that the shell thickness and the cavity size can be tuned by varying the CTAB content. In particular, increased shell thickness was observed with increased CTAB concentration.[76]

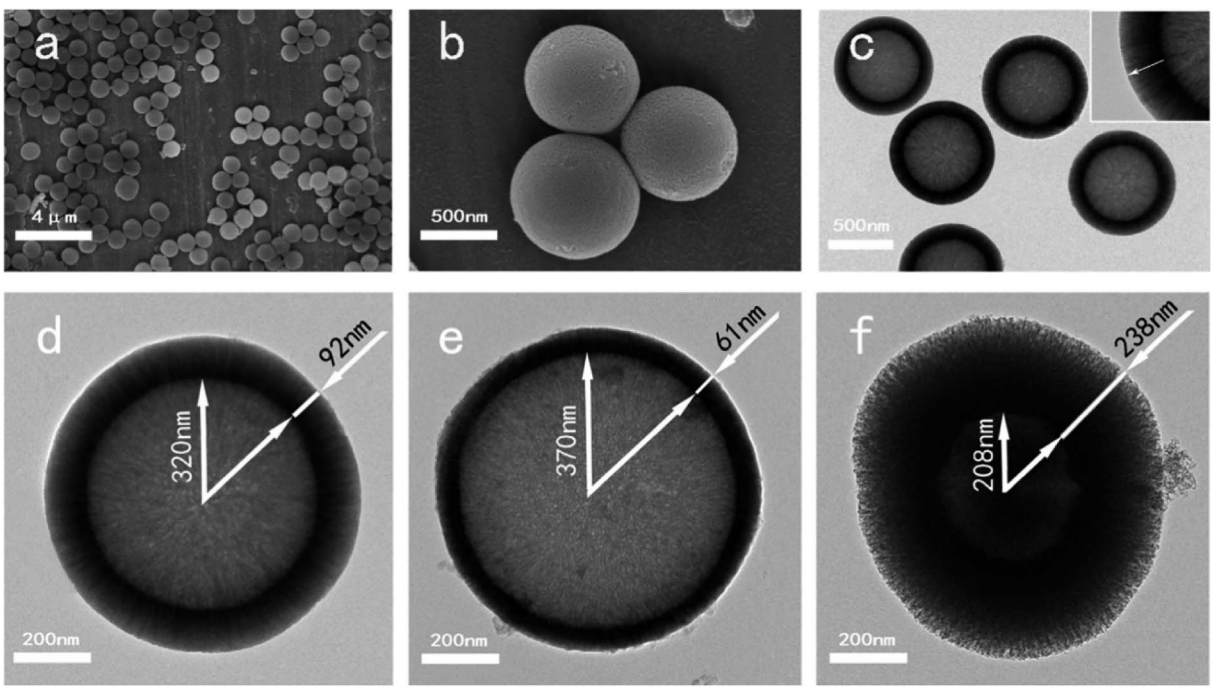

Fig. 2 (a and b) SEM and (c) TEM images of synthesized HMBGs. TEM images of HMBGs with different CTAB concentrations are shown in (d–f). Reproduced with permission from ref. 76. Copyright 2017, Elsevier.

Open Access Article. Published on 11 September 2020. Downloaded on 10/25/2025 7:46:44 PM.
This article is licensed under a Creative Commons Attribution-NonCommercial 3.0 Unported Licence.

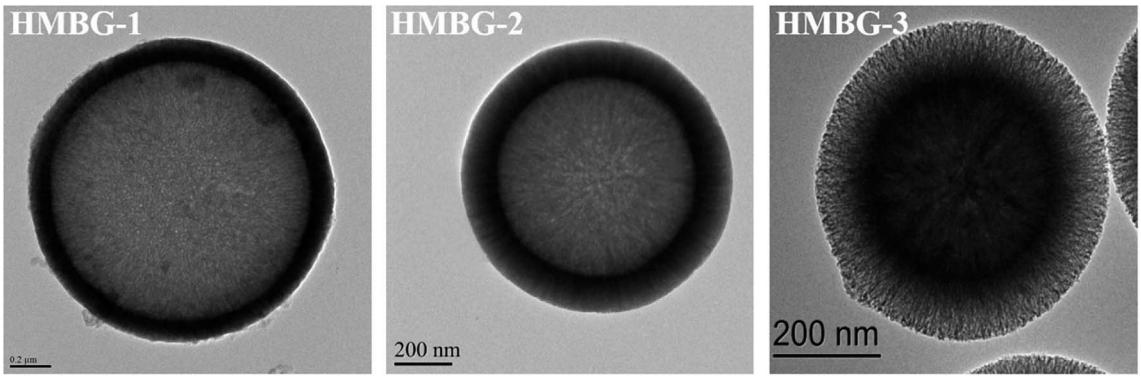

Fig. 3 TEM images of synthesized HMBGs nanoparticles. Adapted from ref. 79. Copyright 2019, Wang, Pan and Chen.

Using a similar approach, Wang *et al.*[79] prepared HMBGs nanoparticles in presence of CTAB, cyclohexane, ethanol and water-based emulsion where CTAB played a key role in modulating the interior mesoporous structure, morphology and the dispersion of the HMBGs nanoparticles. The CTAB concentration was varied as 2, 4 and 6 mM and the corresponding HMBGs nanoparticles synthesized were named HMBG-1, HMBG-2 and HMBG-3 respectively.[79] The TEM micrographs depicted in Fig. 3 demonstrate that all HMBGs nanoparticles exhibited a hollow structure with different shell property thereby influencing their drug release behaviours. The HMBG-1 nanoparticles exhibited compact shell structure while HMBG-2 showed a peculiar

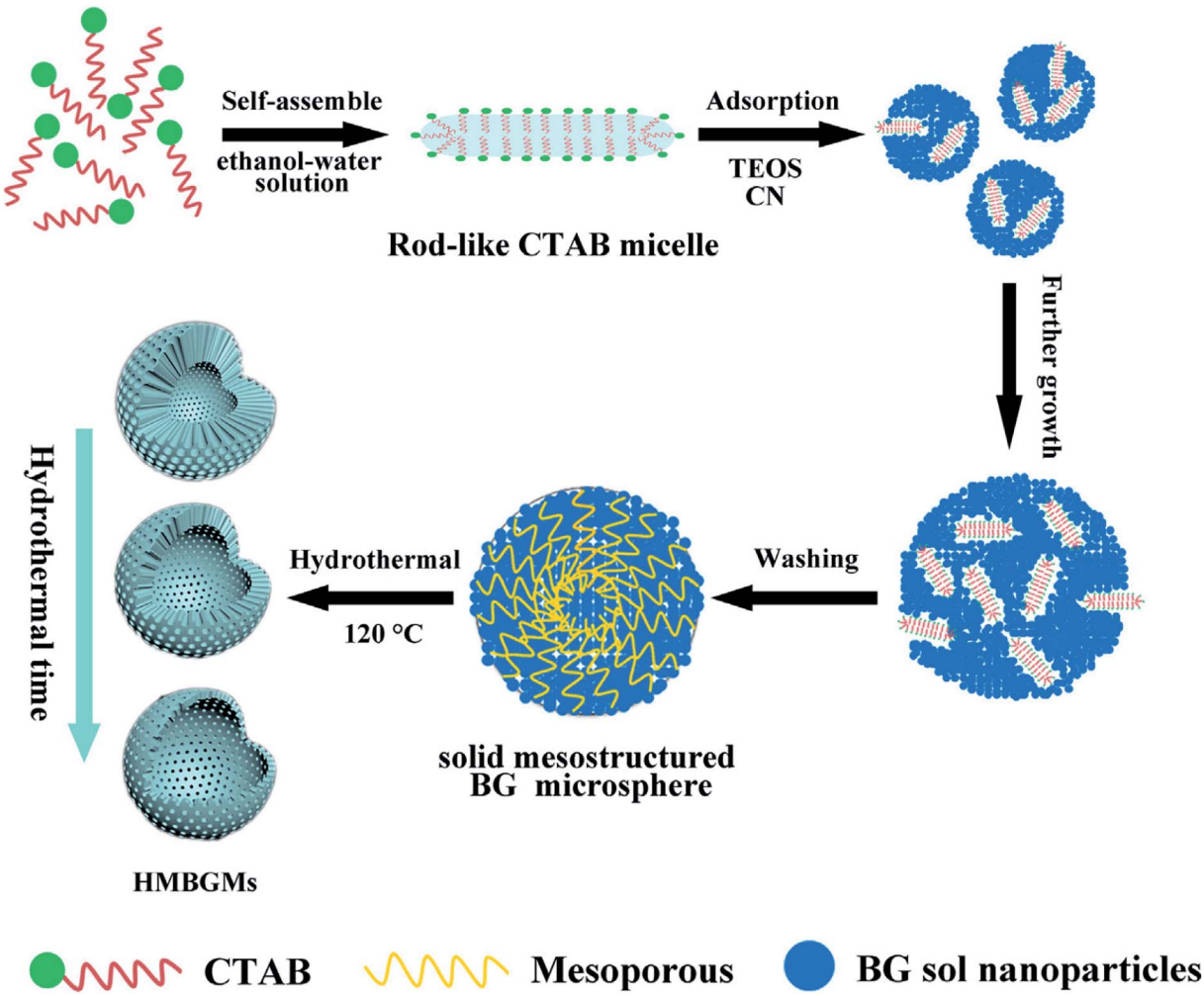

Fig. 4 Mechanism of HMBGs microsphere formation. Reproduced with permission from ref. 81. Copyright 2016, Elsevier.

Open Access Article. Published on 11 September 2020. Downloaded on 10/25/2025 7:46:44 PM.
This article is licensed under a Creative Commons Attribution-NonCommercial 3.0 Unported Licence.

microstructure comprising several penetrative tunnels.[79] Moreover, the HMBG-3 demonstrated several mesoporous tunnels similar to HMBG-2. The synthesized HMBGs nanoparticles exhibited a high specific surface area (749.619 $m^2 g^{-1}$) and excellent drug loading efficiency (55.1%) with stable drug release behavior and excellent drug storage ability owing to their hollow structure and the penetrative mesopores on the shell.[79] The *in vivo* studies further revealed that HMBGs nanoparticles can promote bone tissue regeneration with enhanced bone repair capability.

Hu *et al.*[80] reported CTAB assisted facile method for the sol–gel synthesis of HMBGs microspheres with tailorable cavity sizes. The authors demonstrated that CTAB acted as a structure-directing agent and favoured the synthesis of HMBGs with hollow mesoporous structure, high surface area and homogeneous particle size. In this study, the size of HMBGs particles and the cavity sizes were determined by CTAB concentration. Therefore, the CTAB concentration was varied as 3.3, 4.6 and 5.9 mM and the corresponding HMBGs synthesized were named as HMBGs-1, HMBGs-2 and HMBGs-3 respectively.[80] The authors demonstrated that with an increase in CTAB concentration, the particle size of HMBGs decreased and the morphology changed from hollow spheres to solid spheres. The average particle size for the synthesized HMBGs was reported to be 294 nm for HMBGs-1, 264 nm for HMBGs-2 and 187 nm for HMBGs-3.[80] All the synthesized HMBGs displayed narrow particle size distribution, good dispersibility and high specific surface areas.[80] Similarly, Duan *et al.*[81] demonstrated the synthesis of HMBGs microspheres *via* hydrothermal self-transformation method using CTAB as a mesoporous template. Fig. 4 demonstrates the mechanism of the formation of HMBGs microspheres.[81] The authors demonstrated that the solid HMBGs spheres prepared in Stöber solution can readily transform into the hollow structure after incubation in hydrothermal conditions.[81] Also, the shell thickness of HMBGs microspheres can easily be controlled by adjusting the hydrothermal time. The synthesized HMBGs microspheres displayed mesoporous structure, tunable shell thickness, excellent drug loading capacity and remarkable sustained-release property.[81] Besides, HMBGs microspheres exhibited narrow particle size distribution in the range of 300–650 nm and high specific surface area (444.11 $m^2 g^{-1}$).[81] These outstanding characteristics of HMBGs microspheres make them a potential drug carrier material for bone tissue regeneration and controlled drug release.[81]

Recently, Xiao *et al.*[82] reported novel method for template assisted sol–gel synthesis of HMBGs nanofibers which were later utilized for fabricating 3D scaffolds using bacterial cellulose (BC) and pluronic P123 as co-templates. It was emphasized that the presence of hydroxyl groups on the surface of BC acted as a catalyst and accelerated the hydrolysis and condensation reaction of precursors and as a result promoted the formation of HMBGs. Fig. 5 schematically represents the fabrication process of HMBGs nanofiber-based scaffold.[82] The diameter of the synthesized HMBGs nanofibers was found to be around 40 nm with the wall thickness of 8 nm while the specific surface area of the resulting scaffold was found to be 579.0 $m^2 g^{-1}$. The reported diameter of the synthesized HMBGs nanofibers is the

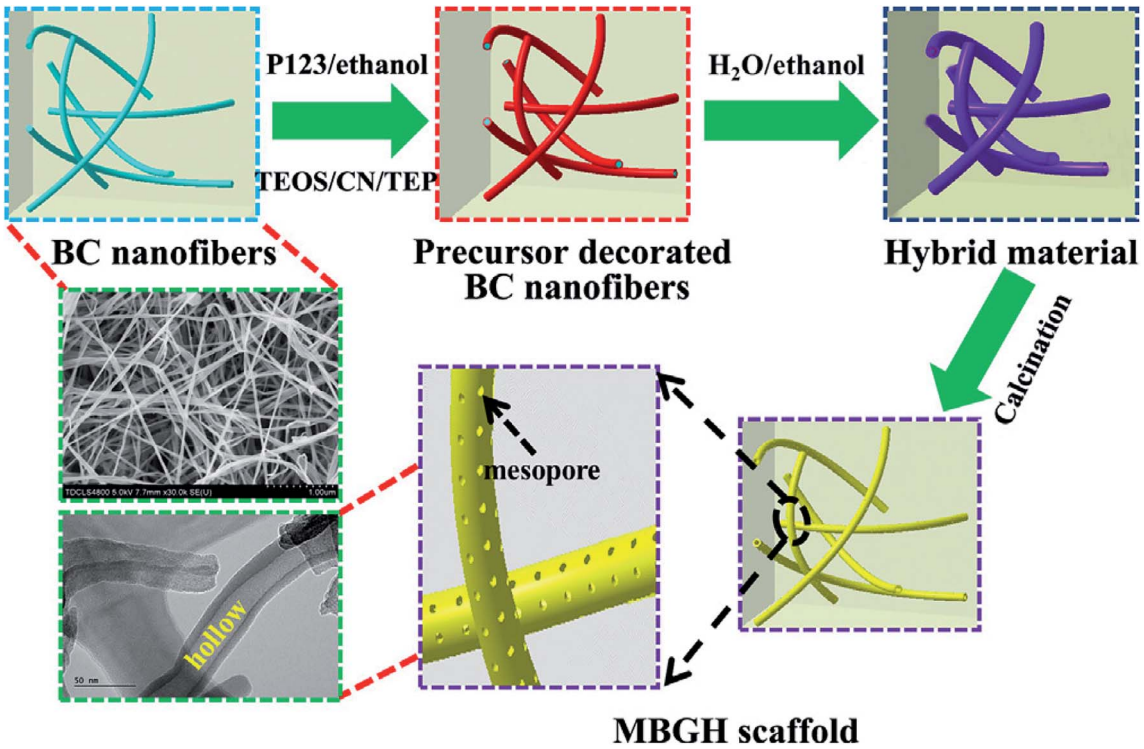

Fig. 5 Schematic illustration showing the fabrication process of HMBGs nanofiber based scaffold. Reproduced with permission from ref. 82. Copyright 2019, Elsevier.

Open Access Article. Published on 11 September 2020. Downloaded on 10/25/2025 7:46:44 PM.
This article is licensed under a Creative Commons Attribution-NonCommercial 3.0 Unported Licence.

smallest among all the HMBGs nanofibers reported so far while specific surface area is the largest among all the HMBGs currently reported.[82] The HMBGs scaffold exhibited nanopore sizes of 3.9 nm (pores present on the wall) and 15.1 nm (pores formed by neighboring tubes).[82] The authors further emphasized that the small fiber diameter and the mesoporous structure of the fabricated scaffold with high specific surface area impart excellent bioactivity and renders the HMBGs scaffold as a promising material for controlled drug release and bone tissue engineering.[82]

2.2 Acid catalyzed sol–gel synthesis

The sol–gel synthesis procedure can occur under acidic or basic conditions which eventually can influence the properties such as porosity, transparency and structure of the resulting materials. The catalyst can be selected based on the desired properties of the final product.[83] It was mentioned that the hydrolysis and condensation reactions do not depend on the catalyst type employed but also heavily reliant on the solution pH.[84] Strong inorganic acids such as sulphuric acid (H_2SO_4), hydrochloric acid (HCl) and nitric acid (HNO_3) are frequently used as catalysts because they activate the hydrolysis reaction very quickly.[85] Bioactive glasses can be prepared by employing a strong acid as a catalyst. However, employing base catalysts can help in inducing the particle formation as they enhance the pH value which in turn can be useful in preventing the development of bulky gel structure of bioactive glasses.[86,87] In sol–gel synthesis based on acid/base co-catalysis, first TEOS is mixed with metal ion precursors under acidic conditions and later concentrated basic catalyst is added to accelerate the reaction.[66] However, under acidic conditions, tiny colloidal particles are susceptible to form 3D gel network but the presence of salt decreases the stability of nanoparticles.[66] Due to these reasons, bioactive glasses usually exhibit polydispersity or agglomerated morphology.[86,88] Using acid/based co-catalyzed technique, monodispersed glasses can be obtained by employing weak organic acids such as citric acid ($C_6H_8O_7$). However, the obtained glasses usually exhibit a rough surface.[66,89] Polymeric materials which act as steric berries can also be included during the acid/base co-catalysis to improve the dispersibility of bioactive glasses.[66,90] For instance, after the addition of a base catalyst, polyethylene glycol (PEG) has been added as a non-ionic surfactant to tailor the particle size as well as to improve the dispersibility of the bioactive glasses produced.[91] Using this strategy, several bioactive glasses have been produced. For example; Nagayama *et al.*,[92] synthesized lanthanum trifluoride (LaF_3) doped silica glasses using hydrofluoric acid (HF) acid-catalyzed sol–gel method. HF was employed as a catalyst for sol–gel reaction and as a fluorine source. Fig. 6 depicts the photographs of cracked free dried gel (Fig. 6a) obtained after drying the aged wet gels for 6 to 7 days at 40 °C. The subsequent sintering of the dried gel for one hour at 1150 °C resulted in the formation of monolithic silica glass (Fig. 6b).[92] The gel processing time was found to be one week.[92]

3. Types of sol–gel derived glasses

3.1 Silicate based glasses

Sol–gel derived porous bioactive glasses were first time discovered by Li *et al.*[93] in the early 1990s. Since then these bioactive glasses have been studied extensively.[94–98] Silicate glasses are the most widely explored sol–gel derived bioactive glass compositions. Understanding the bioactive glass structure is important to demonstrate the role of each component on its bioactivity. The glass structure is frequently explained based on three different components and these are network formers, network modifiers and intermediate oxides.[99] Usually, network formers namely silica (SiO_2), phosphorous pentoxide (P_2O_5) and boron trioxide (B_2O_3) can form glasses without the necessity of additional components.[99] Bioactive silicate glasses are amorphous solids that are characterized by a 3D network structure consisting of SiO_4 tetrahedron building blocks which are bonded to upto a maximum of four neighboring SiO_4 tetrahedra *via* covalent Si–O–Si bonds, usually known as bridging oxygen (BO) atoms.[99,100] Usually, the tetrahedral structures are illustrated by the symbol Q^n units (Q stands for quaternary), where n

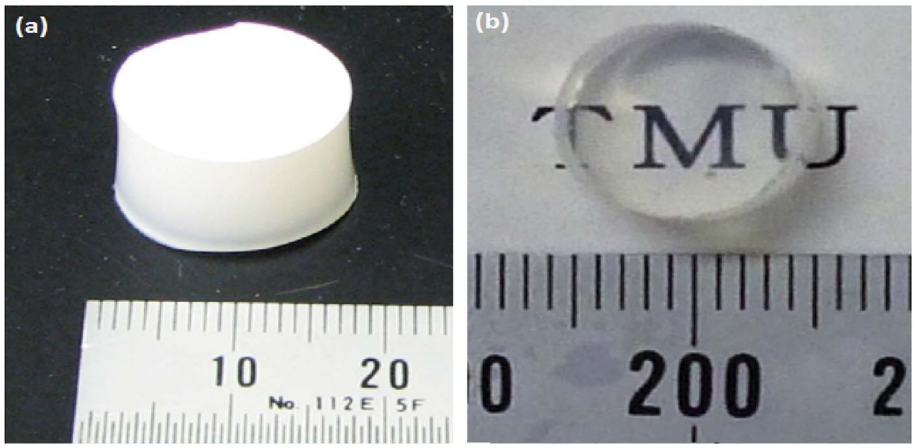

Fig. 6 Photographs of (a) dried silica gel and (b) silica glass obtained by sintering at 1150 °C for one hour. Reproduced with permission from ref. 92. Copyright 2012, Elsevier.

Open Access Article. Published on 11 September 2020. Downloaded on 10/25/2025 7:46:44 PM.
This article is licensed under a Creative Commons Attribution-NonCommercial 3.0 Unported Licence.

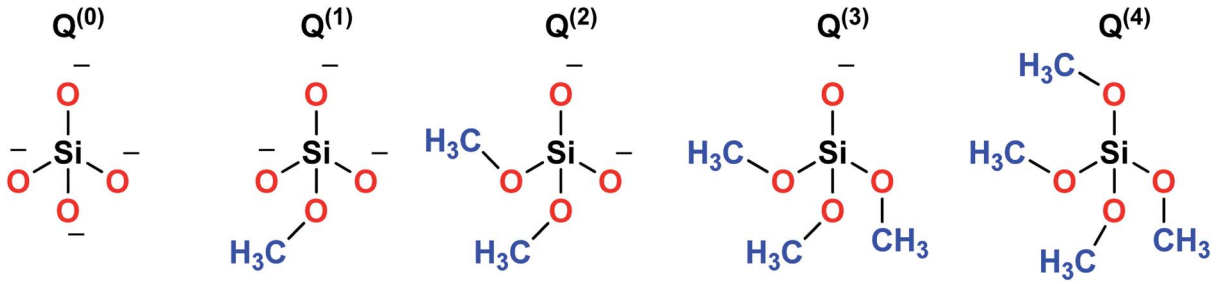

Fig. 7 Schematic representation of Si tetrahedral sites of silicate glasses.

represents the number of BO atoms which are connected to each tetrahedron.[94,98] A schematic representation of Si-tetrahedral sites of silicate glasses is given in Fig. 7. In the case of vitreous SiO_2, each and every tetrahedron is connected to another tetrahedron of its four corners ascribing to four BO atoms per tetrahedron.[99] On the contrary, network modifiers, change the glass structure by turning BO atoms into non-bridging oxygen (NBO) atoms.[99,101] The properties of silicate bioactive glasses to a great extent depends on the portion of NBO atoms. Typically, oxides of alkali or alkaline earth metals such as Na^+, K^+, Ca^+, Mg^+ are used as network modifiers.[99] The bond between the metal ion modifier and NBO is predominately ionic while the bond within Si and BO is covalent.[102] Fig. 8 schematically depicts a two dimensional (2D) representation of glass modifiers and network formers. The third type of a glass component is intermediate oxides (*e.g.* ZnO, MgO, Al_2O_3) which generally served as a network modifier (depolymerize the structure)[103] or can be penetrated into the backbone of the glass structure (act like a network former) depending on their content.[104] The polymerization of the network *i.e.* the average number of BO per SiO_4 tetrahedron is typically described as the network connectivity of the glass.[105] The network connectivity of bioactive glasses tends to be low with values typically in the range of 2 and 2.6. The higher the value of network connectivity, the more connected the network. With the addition of modifier, the Si–O bond breaks down leading to the formation of Q^3, Q^2 and Q^1 units which share 3, 2 and 1 oxygen ions with their respective neighboring units.[100] Bioactive glasses mainly consist of Q^2 and Q^3 units, since they contain low silica content (45–55%).[106,107] A metasilicate glass having a chain or ring structure of Q^2 group exhibits network connectivity of 2.0 while an increase in the connectivity leads to enhanced polymerization of silicate structure with a subsequent increase in Q^3 and Q^4 groups.[100] The network connectivity in silicate glasses varies

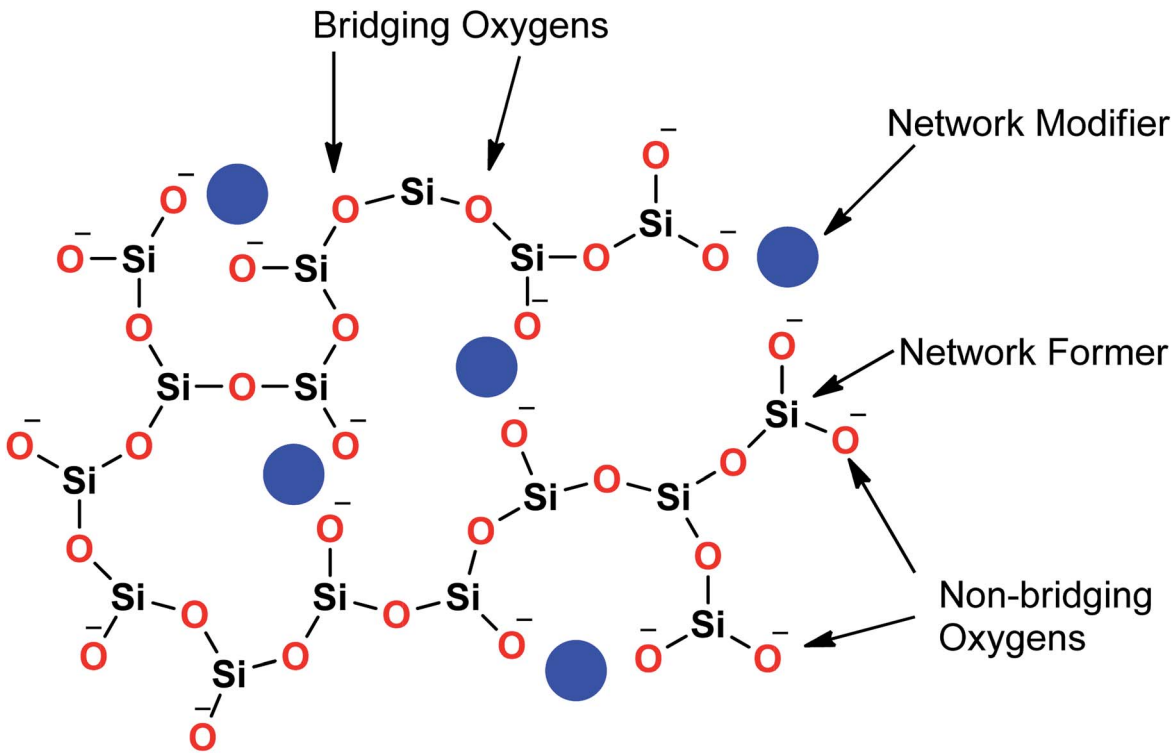

Fig. 8 Schematic representation of glass network formers and modifiers.

Open Access Article. Published on 11 September 2020. Downloaded on 10/25/2025 7:46:44 PM.
This article is licensed under a Creative Commons Attribution-NonCommercial 3.0 Unported Licence.

from 4 for pure silica glass to 2 for a chain-like structure.[100] Thus, network connectivity gives information about the average polymerization of the network[108] while it is also useful for estimation of properties of glasses such as crystallization tendency, glass transition temperature as well as bioactivity.[105,109] For bioinactive compositions, the network connectivity is usually greater than 3 while the network connectivity around 2–3 suggests appropriate dissolution and bioactivity.[105,108]

Silicate glasses have been extensively investigated as inorganic bioactive biomaterials in the field of regenerative medicine since the discovery of first bioactive glass (traditionally known as 45S5 Bioglass®) of composition $45SiO_2$–$24.5Na_2O$–$24.5CaO$–$6P_2O_5$ wt% in the early 1970s.[110,111] Originally, Hench and coworkers used the traditional melting method for producing silicate-based bioactive glasses and later focused on the sol–gel method for synthesizing different glasses and glass derived ceramics.[93,112] Since then, there is a growing research activity in this field where innumerable research groups across the globe are seeking novel biomaterials in varied forms and compositions.[113–115] The key feature in the bioactivity of the silicate glasses is their composition which is mainly premised on silica as the glass network former which offers stability to the material. In sol–gel silicate glasses, the tetrahedral SiO_4 unit condensates as scattered branches or as 3, 4 or 5 SiO_4 member ring based on the stabilizing temperature.[116] This confirmation leads to high microporosity resulting from the high surface area which further provides characteristic reactivity of silicate glasses.[117,118] The addition of a high level of glass network modifiers namely Na_2O, CaO, MgO and K_2O have been demonstrated to influence the bioactivity of silicate glasses.[119] Also, a relatively high CaO/P_2O_5 ratio was found to transform high reactivity to the glass surface in a physiological environment.[120] Therefore, several bioactive glass compositions have been developed over the years having no sodium or containing other elements namely fluorine, magnesium, strontium, iron, silver, boron, potassium or zinc incorporated in the silicate network.[114,121–126]

Bioactive silicate glasses have instigated tremendous research interest in mineralized bone tissue engineering owing to their ability to form the HCA layer when in contact with biological fluids.[127] These glasses are identified by their strong capability to react chemically with the living tissues thereby forming strong and stable bonds with them.[128] The high biocompatibility and the favourable biological effects of their reaction products constituted after implantation has made silicate glasses the most promising and interesting group of biomaterials for the last five decades. However, the inferior mechanical properties of these glasses have severely limited their clinical applications.[118,129] Nevertheless, silicate glasses display the majority of the chemical as well as biological properties that are relevant to an ideal grafting and scaffolding material namely high surface area, porous structure with regards to overall porosity and the pore size that can foster cell-material interaction and cell invasion.[130] Studies have shown that the porous structure of silicate glasses provides a higher surface area that depicts enhanced tissue bonding rates.[59] These features promoted new perspectives of silicate glasses as third-generation biomaterials for bone tissue regeneration.[131] Moreover, the high reactivity of silicate glasses is the primary advantage for the repair or regeneration of periodontal tissue and bone augmentation because the reaction products acquired from such kind of glasses and physiological fluids promote crystallization of apatite layer which is analogous with the inorganic components of the bone invertebrate species.[118] However, as far as scaffold preparation for tissue engineering applications is concerned, it is a drawback to have a high content of Na_2O in the bioactive glass composition and thus silicate glasses with low alkali content needs to be designed with good sintering ability, enhanced bioactive properties, controlled chemical dissolution and high mechanical strength.[132]

The formulation of bioactive glasses using the sol–gel technique opens the possibility of increasing the range of compositions displaying bioactive behavior. The bioactivity and the biocompatibility of sol–gel derived silicate glasses based on the SiO_2–CaO–P_2O_5 system have been widely examined for various biomedical applications.[133,134] A rapid *in vitro* HCA formation was noticed for compositions consisting of 80 mol% of SiO_2 in SiO_2–CaO–P_2O_5 and SiO_2–CaO glass systems.[135,136] A comparative *in vivo* study of sol–gel silicate glasses based on 58% SiO_2–38% CaO–4% P_2O_5 (58S) and 77% SiO_2–19% CaO–4% P_2O_5 (77S) with melt derived 45S5 bioglass revealed that sol–gel glasses display similar cell response with minor changes in the environmental conditions owing to the lower content of Na^+ and Ca^+ cations in the glass composition. The long term *in vivo* studies further validated that 58S and 77S based sol–gel glasses displayed similar responses to melt derived 45S5 bioglass.[137] In another study, the *in vivo* behavior of sol–gel silicate glasses was evaluated to check their eligibility as a material for bone substitution or repair[138] while another investigation reported *in vitro* HCA formation correlated with *in vivo* behavior of the sol–gel glass.[139] Lin *et al.*[140] studied the effect of different bioactive glass compositions on cutaneous wound healing in both normal as well as streptozotocin induced diabetic rats. The bioactive glass ointments developed *via* mixing the sol–gel synthesized silicate glass of composition 58% SiO_2–33% CaO–9% P_2O_5 (58S), nano bioactive glass (58S) and melt derived 45S5 bioglass powder with 18 wt% of Vaseline were employed for healing the full thickness excision wound. In all three cases, the addition of bioactive glass to Vaseline was found to improve and expedite the wound healing and vascularization process. Moreover, sol–gel derived silicate glasses exhibited significantly higher healing rates than that of melt derived 45S5 bioglass.[140] Xie *et al.*[141] synthesized different compositions (60S, 70S, 80S, and 90S) of sol–gel derived silicate bioactive glasses and found that 90S silicate bioactive glass with composition $90SiO_2$–6CaO–$4P_2O_5$ (mol%) displayed excellent support for the proliferation of human foreskin fibroblasts. Therefore, silicate glass particles of 90S composition were utilized as a model for systematic investigation of the wound healing related cellular response of fibroblasts. The results related to the gene expression of extracellular matrix (ECM) demonstrated that 90S silicate bioactive glass particles modified the capacity of critical ECM molecules comprising type I and III collagen, fibronectin, and tenascin-C.

Open Access Article. Published on 11 September 2020. Downloaded on 10/25/2025 7:46:44 PM.
This article is licensed under a Creative Commons Attribution-NonCommercial 3.0 Unported Licence.

Furthermore, it was illustrated that the 90S silicate bioactive glass particles significantly inhibited the differentiation of fibroblasts to myofibroblasts. Finally, the authors concluded that Si^{4+} ions played a key role in the regulation of cell behavior during the wound healing process thereby accelerating the healing rate with minimum scaring.[141] Salinas *et al.*[142] investigated the role of P_2O_5 on the bioactivity (*in vitro* behavior) and the textural properties of three different compositions of SiO_2–CaO–P_2O_5 sol–gel glasses. The porosimetry studies revealed that the surface area increased while the pore volume and the pore diameter was reduced as P_2O_5 content in glasses increased.[142] *In vitro* investigations revealed that all the three compositions were bioactive owing to the formation of the apatite layer after soaking in simulated body fluid (SBF). The glass composition with S75 exhibited the highest initial reactivity and the lowest crystallization rate of the apatite-like phase. For glass compositions with S72.5P2.5 and S70P5, the formation of an amorphous CAP layer was slower than for S75, however, the crystallization of apatite was noticed after shorter periods in SBF. Besides, after soaking for 7 days, the layer thickness was decreased with an increase in the P_2O_5 content in the glasses. Thus, it was found that P_2O_5 played a very complex role in SiO_2–CaO–P_2O_5 sol–gel glasses where more than 10 mol% of this component leads to non-bioactive compositions.[118] Moreover, several investigations[123,143–145] have shown that the addition of network modifiers such as MgO into SiO_2–CaO–P_2O_5 sol–gel glasses compositions induce changes in the apatite layer formation when they are soaked in SBF. The existence of Mg^{2+} cations in the glass composition reduces the apatite layer formation rate but with increased layer thickness in comparison with the glasses without MgO content.[118] Also, Saboori *et al.*[146] have shown that the quaternary sol–gel derived bioactive glass system comprising SiO_2–CaO–P_2O_5–MgO exhibits the ability to support human fetal osteoblast cell growth. These bioactive glasses were turned out to be non-toxic and found to be compatible with the segmental defects in the goat model *in vivo*.[146]

The doping of various metal ions in the sol–gel silicate glasses has been widely studied with an aim to enhance their bioactivity in a relevant physiological environment and to stimulate the effect of bioactive glasses on osteogenesis and angiogenesis while promoting their antimicrobial properties.[46] For example; Bellantone *et al.*[147] reported *in vitro* bioactivity and antibacterial properties of silver (Ag) doped sol–gel silicate glasses based on the $76SiO_2$–$19CaO$–$2P_2O_5$–$3Ag_2O$ wt% with controllable degradation properties. The addition of 3 wt% of Ag in the silicate glass conferred antimicrobial properties without sacrificing its bioactivity. Ag-doped bioactive silicate glass exhibited a striking antibacterial effect against *Escherichia coli* with a lowest concentration of 0.2 mg (biomaterial) per mL (culture solution). Above this concentration, the bacterial growth was decreased to 0.01% of that of the control culture solution.[147] Similarly, Hu *et al.*[148] studied the potential of Ag-doped SiO_2–CaO–P_2O_5–Ag_2O silicate bioactive glass with nanoporosity (pore size ~6 nm) and high surface area (467 $m^2\ g^{-1}$) prepared *via* the sol–gel method for wound healing applications. The synthesized silicate bioactive glass containing 0.02 wt% Ag exhibited good antibacterial properties against *Escherichia coli* without cytotoxic effect while the antibacterial rate reached 75% in one hour and 99% in twelve hours. Furthermore, these silicate glasses successfully promoted blood clotting and obtained hemorrhage control in the animal model while the high surface area caused an exceptional hemostatic performance.[148] Pratten *et al.*,[149] performed *in vitro* studies to investigate the ability of Ag-doped bioactive silicate glass coating to prevent bacterial colonization on surgical sutures. The antibacterial effect was studied against *Staphylococcus epidermidis* with the Ag-doped bioactive silicate glass coating having the greatest effect on limiting the bacterial attachment as compared to the 45S5 Bioglass® coated and the uncoated sutures.[149] Catauro *et al.*[150] studied the effect of Ag ion addition on the antimicrobial properties of Na_2O–CaO–SiO_2. The sol–gel derived silicate glasses showed high antimicrobial effects against *Escherichia coli* and *Streptococcus mutans*. Similar studies were later reported by Jones *et al.*[112] where Ag ions were added to sol–gel glass scaffolds for bone tissue engineering applications. Moreover, sol–gel based silicate glasses were doped with other metal ions such as zinc (Zn^{2+}),[151–154] and strontium (Sr^{2+})[155–158] in order to enhance their bioactivity and biocompatibility in relevance to their tissue engineering applications.

3.2 Phosphate based glasses

The sol–gel synthesis of phosphate-based glasses is considerably more stringent than the synthesis of silicate glasses. Phosphate based glasses are inorganic polymers consisting of highly degradable tetrahedral phosphate anion (PO_4^{3-}) which forms the backbone of the structure and the metal cations charge to balance the phosphate chains.[159] The basic building blocks of phosphate-based glasses are the PO_4^{3-} tetrahedra which is analogous to silicate glasses.[160] The PO_4^{3-} tetrahedra are interconnected in the glass structure *via* covalent bonds to form various phosphate anions as shown in Fig. 9. Phosphate based glasses are mainly based on phosphorus pentoxide (P_2O_5) which acts as a glass network former. P_2O_5 is chemically unstable and the incorporation of metal oxides improves its stability. Phosphate based glasses containing various metal oxides such as titanium dioxide (TiO_2), ferric oxide (Fe_2O_3), copper oxide (CuO), zinc oxide (ZnO), and aluminium oxide (Al_2O_3) have been prepared for different end applications.[161–165] However, the most commonly used oxides are sodium oxides (Na_2O) and calcium oxides (CaO) which are usually employed in a specific molar ratio to synthesize biologically active glasses.

The sol–gel derived phosphate-based glasses for the biomedical application were originally presented by Knowles.[166] Later, Carta *et al.*,[11,167] described the synthesis of ternary (P_2O_5–CaO–Na_2O) and quaternary (P_2O_5–CaO–Na_2O–SiO_2) sol–gel derived phosphate glasses. Further, the same research group investigated these phosphate-based glasses and found structural similarities between the sol–gel derived glasses and the melt derived glasses of the same composition. Hence, indistinguishable bioactivity was anticipated for varied biomedical applications.[167] Pickup *et al.*[168,169] reported the low-temperature

Open Access Article. Published on 11 September 2020. Downloaded on 10/25/2025 7:46:44 PM.
This article is licensed under a Creative Commons Attribution-NonCommercial 3.0 Unported Licence.

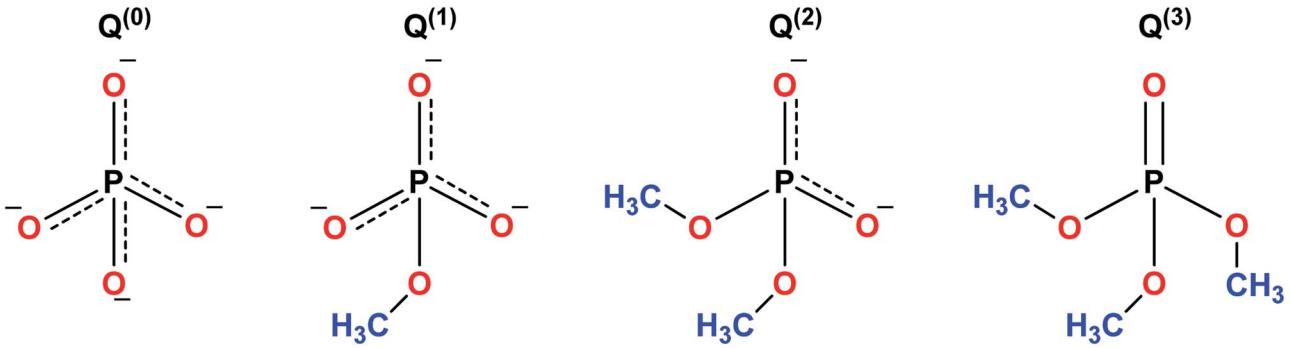

Fig. 9 Schematic representation of PO_4^{3-} tetrahedral sites of phosphate glasses.

sol–gel synthesis of binary (P_2O_5–TiO_2) and ternary (P_2O_5–CaO–Na_2O) glasses. These glasses were later tested for drug delivery applications by subsequently releasing the drug molecules in aqueous medium.[170] From the biomedical application point of view, phosphate-based glasses have several unique and interesting properties such as the ability to be completely dissolved in the aqueous medium. Furthermore, the dissolution rate can be easily controlled to give glasses with the dissolution rates of several orders of magnitude.[166] The degradation of these glasses deviates from a few hours to years depending on the composition and the targeted applications. Phosphate-based glasses can be synthesized in different forms such as discs,[171–173] microtubes,[174] microspheres[175] and fibers.[164,176,177] Fibers can be utilized for cell transportation and device expansion,[175] nerve conduit[178] and as a scaffold for muscle regeneration.[165] The key goal of using phosphate-based glass fibers in biomedical applications is to produce tissue-like fibrous constructs which can guide the cell growth. Copper (Cu)-containing fibers with antimicrobial properties have been used as wound dressing meshes for treating severe burns and leg ulcers.[162] Phosphate based glass microspheres have also been reported for radiotherapy applications.[179] The microsphere morphology provides a stable surface for proliferation and cell attachment preventing tissue damage and hemorrhage during radiotherapy.[179] The phosphate-based glass fibers have fascinating properties to form microtubes and hence can be integrated with a wide range of polymers to help nutrients diffusion and ingrowth of vascularization when employed as scaffolds for hard and soft tissue regeneration.[180]

Phosphate-based glasses belong to the group of unique materials owing to their fully controllable bioresorbable nature and easy doping with a wide variety of ions. In recent years, various glasses have been developed with chemical compositions similar to the mineral phase of bone making phosphate-based glasses promising candidates for the development of implantable biomaterials for repair and regeneration of hard tissues.[181] The stability of individual phosphate-based material depends not only on the small changes in the composition but also on the pH and the reaction.[1] Phosphate-based glasses containing calcium (Ca^{2+}) and sodium (Na^+) ions are the potential materials for applications such as soft and hard tissue engineering because the ions released from them are natural components of the human body.[166] In addition to actively taking part in the dissolution process of glasses, Ca is a primary constituent of bones which can trigger bone remodeling. Ca is necessary for the normal functioning of nerves, cells, muscles and bones. Ca^{2+} ions play an essential role in cell activation mechanisms and control various growth-related processes and cell functioning.[182] Furthermore, to confer additional beneficial properties, it is possible to include other cations such as Mg^{2+}, aluminium (Al^{3+}), Zn^{2+}, silver (Ag^+) and potassium (K^+) within the glass network besides Na^+ and Ca^{2+}.[46] Also, it has been reported that the extracts of the less soluble glass compositions accelerate cell proliferation and improves gene expression.[183] Besides, the cells can be attached, spread and proliferate in a controlled manner in addition to the development of a collagen-rich mineralized matrix.[184]

Like silicate and phosphate-based glasses, calcium phosphates (CaP) based ceramics also exhibit natural components found in the human body.[1,185] However, their biological properties are different. CaP based ceramics are frequently utilized in the field of medicine as bone replacements and as implants coating on dental and orthopedic prostheses.[185] HA is the frequently studied CaP material which is analogous to natural tooth and bone and it also represents the highly stable mineral phase in simple aqueous solutions (deionized water). This means that the degradation of CaP based materials in deionized water leads to the development of HA crystals.[1] HA and other CaP based materials such as α or β tricalcium phosphate (TCP) are manifested by exceptional biocompatibility due to their structural and chemical resemblance with the inorganic phase of human bone. Several CaP compositions such as α-TCP or tetra calcium phosphate (TTCP) have the ability to become hard (like cement) in aqueous solution making them useful as an injectable biomaterial for treating bone defects.[1] Recently, biphasic materials comprising of HA/β-TCP[186] and silicon substituted HA were demonstrated for clinical applications.[187] The most relevant features of these materials include their biological effect on tissues and in particular on their dissolution behavior which can be ascertained by their morphology, surface topology and chemical composition. Hence, proper designing of material creates the possibility to use CaP based materials in hard tissue regeneration.

Open Access Article. Published on 11 September 2020. Downloaded on 10/25/2025 7:46:44 PM.
This article is licensed under a Creative Commons Attribution-NonCommercial 3.0 Unported Licence.

Phosphate based glasses containing various therapeutic ions such as Ag^{+} (antibiotic),[188] Ti^{4+} (promotes growth of new bone),[172] fluorine (F) (helps in preventing dental caries/cavities),[189] strontium (Sr^{2+}) (taken up in a new bone as a treatment for osteoporosis)[190] and cisplatin (chemotherapy drug)[170] have also explored. The inclusion of these therapeutic ions certainly changes the structure of phosphate-based glasses and consequently affects their dissolution behaviour. Fig. 10 demonstrates a few selected biotherapeutic ions that can be released from CaP glasses thereby playing a key role in bone repair and regeneration.[191] Ca^{2+} ions are well known for stimulating proliferation of osteoblasts and mineralization of ECM[192] whereas Mg^{2+} ions promote the formation of new bone.[193] Furthermore, PO_4^{3-} ions are required for the deposition of CaP crystal and the mineralization of ECM,[194] whereas Na^{+} ions are usually found in extracellular fluid.[195] Other therapeutic ions such as Sr^{2+},[196] Ag^{+} [197] and Cu^{2+} [162] can also be released from the CaP glasses simply by doping the glass composition with the metal oxide of interest. Moreover, both Cu^{2+} and Ag^{+} ions have demonstrated antimicrobial properties[162,198] whereas Sr^{2+} ions prevent osteoclast activity while fostering osteogenesis of mesenchymal stem cells *in vitro* and *in vivo*.[199,200]

3.3 Silica–titania based glasses

The sol–gel chemistry-based preparation of silica glasses has been reviewed to a great extent by several authors. However, despite a large amount of work already reported on sol–gel silica-based glasses, considerably less information is available about the sol–gel glasses derived from silica–titania (Si–Ti) based binary systems, particularly for biomedical application. Over the past few years, Si–Ti binary systems have been largely used as a catalyst in the forms of amorphous oxides, crystalline titanium silicates *etc.*[201,202] In addition to the catalytic application, one can also anticipate enhanced thermal stability, mechanical strength, resistance to alkali and zero thermal expansion upon addition of Ti in the Si network.[203,204] For developing sol–gel derived Si–Ti based materials, control over hydrolysis reaction is essential for obtaining homogeneous gels. This is because the hydrolysis and the condensation reaction rates of titanium alkoxide are considerably higher than that of silicon alkoxide owing to the low electronegativity of titanium and its propensity to display several coordination states.[205] To compensate for their hydrolysis rate differences, bulky alkoxy groups for titanium and methoxy or ethoxy groups for silicon have been used.[206,207] In some cases, chelating reagents such as acetylacetone (Acac)[208,209] have been used and in some cases, the two-step hydrolysis[210] method was adopted to obtain homogeneous Si–Ti based gels. Konishi *et al.*[211] demonstrated the formation of a well-defined interconnected gel network with Ti system with macroporous morphology using the phase separation method. The phase separation is generally induced by the organic polymer present in the system. The phase separation also enables control over gel morphology to a great extent.[212] Zhu *et al.*[201] illustrated the preparation of Si–Ti based mesostructured monoliths *via* the sol–gel method combined with the liquid crystalline templating approach. The authors suggested that the synthesized monoliths could be used as excellent support for gold catalysts.

Ruzimuradov[213] reported the synthesis of Si–Ti monoliths with bicontinuous macropores by sol–gel method combined with phase separation using various titanium precursors. TEOS, titanium(IV) isopropoxide (TIP), titanium tetrabutoxide (TBOT),

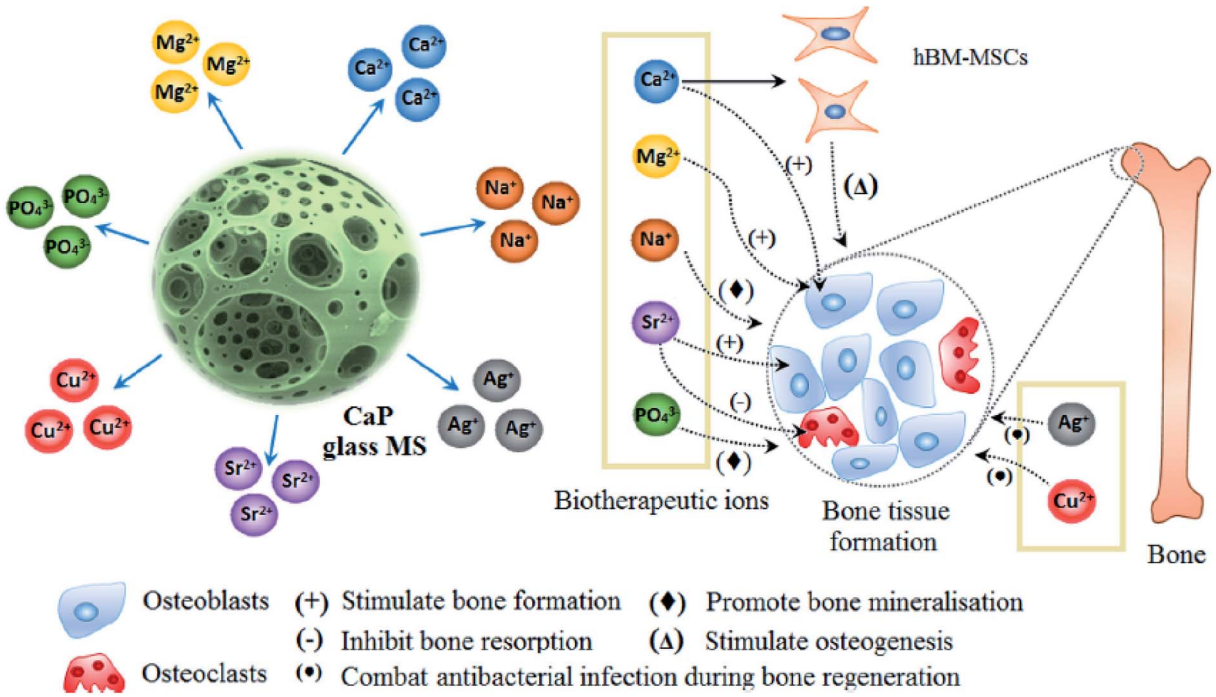

Fig. 10 Releasing of various biotherapeutic ions from CaP glasses and their respective roles in the bone tissue regeneration. Reproduced with permission from ref. 191. Copyright 2018, Elsevier.

Open Access Article. Published on 11 September 2020. Downloaded on 10/25/2025 7:46:44 PM.
This article is licensed under a Creative Commons Attribution-NonCommercial 3.0 Unported Licence.

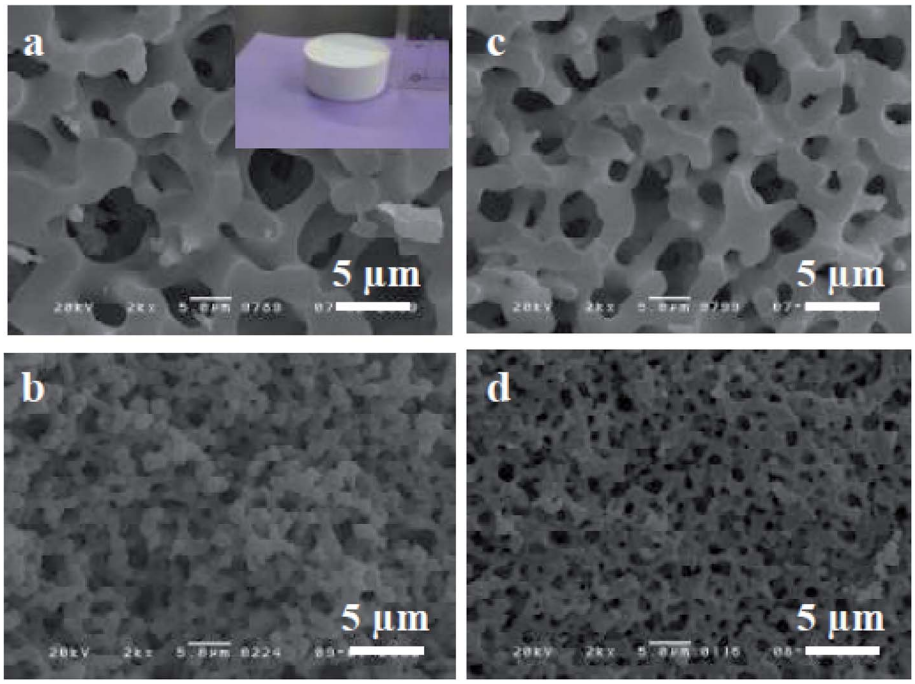

Fig. 11 SEM micrographs of dried gels prepared using (a and b) TIP–Acac and (c and d) TBOT. The figure inset shows the photograph of the synthesized Si–Ti based monolith. Adapted from ref. 213. Copyright 2011, IOP Publishing Ltd.

titanium tetrachloride ($TiCl_4$) and titanium sulfate (Ti $(SO_4)_2$) was used as the source for Si and Ti respectively. Furthermore, Acac was utilized as a modifier to prevent the reactivity of TIP. PEG was utilized as a polymeric constituent to instigate phase separation. It was observed that the Si–Ti based monoliths comprise a bimodal porous structure with homogeneously dispersed Ti in the Si network. Fig. 11 and 12 depicts the microstructure of the dried gels obtained using different types of titanium precursors. For all the compositions, the interconnected macroporous structure was observed when the

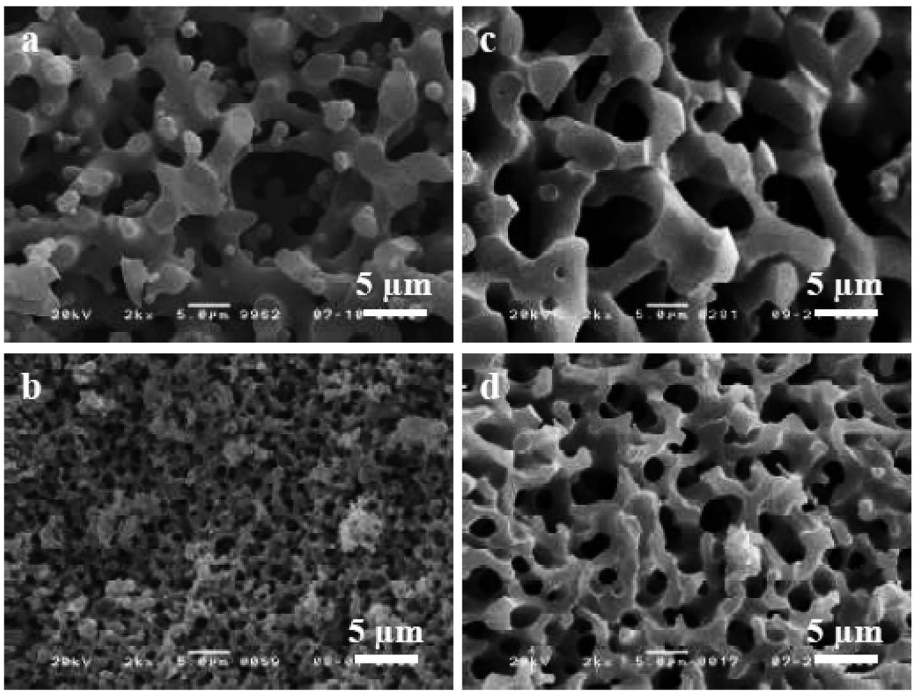

Fig. 12 SEM micrographs of dried gels prepared using (a and b) $TiCl_4$ and (c and d) $Ti(SO_4)_2$. Adapted from ref. 213. Copyright 2011, IOP Publishing Ltd.

Open Access Article. Published on 11 September 2020. Downloaded on 10/25/2025 7:46:44 PM.
This article is licensed under a Creative Commons Attribution-NonCommercial 3.0 Unported Licence.

transitional structure during phase separation was frozen due to sol to gel transition of inorganic constituents.[213] Nevertheless, a large difference in phase separation tendency and the dispersion of Ti in the Si network was observed with different titanium precursors used. Furthermore, for titanium alkoxide system the interconnected porous structure was observed at 30 °C with Ti content of 7.5 wt% (Fig. 11a and c) and 11.2 wt% (Fig. 11b and d) and no phase separation was noticed at 50 °C. When $TiCl_4$ and $Ti(SO_4)_2$ were used as titanium precursors, the gels with macroporous structures were obtained at 50 °C with the 7.5 wt% Ti content (Fig. 12a and c), 14.7 wt% (Fig. 12b) and 18.2 wt% (Fig. 12d). Also, the authors observed that the phase separation tendency largely decreased when titanium alkoxides were incorporated into the pure silica sol–gel system. On the other hand, when the titanium salts were utilized, the phase separation propensity changed a bit as compared with the pure silica system.

In another study, the same group of authors demonstrated the synthesis of macroporous Ti–Si monolith through co-gelation, two-step hydrolysis and Acac complex methods.[205] The authors also investigated the effect of different Ti precursors on the propensity of phase separation and the homogeneity of the resultant Ti–Si based gels. Fig. 13 depicts SEM micrographs of Si–Ti based monoliths prepared using three different methods. All the three specimens showed similar morphology where macropores were arranged bi-continuously. For these three samples, it was considered that the phase separation occurs *via* spinodal decomposition within the sol–gel reaction. In spinodal decomposition, the morphology became a superposition of an infinite number of sinusoidal compositional waves having a constant wavelength and randomly oriented in 3D space.[205] Besides, the macroporous morphologies were obtained for the specimens synthesized using co-gelation and two-step hydrolysis method when the reaction temperature was between 25–30 °C.

Recently, our group has demonstrated a similar approach for the sol–gel synthesis of Si–Ti based porous glasses where PEG has been used to induce phase separation, HNO_3 have been utilized as a catalyst while TEOS and TIP has been employed as a source for Si and Ti respectively.[214] The SEM micrograph of the prepared Si–Ti based dried gel is shown in Fig. 13d which revealed the interconnected macroporous network structure. Such type of microstructure is generally observed due to the occurrence of phase separation during sol–gel reaction.[205,214]

Nakanishi *et al.*[215] prepared Ti–Si based gels with a well-defined interconnected porous structure using the phase separation method. The author prepared these samples by a co-gelation method where acidic water was added to a mixed

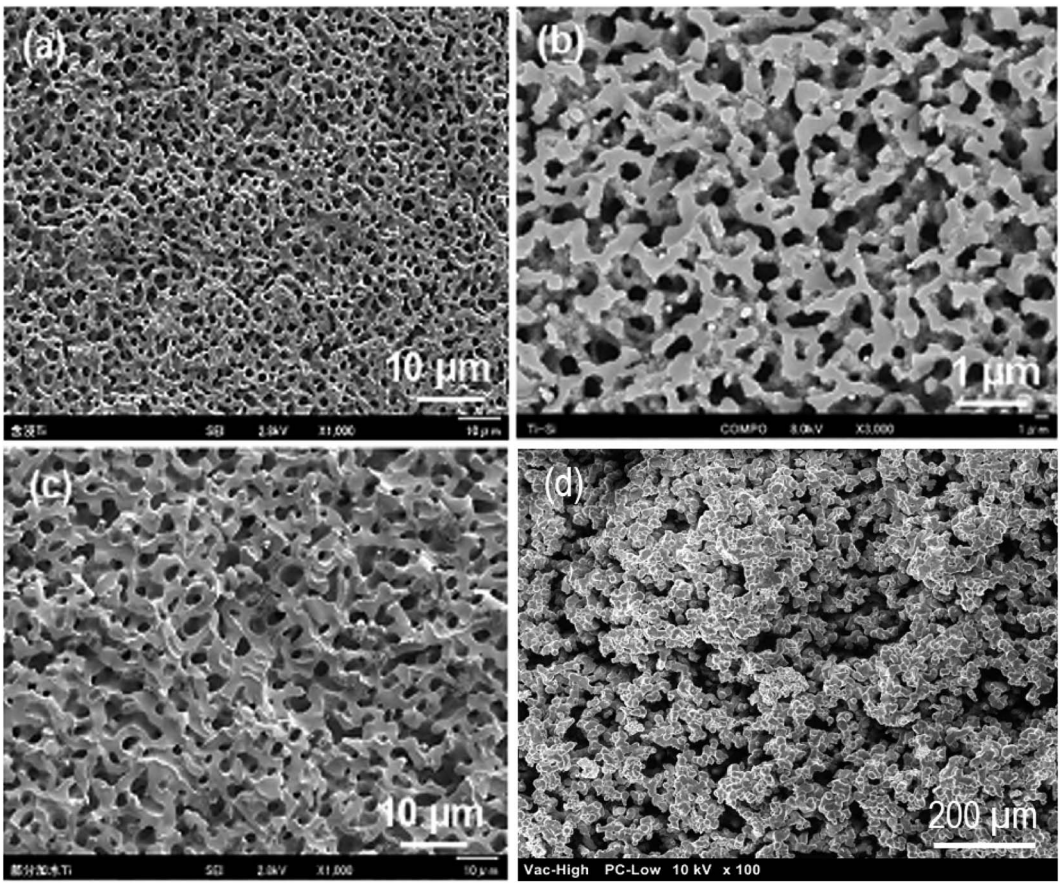

Fig. 13 SEM micrographs of fractured surface of Ti–Si based samples prepared with (a) impregnation (b) co-gelation, (c) two step hydrolysis with 0.6 g PEG and 11 g water. Adapted from ref. 205. Copyright 2012, Springer Nature. (d) SEM micrograph of Si–Ti sol–gel glasses prepared *via* similar method using PEG as phase separating agent and HNO_3 as catalyst.

Open Access Article. Published on 11 September 2020. Downloaded on 10/25/2025 7:46:44 PM.
This article is licensed under a Creative Commons Attribution-NonCommercial 3.0 Unported Licence.

alkoxide solution of TMOS and TBOT. However, the dispersion of Ti in the Si network was not studied in detail but it was expected that the dispersion of Ti in macroporous Ti–Si based materials can be modified by changing the synthesis method.[205] In another investigation,[216] hierarchically organized Si–Ti monoliths with the high specific surface area were synthesized by the sol–gel technique under purely aqueous conditions using 3-[3-{tris(2-hydroxyethoxy)silyl}propyl]acetylacetone as a precursor modified by ethylene glycol. Aravind *et al.*[217] illustrated the synthesis of crack-free Si–Ti-aerogel monolith with a high specific area and mesoporous structure for catalytic applications. A 3D printing method in combination with the sol–gel technique has also been reported for the synthesis of optically transparent Si–Ti glasses.[218] The characterization of 3D printed Si–Ti glass demonstrated that their properties including chemical composition, refractive index, optical transmission and thermal expansion coefficient are comparable to commercially available Si–Ti glasses.[218] The addition of Ti to Si decreases the thermal expansion and increases the refractive index of the resulting glass. Moreover, it has been shown that the addition of Ti to Si improves the network flexibility and the free volume of the glass while its tetrahedral structure was preserved.[219] Besides, Si–Ti glasses have also been used for the fabrication of optical parts such as mirrors, optical waveguides[220] and gradient index glass optics.[221]

Si–Ti based aerogels are actively used as a catalyst due to prominent mesoporosity and also due to the homogeneous dispersion of Ti in the Si network. The effectiveness of Si–Ti based catalysts greatly depends on the molecular level dispersion of Ti atoms, large surface area as well as pore diameters in the mesoporous range.[77] The high-temperature treatment induces considerable Si and Ti segregation which nullifies the porous structure established during sol–gel processing. In the literature, there are several strategies suggested for the sol–gel synthesis of Si–Ti based aerogels. The Si–Ti based aerogels synthesized by co-gelation of alkoxide have a surface area of 400–700 $m^2\ g^{-1}$, a pore size of 10–30 nm, a pore volume of 2–3 $cm^3\ g^{-1}$ and pore densities within 0.34–0.38 g cm^{-3} range.[217,222] Supercritical drying at low temperatures has been suggested to produce aerogels with low micro porosity and high surface area and amorphous mixed oxide aerogels.[223] Deng *et al.*[222] and Xu *et al.*,[224] reported the synthesis of Si–Ti based aerogels which exhibit high mechanical strength and high porosity with Ti/Si molar ratio of 1 : 5. The addition of Ti to a great extent modify the pore structure of the gel system. Pure Ti aerogels possess a surface area of ~100 $m^2\ g^{-1}$. It was found that the higher content of Ti in the Si–Ti based aerogels yields low surface area at all the compositions, which could be either due to decreased pore accessibility or due to the occupancy of Ti in the aerogel pores.[217,225] Another reason for the decrement of specific surface area with increment in Ti content could be the poor interactions between TiO_2 and SiO_2 in the Ti–Si based aerogels and the high amalgamation of TiO_2 particles in the gel.[222]

The sol–gel technique has also been utilized for the synthesis of bulk Si–Ti based glasses. Deng *et al.*[226] reported colloidal sol–gel method and succeeded in preparing bulk Ti–Si based glasses with large crack free specimens in different shapes such as glass rods (50 mm length, 5 mm diameter) and glass disc (5 mm thick, 40 mm diameter). A dense and transparent glass was obtained which is the same as the glass obtained using the melt quenching method. In another study, Satoh *et al.*[227] demonstrated the synthesis of Ti–Si based bulk glasses using silicon and titanium alkoxides. Recently, El-Bashir[228] fabricated Si–Ti based glass monoliths doped with Nd^{3+} ions. The synthesized glasses were recommended as a potential material for photo-resistive and photo-capacitive sensor applications. Guangwu and Yangang[229] reported the synthesis of Si–Ti based aerogel monolith with a Ti content of 26% by mass and drying under supercritical conditions using ethanol as a drying agent. Fig. 14 demonstrates the synthesized crack free monoliths of Si–Ti based aerogels with a density of 0.135 g cm^{-3}. The results from SEM analysis revealed that Si–Ti based aerogel was more compact than the pure silica aerogel with discontinuous microdomains of ordered porosity. Besides, the Si–Ti based aerogel revealed broad pore size distribution which was reasoned to be due to ethanol supercritical drying.[229]

3.4 Organic–inorganic hybrids

Sol–gel based organic/inorganic hybrid materials are rapidly becoming a fascinating research field in materials science. In the past decades, there has been tremendous progress in the synthesis of new organic/inorganic hybrids for various specific applications.[230] Hybridization is a multifaceted strategy by which multifunctional materials can be designed and produced with the synergistic effect of both organic and inorganic components leading to improved performance.[231] The organic/inorganic hybrid materials are comprised of interpenetrating

Fig. 14 Photographs of sol–gel derived (a) Si (b) Si–Ti based aerogel monoliths. Adapted from ref. 229. Copyright 2016, IEEE.

Open Access Article. Published on 11 September 2020. Downloaded on 10/25/2025 7:46:44 PM.
This article is licensed under a Creative Commons Attribution-NonCommercial 3.0 Unported Licence.

networks (IPNs) of various organic and inorganic phases with the scale of each phase in the range of 1 to 100 nm. These phases have nanoscale interaction with each other and enable the whole material to become a single phase contrary to traditional nanocomposites.[96,232] This facet of hybrid materials is accountable for highly controllable degradation rates and the potential for tailoring the mechanical properties as per the specific application needs. Furthermore, the molecular level dispersion of constituents facilitates an improved interaction with the cells resulting in instantaneous cell adhesion on the surface of the material.[196] For the synthesis of organic/inorganic hybrids, a polymeric component is induced in the sol–gel method right after the hydrolysis of TEOS. This allows the development of an inorganic network in the vicinity of organic molecules leading to molecular level interactions.[233] The gelation of organic and inorganic phases occurs simultaneously and results in the formation of 3D IPNs.[1] Therefore, this process can be employed for producing elastic hydrogels, flexible rubber and glasses with mesoporous structures, good physicochemical stability, high biocompatibility and reduced shrinkage.[234]

The organic/inorganic hybrid materials can be categorized as Class I and Class II hybrids depending on the type of interaction between organic and inorganic phases.[235] Class I hybrids represent the materials exhibiting non-covalent or ionic–covalent bonds within the organic and inorganic phases. In this case, the constituents of the hybrid interact with each other *via*

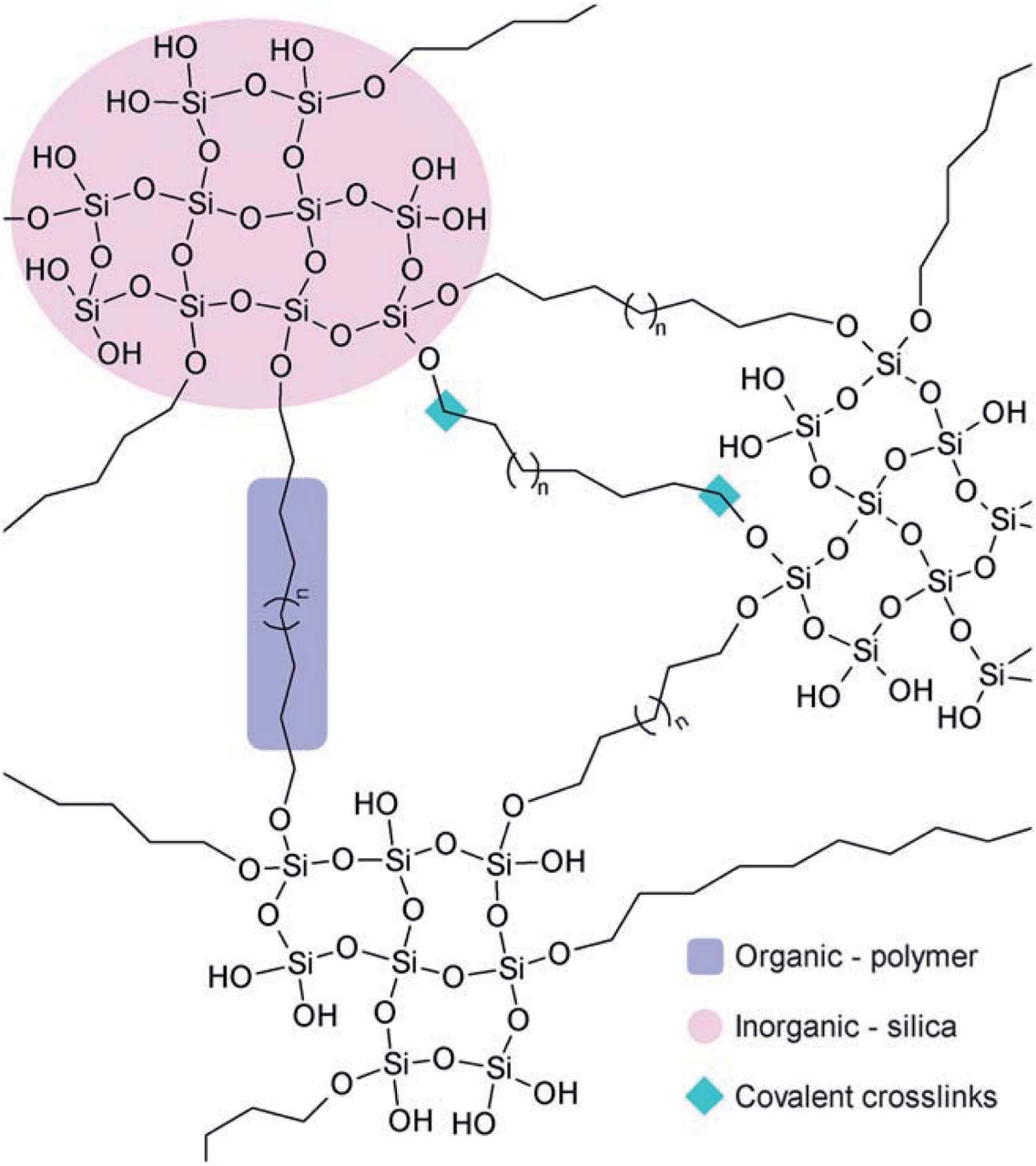

Fig. 15 Schematic representation of polymer–silica Class II hybrids. Adapted from ref. 235. Copyright 2011, the Royal Society of Chemistry.

Open Access Article. Published on 11 September 2020. Downloaded on 10/25/2025 7:46:44 PM.
This article is licensed under a Creative Commons Attribution-NonCommercial 3.0 Unported Licence.

weak hydrogen bonding interactions, van der Waals forces, π–π interaction or electrostatic forces. Class I hybrid materials can be obtained *via* approaches such as hydrolysis and condensation of alkoxides in the presence of organic polymers and blending alkoxide and organic constituents. Few examples of Class I hybrids are polyphosphazene-metal oxide,[236] silica–poly(*N*,*N*′-dimethyl acrylamide) (PDMAAm),[237] silica–polyvinylpyrrolidone (PVP),[238] polydimethylsiloxane (PDMS)–silica,[239] polymethylmethacrylate (PMMA)–silica[240] and poly(*n*-butyl methacrylate)–TiO_2 hybrids.[241] The drawback of Class I hybrids for tissue engineering applications is the absence of chemical bonds within the organic and inorganic phases that leads to rapid dissolution in presence of water because of the chain separation caused by water molecules.[235] Class II hybrids represent the materials in which the organic and inorganic constituents interact mutually *via* strong covalent or ionic–covalent bonds.[1] Crosslinking is the main feature of Class II hybrids. Generally, coupling agents are utilized for forming covalent bonds between a polymer matrix and the silicate network.[235] For the synthesis of these hybrids materials, the polymer is first functionalized using a coupling agent before it is introduced in the sol–gel process.[96] Fig. 15 schematically represents the possible interaction mechanism where the polymer matrix is incorporated at the beginning of the process to form inorganic silica chains around the polymeric molecules which lead to the formation of a hybrid having molecular level interaction.[235] It has been suggested that the molecular level interactions within organic and inorganic phases lead to controlled and uniform biodegradation with tailored mechanical properties.[242] Moreover, the molecular level interaction also suggests that the cells will contact the organic and inorganic phases simultaneously when they interact with the surface of the hybrid and thereby retaining the biological properties of bioactive glass.[235]

As far as biomedical applications are concerned, bioactive glasses represent the most proficient inorganic phase for obtaining hybrid structures. The bioactive glasses are generally comprised of binary SiO_2–CaO system or SiO_2–CaO–P_2O_5 and SiO_2–CaO–Na_2O ternary systems having a good bioactive response and identical degradation rates. The addition of sol–gel derived glass particles into a suitable polymer matrix is a promising strategy to ameliorate the performance of the base polymer, especially mechanical strength and biological activity.[233] For instance, Kamitakahara *et al.*,[243] investigated the biological activity and mechanical behaviour of PDMS–CaO–SiO_2 hybrids prepared with the varied calcium content. These hybrids were reported to form HA in SBF solution when tested *in vitro*. In another study, Sanchez-Tellez *et al.*[244] studied the sol–gel derived SiO_2–CaO–P_2O_5 hybrids for bone tissue regeneration. Several other synthetic or natural biopolymers such as PVA,[245,246] PEG,[247] gelatin,[248] chitosan[249,250] and poly(ε-caprolactone) (PCL)[251,252] were also used in the preparation of hybrids for biomedical applications. Such kinds of hybrids are generally synthesized by blending a polymer solution with silica sol followed by gelation. Recently, Catauro *et al.*[253] investigated the sol–gel derived PCL/zirconium oxide (ZrO_2) hybrids for implants coatings. In another study based on a gelatin–SiO_2 hybrid system, an improved apatite forming ability and osteoblast biocompatibility were observed.[254,255] Besides, nanostructured chitosan–siloxane hybrids also showed improved HA forming ability with fascinating photoluminescent properties.[256] Ohtsuki *et al.*[257] synthesized bioactive organic/inorganic hybrid comprising 3-methacryloxypropyltrimethoxysilane (MTMOS) and 2-hydroxyethyl methacrylate (HEMA) using sol–gel technique. These bioactive hybrids demonstrated the apatite formation ability when mixed with calcium chloride ($CaCl_2$) and recommended to be used as a novel material for bone repairing with both biological and mechanical behaviour closely matching with the conventional PMMA cement.[258] Thus, from these studies, it has been ascertained that the bioactivity or biodegradability of the sol–gel synthesized inorganic/organic hybrid materials can be controlled by varying the compositions of organic and inorganic phases which ultimately results in the better material properties.

4. Properties of sol–gel derived porous glasses

4.1 Mesoporous structure

The intrinsic characteristic of the sol–gel process is the production of materials with micro and mesoporous structures. In general, for sol–gel based glasses the porous structure is established either during synthesis or by successive treatment. On the basis of ascendant pore size and as per the classifications of IUPAC, the porous materials are classified as; (i) microporous materials possessing pore diameter up to 2.0 nm (ii) mesoporous materials exhibiting pore sizes in the range of 2 to 50 nm and (iii) macroporous materials comprising pore sizes greater than 50 nm.[259,260] The defining properties of any mesoporous material are most often the pore size and structure. The pores can be isolated or can be interconnected with the homogeneous (similar) or heterogeneous (dissimilar) shape and size distributions. The silicate materials acquired by the traditional sol–gel technique are most often manifested by mesopores with an average pore size in the range of 10–20 nm.[261] The small size mesoporous materials can be synthesized *via* sol–gel method combined with supramolecular chemistry in which surfactant is generally employed as a mesopore template.[233,262] Using this approach, the mesopore size can be finely tuned which is very much crucial especially for the materials to be designed for biomedical applications namely drug delivery systems.[263] This route is generally adapted for developing MBGs with a highly controlled mesopore size.[264] Primarily for biomedical applications, the larger pores can be advantageous to fit in certain cell types for the promotion of tissue engineering or regeneration activities while smaller surface pores can be advantageous to control the drug release or the release of small biological components or biomolecules.[191]

The surfactants are frequently used in the synthesis of mesoporous silica where they are served as a template for *in situ* polymerization of *ortho*-silicic acid. Typically, the surfactant is a kind of liquid crystalline mesophase comprising amphiphilic

Open Access Article. Published on 11 September 2020. Downloaded on 10/25/2025 7:46:44 PM.
This article is licensed under a Creative Commons Attribution-NonCommercial 3.0 Unported Licence.

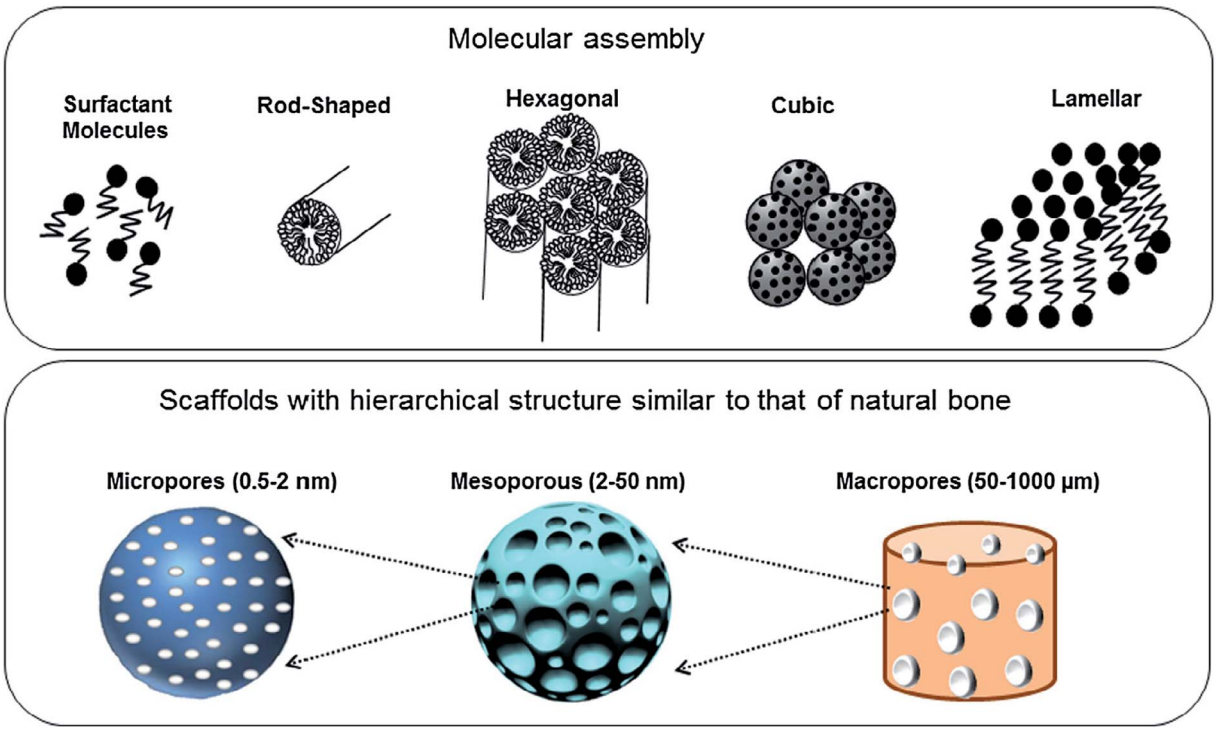

Fig. 16 Molecular assembly and different levels of pores created to design scaffolds for bone tissue repair. Adapted from ref. 1. Copyright 2016, Elsevier.

molecules which form micelles in the water-containing medium.[233] The pore size can be under the influence of several factors such as the chain length of the surfactant employed within the synthesis or the inclusion of auxiliary organic molecules for attaining more efficient control over pore dimensions.[233] These methods create the possibility to incorporate large molecules and influence their release rate as the pore size also has a negative impact on the diffusion of drugs which are loaded in the delivery medium.[265] Several features such as pore interconnectivity, pore shape and size distribution of the pore need to be considered for the characterization of porosity. The pore size should be regulated to meet the requirements of various applications as depicted in Fig. 16.[1] The pore structure and size control is pivotal for producing the living cell substitutes since porosity features are critical in ascertaining the existence of the interaction between the living cells and the surrounding environment.[233] Fig. 17 demonstrates that the surface area, pore diameter, pore volume and the surface functionalization of pore using organic molecules can have an impact on the loading and release rate of

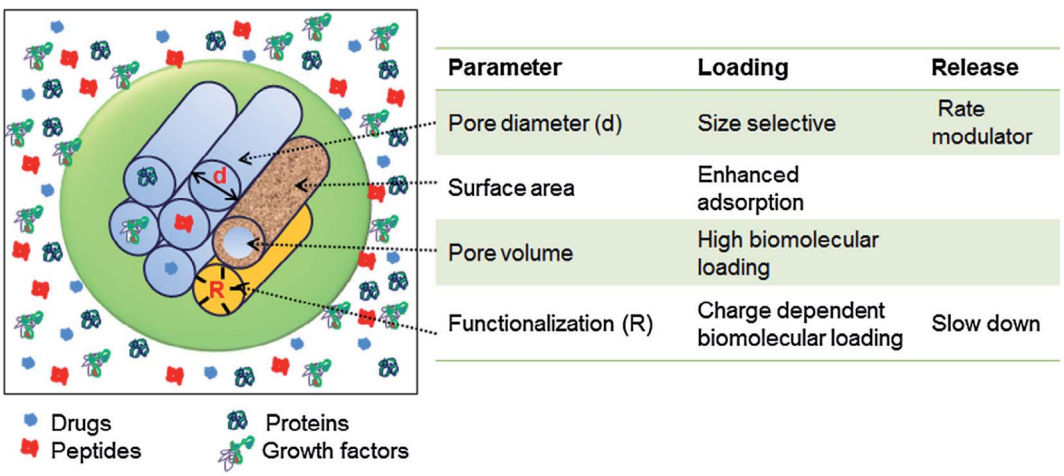

Parameter	Loading	Release
Pore diameter (d)	Size selective	Rate modulator
Surface area	Enhanced adsorption	
Pore volume	High biomolecular loading	
Functionalization (R)	Charge dependent biomolecular loading	Slow down

Fig. 17 Various parameters controlling the loading capacity and the release rate of biomolecules in mesoporous materials. Adapted from ref. 1. Copyright 2016, Elsevier.

Open Access Article. Published on 11 September 2020. Downloaded on 10/25/2025 7:46:44 PM.
This article is licensed under a Creative Commons Attribution-NonCommercial 3.0 Unported Licence.

biomolecules.[1] For certain drug delivery systems, it can be beneficial to have a bilateral pore size distribution (formation of dual mesoporous material) which can be achieved using binary surfactants having different molecular weight during the fabrication of surfactant constituted mesostructures.[1]

Hollow mesoporous bioactive glass (HMBG) spheres have also been produced by template-assisted or microemulsion based sol–gel synthesis.[266,267] The hollow structure is capable of providing large specific surface area and voids for bioactive glasses which is especially fascinating for drug delivery applications. For achieving hollow mesoporous architectures, co-templates are most often investigated.[76,91,266] Mesoporous shells can be developed using templates such as CTAB or pluronic P123 and the voids in the bioactive glasses can be created by hard templates such as polymeric particles[268] or soft templates such as microemulsion drops and micelles.[76] Furthermore, porosity in fact can be controlled by altering the type of template. For example; radial MBGs were obtained by sol–gel synthesis using cetyl pyridine bromide (CPB) as a template[269] whereas hexagonal bioactive glass spheres were obtained using pluronic F127 as templates for bone grafting and drug delivery applications.[270] Thus, MBGs with relatively large pore sizes can be realized by the microemulsion assisted sol–gel method.[73]

4.2 Morphology, shape and size

Using the sol–gel process, materials with a broad range of shapes and morphologies can be generated at the micro and macro scale. For example, thin films, bulk glasses, porous foams, fibers, microspheres and nanoparticles *etc.* The morphological features such as the size and shape of mesoporous glasses are essential and need to be controlled significantly for their efficient biomedical applications. Mesoporous glasses with small particle size stimulate apatite formation at a faster rate when exposed to body fluid which is favorable for applications such as orthopedic implants coating. The small size also facilitates cellular uptake thereby it is useful for drug delivery or delivery of biologically active ions. Furthermore, mesoporous glasses with small sizes also exhibit a larger surface to volume ratio which enables them to be incorporated with polymer matrices to form polymer nanocomposites.[233] The size of the bioactive glass can be adjusted by the processing parameters used in the synthesis. The size of bioactive glass particles is inescapably due to the concentration and the time at which the precursors are included in the synthesis process.[271,272] Also, the use of organic species tenders a manageable approach for adjusting the size of bioactive glasses. By merely varying the concentration of such organic species, the size of the bioactive glass can be easily controlled. The particle size also gets affected by the kind of template used during the synthesis.[273] In microemulsion based sol–gel synthesis of bioactive glasses, the particle size can be adjusted by fine-tuning of microemulsion droplets, for example by changing the concentrations of the catalyst.[73]

The sol–gel derived bioactive glass particles are generally spherical. The spherical shape tenders suitable flow properties for directly contacting the body fluids. Nevertheless, non-spherical particles are also useful for certain biomedical applications.[67] For instance; nanoparticles with rod-like shape and high aspect ratio can have more efficient cell attachment than spherical nanoparticles making them beneficial for specific anticancer drug delivery.[274] Furthermore, when employed as a bioactive reinforcing filler, rod or fiber-like bioactive glass particles demonstrate enhanced mechanical properties in comparison with the spherical shape particles.[275] Liang *et al.*[73] reported a synthesis of two different types of MBGs (i) spherical shaped bioactive glasses with radial mesostructure and (ii) pineal shape mesoporous glasses with lamellar mesostructure *via* the sol–gel process combined with liquid template method. Recently, Li *et al.*[276] described the fabrication of MBGs with distinctively different shapes where CTAB was used as a template for shaping mesoporous glasses. The high concentration of CTAB resulted in the formation of mesoporous glasses with rod-like shapes and low concentrations of CTAB tend to form spherical shaped particles. The addition of surfactants such as CTAB, pluronic P123 and pluronic F127 is crucial in achieving well-ordered structures. It was reported that the structure controlling agents have an influential role on the shape and size of mesopore, surface area as well as pore volume of MBGs.[1] Usually, CTAB induced mesoporous glasses exhibits smaller pore size (2–3 nm) as compared with P123 or F127 induced glasses (4–10 nm). Moreover, P123 induces a 2D hexagonal mesoporous structure, whereas F127 induces a worm-like mesoporous structure.[48]

A number of chemical and structural modifications to sol–gel bioactive glasses have been introduced to achieve improved biocompatibility and mechanical integrity. For example; El-Meliegy *et al.*[277] reported enhanced bone metabolism, in particular osteoblastic proliferation, differentiation and calcification through the presence of iron oxides (below the toxic level in the human body). The authors designed 3D scaffolds by combining Fe_2O_3-doped sol–gel bioactive glass (SiO_2–CaO–Na_2O–P_2O_5) with chitosan and obtained varied scaffold compositions using the freeze-drying technique. It was found that the interconnected open porosity was in the range from 64% to 75%. Furthermore, it was noted that, the presence of Fe_2O_3 up to 10 wt% led to the reduction in the porosity of formed bioactive glass scaffolds, however, the crosslinking between the bioactive glass and the polymer matrix was increased. In addition to that, the density and the compactness of the scaffolds led to an enhancement of mechanical strength. Besides, the authors also proved that the higher concentrations of bioactive glass and Fe_2O_3 in the scaffolds increase the cell viability as compared with the normal cells and pure chitosan scaffold.[277] In another study, the same group of authors demonstrated that the incorporation of hematite (Fe_2O_3) in the bioactive glass/chitosan scaffolds leads to an enhanced drug release for delivering 2% chlorhexidine gluconate (CHX).[278] Furthermore, the *in vitro* drug release and antibacterial studies revealed that incorporation of hematite completely removed the bacterial growth after 14 days. Moreover, the scaffold implantation treating dental infections resulted in outstanding osteoinduction ability.[278]

Open Access Article. Published on 11 September 2020. Downloaded on 10/25/2025 7:46:44 PM.
This article is licensed under a Creative Commons Attribution-NonCommercial 3.0 Unported Licence.

Recently, attempts have also been made using the sol–gel route to fabricate 3D foam scaffolds as a prominent group of biomaterials for tissue engineering applications. These 3D foam scaffolds can be developed to form hierarchically structured macro and mesopores that can be found in many tissues. The advantage of this type of scaffolds is that they exhibit combined properties of conventional glass-based scaffolds with unique qualities of mesoporous materials. Thus, the fabrication of highly porous 3D scaffolds using bioactive glass composition can be useful in bone tissue regeneration thereby taking advantage of both glass compositions as well as the mesoporous morphology. Baino *et al.*[279] demonstrated excellent apatite-forming ability on iron (Fe) doped sol–gel silicate glasses with multiscale hierarchical porosity ranging from the macro (50–600 mm) to the mesoscale (4–20 nm). It was noted that the pore volume, specific surface area and mesopore size decreased with increase in Fe content. Furthermore, the fabricated foams exhibited promising ferromagnetic properties and high biocompatibility which could be beneficial for simultaneously exploiting their ability to treat bone cancer *via* hyperthermia thereby promoting bone regeneration.[279] Of course, the bone-bonding ability of bioactive glasses depends on biodegradability, the dissolution rate of its ions, formation of new bone tissues and the stimulation of osteoblasts upon soaking in SBF.[280] The inclusion of iron oxide is beneficial because it does not induce cytotoxicity and the osteoblast can be grown and proliferated. However, the growth of the HA like layer was slower with increasing iron oxide content. The initial mechanism that was thought to induce bone formation is reduced due to the replacement of Ca^{2+} with Fe ions in the glass network.[280] Mesquita-Guimarães *et al.*[281] emphasized the importance and the influence of macroporosity of bioactive glass on cell viability and proliferation. The authors fabricated zirconia-based open-cell foams using the replica technique followed by coating *via*

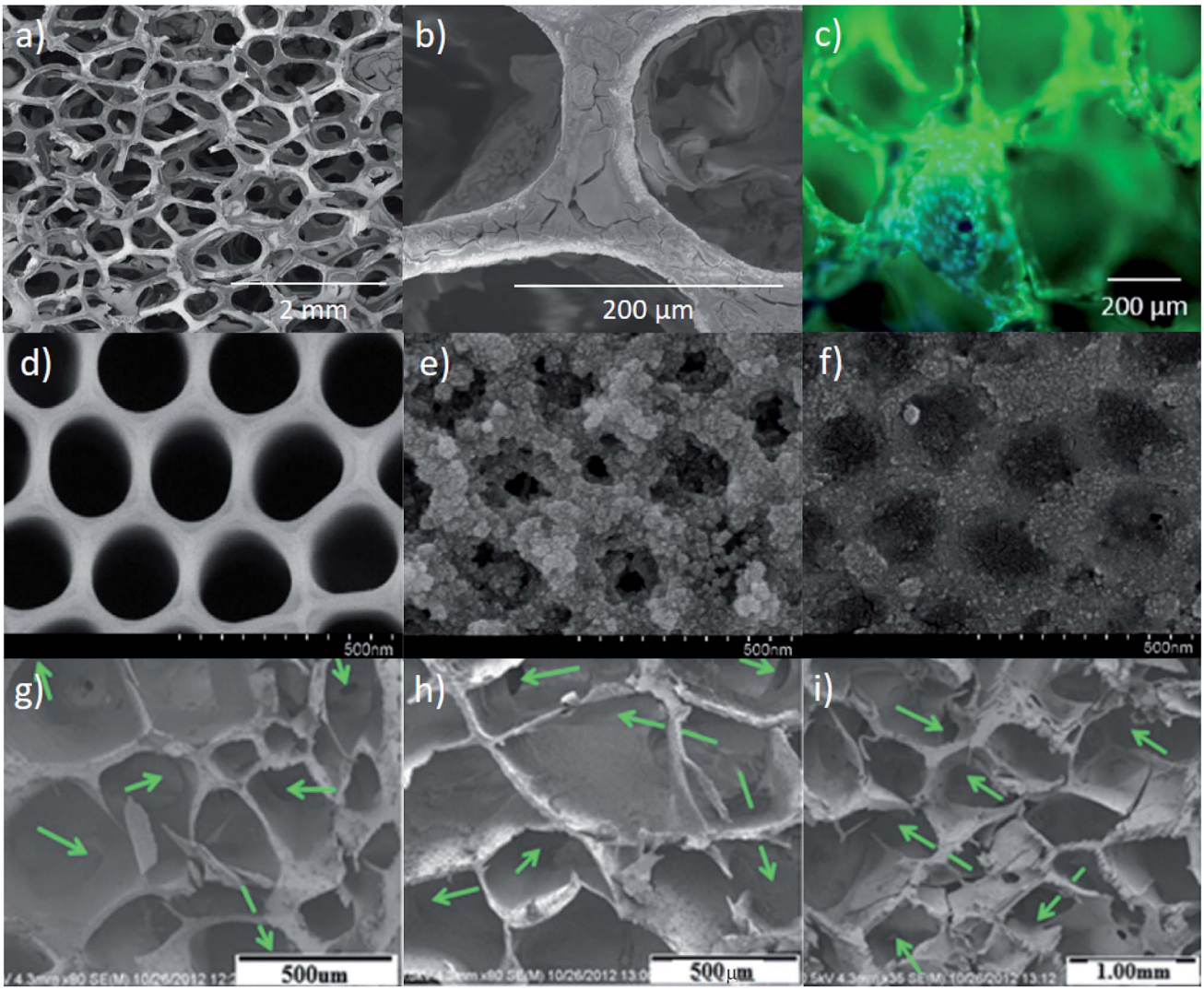

Fig. 18 (a) SEM micrographs of coated scaffolds with three immersions in fresh sol–gel solution. (b) Coated scaffolds with two immersions during 8 h of condensation. (c) Coated scaffolds after 2 days of cultivation. Reproduced with permission from ref. 281. Copyright 2019, Elsevier. (d–f) Micrographs showing surface structure of (d) PAA (e) $CaO–SiO_2$/PAA and (f) $CaO–SiO_2–Ag_2O$/PAA. Reproduced with permission from ref. 282. Copyright 2016, Elsevier. (g–i) SEM micrographs of gelatin/nanosilver/bioactive glass scaffolds with different concentrations (g) BGA0% (h) BGA20% and (i) BGA40%. Adapted from ref. 283. Copyright 2014, American Scientific Publishers.

Open Access Article. Published on 11 September 2020. Downloaded on 10/25/2025 7:46:44 PM.
This article is licensed under a Creative Commons Attribution-NonCommercial 3.0 Unported Licence.

immersing in the sol–gel solution of 58S bioactive glass. Fig. 18a demonstrates the SEM micrographs of coated scaffolds immersed three times in fresh sol–gel solution while Fig. 18b show SEM micrograph of coated scaffolds immersed twice during 8 h of condensation.[281] It was reported that reducing the pore size from 700 to 322 μm led to a 100% increase in cell proliferation. The enhanced cell viability and proliferation tendency was demonstrated by fluorescence microscopy using 4,6-diamidino- 2-phenylindole (DAPI) and calcein staining of MG-63 cells after two days of cultivation as illustrated in Fig. 18c.[281] Another interesting method was reported by Ni *et al.*[282] in which the authors reported about the sol–gel synthesis of bioactive $CaO–SiO_2–Ag_2O$ glasses loaded with porous anodic alumina (PAA) by a sol-dipping method followed by calcination of the gel-glasses. The results from this study revealed that the combination of the nanoporous structure of PAA and materials impregnated into the pores is a promising technique for forming a coating with multifunctional properties. Fig. 18d shows the typical PAA microstructure consisting of ordered hexagonal cells with a uniform nano-pore in the cell center.[282] The results from the pore loading investigation (Fig. 18e and f) revealed that the pore filling can be accomplished using $CaO–SiO_2$ and $CaO–SiO_2–Ag_2O$ bioactive glasses by a simple mechanism which can be influenced by pressure. Moreover, an *in vitro* antimicrobial activity test indicated that the $CaO–SiO_2–Ag_2O$/PAA system was highly effective in preventing the growth of both *Escherichia coli* and *Staphylococcus aureus* bacteria. The enhanced antimicrobial ability is mainly ascribed to the released Ag ions and increased pH values.[282] In another study, macroporous nanocomposite scaffolds based on gelatin/bioactive-glass/silver nanoparticles were developed from an aqueous solution of gelatin by freeze-drying method followed by crosslinking using genipin at ambient temperature. From a structural point of view, the macro-scale 3D interconnected porosity was obtained with pore size ranging from 350 to 635 μm as shown in Fig. 18g–i. Furthermore, by increasing the concentration of silver nanoparticles, the pore size and porosity also increased. As expected, significant prevention of bacterial (*Staphylococcus aureus, Escherichia coli*) growth and reduction of the biofilm formation on the scaffolds was revealed. Furthermore, the antibacterial effect was improved with an increase in the concentration of silver nanoparticles. It was proved through the viability studies of the hMSC on the prepared scaffold that all the scaffolds were cytocompatible.[283] Moreover, Ag ions can be released from sol–gel-derived $SiO_2–P_2O_5–CaO–Ag_2O$ glasses depending on the chemical composition, specific surface area and the diffusion of the biogenic ions present thereby affecting the degree of cytotoxicity.[284]

In a similar study, Jalise *et al.*[285] reported that gelatin and strontium (Sr) based bioactive glasses fabricated *via* freeze-drying technique exhibit an interconnected porous structure with an average diameter of 100–300 μm. Furthermore, increasing the Sr concentration leads to a decrease in the average pore size. The fabricated Sr-containing scaffolds with 15% Sr content revealed excellent stiffness (five times greater than glasses without Sr content) and high porosity (>80%). Moreover, *in vivo* angiogenesis studies confirmed superior cell infiltration and stimulated neovascularization in scaffolds containing 15% Sr ions in the bioactive glass as compared with the glass without Sr content. Shaltooki *et al.*[286] successfully produced a nanocomposite scaffold made of chitosan-coated polycaprolactone (PCL) and 45S bioactive glass (5, 10 and 15 wt%) with 7 wt% Sr using solvent casting technique. Porous nanocomposite scaffolds containing 15 wt% of bioactive glass particles was optimized and coated with chitosan layer which revealed no cytotoxic effect, acceptable degradation behavior and enhanced bioactivity, alkaline phosphatase activity and cell attachment.[286] Such modification can be beneficial in controlling the engineering properties of bioactive glasses. Amudha *et al.*,[287] proved that cell viability and proliferation can be significantly enhanced in 45S5 bioactive glass by Sr ions doping. The doping of a small quantity (0.2 wt%) of Sr led to significant changes in the physicochemical, mechanical, surface, drug release and biological properties. For Sr doped glasses, the pore volume and the surface area were improved to 96 and 108% respectively as compared with Sr free glasses. Besides, the interconnected porous structure facilitated the controlled and sustained drug release of about 58% in 720 h. Furthermore, the mechanical strength of the bioactive glass was significantly improved after Sr doping. In another investigation, Zamani *et al.*[288] prepared a composite scaffold based on alginate and bioactive glass (60S) having 80% porosity. The incorporation of bioactive glass particles containing zinc and magnesium into the alginate scaffold led to an improvement of mechanical properties and antibacterial efficiency. Furthermore, the results of *in vitro* tests exhibited good MG-63 cell response (viability, attachment and proliferation) and osteoblast differentiation. Moreover, the ion release capability of the scaffold was evaluated after 60 days of incubation in PBS solution using inductively coupled plasma (ICP) spectroscopy which revealed enhanced antibacterial efficiency against *Escherichia coli* and *Staphylococcus aureus* bacteria.

Hong *et al.*[289] fabricated ultrathin MBG hollow fibers *via* electrospinning technique by employing high molecular weight polyethylene oxide (PEO) as a phase separating agent. During electrospinning, quick solvent evaporation and PEO stimulated phase separation process played an important role in the development of bioactive glass fibers with hollow cores and mesoporous walls. In another study,[290] the fabrication of scaffolds with flexible cotton wool-like 3D structures based on 70 mol% silica and 30 mol% CaO (70S30C) has been reported by combining sol–gel and electrospinning method. The fascinating part of this study was the achievement of three orders of porosity *i.e.* pores on the fibers, pores between the fibers and pores in the entangled fiber space. Thus, such hierarchical porosity can be useful in enhancing the cellular attachment and the transfer among the scaffold fibers.[290] The flexible 3D fibrous structure was found ideal for packing into complex defects with larger inter-fiber spaces to promote vascularization, cell penetrations and nutrients transport throughout the scaffold. The authors demonstrated the potential of 70S30C cotton wool-like materials as a bone graft substitute especially for dental bone regeneration as shown in Fig. 19. The 70S30C based bioactive

Open Access Article. Published on 11 September 2020. Downloaded on 10/25/2025 7:46:44 PM.
This article is licensed under a Creative Commons Attribution-NonCommercial 3.0 Unported Licence.

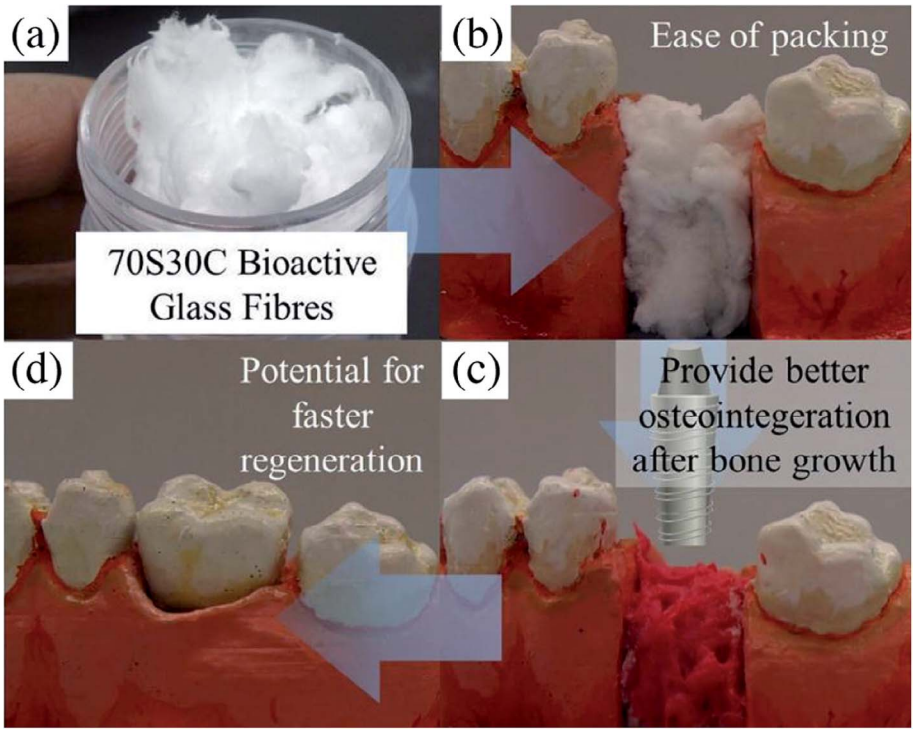

Fig. 19 (a) Photograph showing 70S30C cotton wool like bioactive glass fibers. (b) Demonstration of ease of packing in a tooth extraction socket. (c) Insertion of implant after bone regeneration. (d) Crown placement. Adapted from ref. 290. Copyright 2014, Elsevier.

glass fibers showed excellent flexibility resulting from the large aspect ratio and the entanglement between very long fibers.[290]

4.3 Chemical compositions

In addition to morphology, the chemical compositions of MBGs are also instrumental in determining their properties and it is one of the key aspects that determine the biological activities of glasses in a physiological environment. Thus, it is attractive to explore new applications of mesoporous glasses based on their composition and structure.[67] It has been reported that the sol–gel methods make it possible to study a wider spectrum of glass composition and mesoporous structures than the melt quenching method.[1] In general, the composition of the bioactive glasses can be easily adjusted thereby conferring specific properties to the materials which can be effective in fulfilling the demands of a vast variety of biomedical applications.[291,292] The sol–gel process significantly expands the range of chemical composition of bioactive glasses, including conditions and preparation protocols. Faure *et al.*[293] reported a sol–gel approach for the synthesis of the 45S5 glass by substituting HNO_3 by $C_6H_8O_7$. The use of $C_6H_8O_7$ as a catalyst for the sol–gel synthesis of 45S5 powder has been shown to significantly reduce the concentration (5 mM) of acidic solution which is required to catalyze the hydrolysis reactions of TEOS and TEP. It was demonstrated that the *in vitro* bioactivity level of the sol–gel powder was higher than that of the commercial Bioglass® which can help in speeding the process of bone growth formation by avoiding high pH or temperature conditions.[293] The improved bioactivity is associated with the enhanced porosity and the specific surface area of the sol–gel derived powders. Lopes *et al.*[294] demonstrated that the $C_6H_8O_7$ works as an effective molecular template formed by molecular network elevated from intermolecular forces (*e.g.* hydrogen bonding) resulting from chemical interactions between the COOH and hydroxyl groups (water, ethanol, P–OH, Si–OH).[294] The authors further ascertained that the $C_6H_8O_7$ assisted sol–gel route is an interesting and promising approach to modify the synthesis protocol to control phase segregation during drying and to achieve high structural homogeneity.[294] In another study, Thibault *et al.*,[295] prepared polymer/bioactive glass 45S5 composites comprising boronic acid (PBA) functionalized chitosan by a freeze-drying technique and demonstrated the potential of PBA to improve the bioactivity of the resulting composite. It was ascertained that chitosan–PBA samples exhibit interconnected porosity with pore size ranging from 32 to 476 μm. Moreover, it was revealed that sol–gel modified bioactive glass 45S5 containing PBA exhibit no toxicity for mouse Sertoli (TM4), human embryonic kidney 293 (Hek293) and human bone marrow/stroma (HS-5) cells, as compared with composites prepared using unfunctionalized chitosan.[295]

The hypothesis behind choosing the chemical compositions of glasses is that the bone comprised collagen fiber, bone cells and HA crystals, the implant material should be capable of forming the HA layer on the surface in the biological fluids.[296] Since their discovery, most of the research work being carried out on bioactive glasses is dealing with the compositions that form interfacial bonding with the tissue. The formation of the HA layer on the surface *in vitro* or *in vivo* is considered as an

Open Access Article. Published on 11 September 2020. Downloaded on 10/25/2025 7:46:44 PM.
This article is licensed under a Creative Commons Attribution-NonCommercial 3.0 Unported Licence.

indicator of the glass bioactivity.[297] The interaction of HA crystals with cellular processes leads to glass bonding with the surrounding tissues. The role of the bioactive glasses in bone tissue regeneration is associated with its proficiency to release the critical concentration of calcium and silicon ions at the rate required for cell proliferation and differentiation.[298] Calcium is an essential element of bioactive glasses which plays a pivotal role in inducing osteogenic differentiation of cells.[46] The controlled dissolution and the ion release rates along with the glass network structure are the fundamental criteria for designing novel glass compositions for specific applications. The durability can also be adjusted easily from almost inert to quickly dissolving glasses by simply changing the compositions. The wide range of future applications also rests upon adjusting the glass compositions containing specific inorganic ions that can have controlled effects on the cellular process. The release rate of the therapeutic ions, overall glass dissolution kinetics and on surface HA formation depends on the chemical durability of the glass in the target applications.

Recently, tremendous research interest has been shown in designing phosphate and borate-based glass compositions. Hench *et al.*,[296] explored phosphate-containing silicate glasses based on Na_2O–CaO–P_2O_5–SiO_2 compositions fulfilling the criteria of tissue bonding. CaO and P_2O_5 deliver essential constituents of HA ($Ca_5(PO_4)_3OH$), namely Ca^+ and PO_4^{3-} ions whereas Na_2O and SiO_2 consist of elements that are abundantly available in the human body. The higher ratio of CaO/P_2O_5 enables the ion release from the material surface when soaked in body fluid and forms the HCA layer very rapidly. This facilitates cell proliferation on the implant surface by sustaining the ion concentration.[296] Borate based glass composition is reported to form HA faster than silicate-based compositions.[299] Li *et al.*[93] demonstrated sol–gel derived Na_2O–CaO–SiO_2 glass compositions which shows bioactivity within far greater compositions than that of melt derived glasses. Since then various compositions of bioactive glasses were thoroughly examined.[94–96,98] Fluoride based bioactive silicate glasses were investigated for bone tissue regeneration and also regarded as a potential material for dental applications.[99,300] Numerous other oxides such as B_2O_3, Fe_2O_3, Al_2O_3, ZnO, TiO_2, BaO, Li_2O, CuO and CoO *etc.* have been included in Na_2O–CaO–P_2O_5–SiO_2 glass systems.[46,119,301–304] CaO can be replaced with MgO or CaF_2 and Na_2O can be replaced with K_2O without affecting the bone bonding. However, the dissolution rate of the glass can be affected. Furthermore, bioactive glasses were doped with several elements including Ag, Cu and gallium (Ga) to study their antimicrobial properties.[162,198,305] Ga doped bioactive glasses have been reported to be promising for wound healing applications.[305] The doping effect of the different elements on the cellular processes has been reviewed by several authors.[46,306,307] Li *et al.*[308] illustrated that the incorporation of Mg, Zn or Cu as a substitute for Ca^{2+} affects the glass bioactivity in a sequence of Cu < Mg < Zn. Ag-doped bioactive glasses demonstrate enhanced bioactivity because Ag^+ is highly mobile than Na^+ thereby it is convenient to exchange with H^+ ions.[309] Zn and Mg show almost the same effects and they can be useful in preventing bone resorption by activating the proliferation, osteoblasts differentiation and bone mineralization ability.[310] Zn exhibits anti-inflammatory properties and can be used in the fabrication of glass-based dental cement and polyakenoate orthopedics showing antimicrobial effects,[311] while Mg was found to be useful in promoting bone cell adhesion.[312]

4.4 Chemical and surface properties

The physical as well as chemical features of sol–gel derived bioactive glasses can be fine-tuned by altering or modifying their surface functional groups. The surface properties of biomaterials play an important role in enhancing their interaction with the surrounding tissues. The surface functionalization of sol–gel based materials is vital in view of their applications in biological fields owing to its advantages such as greater adsorption capacities for biomolecules or drug loading, enhanced inclination to supply these biomolecules to particular targets such as cells or tissues and enhancement in the overall biocompatibility.[7] For example; different functional groups can have an impact on the cell adhesion by simply altering the surface hydrophilicity or hydrophobicity.[313] The surface functional groups can also influence the protein absorption proficiency of the material and subsequently affects the cell adhesion.[314] The surface functionalization of bioactive glasses is a favorable approach to convert the present surface into a more desirable composition or architecture to create opportunities for the preparation of functional biomaterial that can be useful for biological applications.[315] Generally, the surface functionalization of bioactive glasses is intended for enhancing the biological response (bioactivity) as well as for improving the biocompatibility of glass particles with other phases.[316] The surface functionalization of bioactive glass can be carried out by physical approach (altering surface topography) or chemical/biochemical approaches (adsorption of molecules *via* atomic layer deposition (ALD), covalent grafting of biomolecules or drugs *etc.*).[317] By employing different functionalization strategies, the surface reactivity of bioactivity glass can be exploited easily to obtain newly customized functional characteristics such as antibacterial, anticancer and antioxidant properties of bioactive glasses.[318]

Among various strategies described in the literature, silanization is an efficient and widely applied method for covalent modification of bioactive glass surface.[319,320] The main purpose of silanization is to establish bonds within the interface between the inorganic constituents and organic biomolecules so as to enhance the bone tissue interaction. Silanization is also used to ameliorate the dispersion stability of inorganic particles in a diverse range of liquids and for anchoring the drug immobilization.[320] The reaction conditions such as reaction time, type of solvent, temperature, nature and concentration of alkoxysilanes should be carefully chosen in order to avoid the formation of a polymerized thick network of silane on the surface.[320] As a result, the chemical bonds are formed between alkoxysilane and the material surface which can be hydrolyzed under a suitable environment. The hydrolyzed silicon alkoxide contains Si–OH groups condensed with the hydroxyl groups existing on the surface of the material whereas the alkyl chain

Open Access Article. Published on 11 September 2020. Downloaded on 10/25/2025 7:46:44 PM.
This article is licensed under a Creative Commons Attribution-NonCommercial 3.0 Unported Licence.

having functional groups namely carboxyl, epoxy, amine, vinyl, chloro, thiol, cyanide or phenyl are harnessed for further functionalization.[320–322] The amino ($-NH_2$) groups are responsible for the electrostatic interactions and covalent bonding with negatively charged functional groups of various molecules such as DNA and protein.[320] The most frequently used silane for the surface functionalization and for introducing amino group on the bioactive glass surface is 3-aminopropyltriethoxysilane (APTES) which is also known as a protein coupling or protein binding agent.[320] Owing to the plenty of silanol present on the surface of bioactive glass, the surface functionalization using APTES can be achieved within the sol–gel synthesis of bioactive glasses under controlled conditions[323] or *via* adsorption through solution.[324,325] Verne *et al.*[324] reported an optimized procedure for surface functionalization of bioactive glasses in order to use the amino groups for binding proteins. Using *in vitro* test, it was demonstrated that the bioactivity of glass was unaffected when APTES was used as a surface modifying agent.[323,326] Moreover, the grafting of APTES has been achieved from various solvents such as toluene,[327,328] ethanol[324,329,330] and water.[326,331,332] Sometimes glutaraldehyde (GA) is also used with APTES for surface functionalization[331,333] while the silane molecules can be directly implemented during the sol–gel processing of bioactive glasses.[334] In another study, APTES was found useful in promoting the formation of the HCA layer without affecting the bioactivity of glasses.[335] Besides, APTES have been successfully utilized for the functionalization of sol–gel derived bioactive glass (58S) in order to improve its cytocompatibility.[87]

Zhang *et al.*,[336] developed functionalized MBGs which were subjected to the surface functionalization using APTES and triethoxysilylpropyl succinic anhydride (TESPSA). From *in vitro* studies, it was observed that the synthesized bioactive glasses significantly promoted the proliferation as well as osteogenic differentiation of rabbit bone marrow stromal cells. However, this effect was more pronounced in the bioactive glasses functionalized with APTES than with TESPSA. *In vivo* studies revealed that the bioactive glasses functionalized with APTES can facilitate a higher level of bone regeneration in comparison to unmodified and TESPSA functionalized bioactive glasses. It was mentioned that the presence of the amino groups on the bioactive glass surface is expected to play a crucial role in enhancing cell proliferation and differentiation.[320] The surface amino groups of bioactive glasses are less hydrophilic than carboxyl groups and the surfaces containing amino functional groups with balance hydrophilicity and hydrophobicity are beneficial for cell adhesion. Although bioactive glasses demonstrate favorable bioactivity and biodegradability, the relative brittleness and the lack of *in situ* mouldability limit their applications. Hence, polymer/bioactive glass composites have been prepared as biomaterials with improved properties.[337–340] Recently, bioactive glasses have been reinforced with polylactide (PLA) matrix to develop composites for bone tissue repairing.[341] In a similar study, APTES was used as a coupling agent for the surface functionalization of bioactive glasses thereby enhancing the interface between poly(L-lactide) (PLLA) and bioactive glass particles.[342] It was reported that the APTES functionalized bioactive glass particles are homogeneously dispersed in the polymeric phase without any agglomeration as compared with non-functionalized glass particles. Aina *et al.*[323] reported new formulations to develop APTES functionalized bioactive glass using maleic anhydride (MA) or *cis*-aconitic anhydride (CAA) in combination with cysteamine and 5-aminofluorescein as model molecules for stimulating the drug. Fig. 20 schematically represents the procedure for the synthesis of APTES and MA functionalized bioactive glass and models for cell binding and protein absorption.[320] In another study, it was described that the GA enables the control over release kinetics of proteins and sustain the native protein structure completely when used as a protein-binding agent.[333,343,344] In a similar investigation, it was stated that the surface functionalization of a bioactive glass substrate using APTES and GA was not effective enough to stimulate variations in the methemoglobin and 5-methylaminomethyl-uridine which form enzyme structure.[333,344] However, GA is reported to improve the stability of hemoglobin attachment and instigates polymerization on the surface of Ag-doped bioactive glasses.[345]

The surface functionalization of bioactive glasses can also be performed by immobilizing various biological species namely proteins and cells on their surfaces. For example; surface functionalization using proteins enhances the bone integration of bioactive glasses. The biomolecules can be bonded to the bioactive glass surface by either electrostatic and van der Waals forces (weak physical interaction) or by covalent or ionic bonding.[320] The binding of biomolecules can be affected by various physicochemical characteristics such as chemical composition, pH or dissolution behavior, microstructure, crystallization degree, hydrophobicity, surface reactivity, surface roughness, zeta potential and particle size *etc.*, of bioactive glasses.[346] Furthermore, the grafting of biomolecules onto the surface of bioactive glasses was studied by various researchers to improve their bioactivity, cell adhesion and differentiation for bone regeneration application. For this purpose, collagen,[332] lysine,[347] ipriflavone,[327] soybean peroxide,[348] bovine serum albumin,[327,349,350] α-amylase,[327,349] BMPs,[324,351] alkaline phosphate (ALP)[325,329] and commercially available mixture of enamel matrix proteins (Emdogain®)[352] have been considered. Laminin was adsorbed on the APTES surface-functionalized bioactive glass foams and its sustainable and controlled release from modified scaffolds was achieved over a 30 day period making it beneficial for tissue formation.[353] Furthermore, antibiotics and anti-inflammatory agents such as gentamicin,[354,355] tetracycline[356] and ibuprofen[357] have been loaded into MBGs forming biomaterials for localized drug delivery applications. Surface functionalized bioactive glasses have also been reported for localized cancer treatment and for this purpose, various biomolecules and drugs have been proposed such as 5-aminofluorescein for doxorubicin,[334] doxorubicin and cisplatin,[358] dexamethasone,[350] alendronate,[359] curcumin[360] and gallic acid.[361,362] Another important approach for surface functionalization of bioactive glasses is the induction of apatite formation. For this purpose, bioactive glass has been soaked in different solutions to facilitate the CaP layer formation on its surface.[363] Studies have demonstrated that the functionalization of the

Open Access Article. Published on 11 September 2020. Downloaded on 10/25/2025 7:46:44 PM.
This article is licensed under a Creative Commons Attribution-NonCommercial 3.0 Unported Licence.

bioactive glass surface by bio-mineralization of the CaP layer followed by immobilization of particular proteins can improve cell adhesion, proliferation and differentiation.[364] Thus, all the aforementioned studies demonstrate that various strategies can be employed for exploiting the surface reactivity of bioactive glasses for their wide range of biomedical applications.

4.5 Biological properties and biodegradation

Biodegradability is among the most significant characteristics of sol–gel derived bioactive glasses in view of their bone-bonding ability. Generally, biodegradable materials manifest higher reactivity which is closely associated with the formation of the HCA layer.[365] Biodegradation is the key when bioactive glasses are utilized for the preparation of bone tissue scaffolds. Nevertheless, high degradation rates have a negative impact on cell attachment and growth and therefore prevent the progress of new bone formation.[366] Thus, it has been suggested that the surface functionalization of bioactive glasses using organic functional groups (amino or carboxylic groups) can partially decrease the high degradation rates while maintaining the bioactivity. For a variety of applications, materials that degrade easily are best suited than persistent implant materials because degradable materials are resorbable into the body and can be exchanged with regenerated tissues.[367] Nevertheless, managing the degradation rate is a complex process; therefore, it is necessary to understand the degradation mechanism and the determinants that affect the degradation rate of sol–gel based bioactive glasses.[1] Moreover, the dissolution of glass in contact with the body fluids and the release of Ca and P ions are crucial to the bio-mineralization of glasses. The ionic dissolution products from bioactive glasses are well known for stimulating angiogenesis, osteogenesis and vascularization.[368] Thus, the dissolution behavior plays a pivotal role in the bioactivity of the sol–gel glasses.

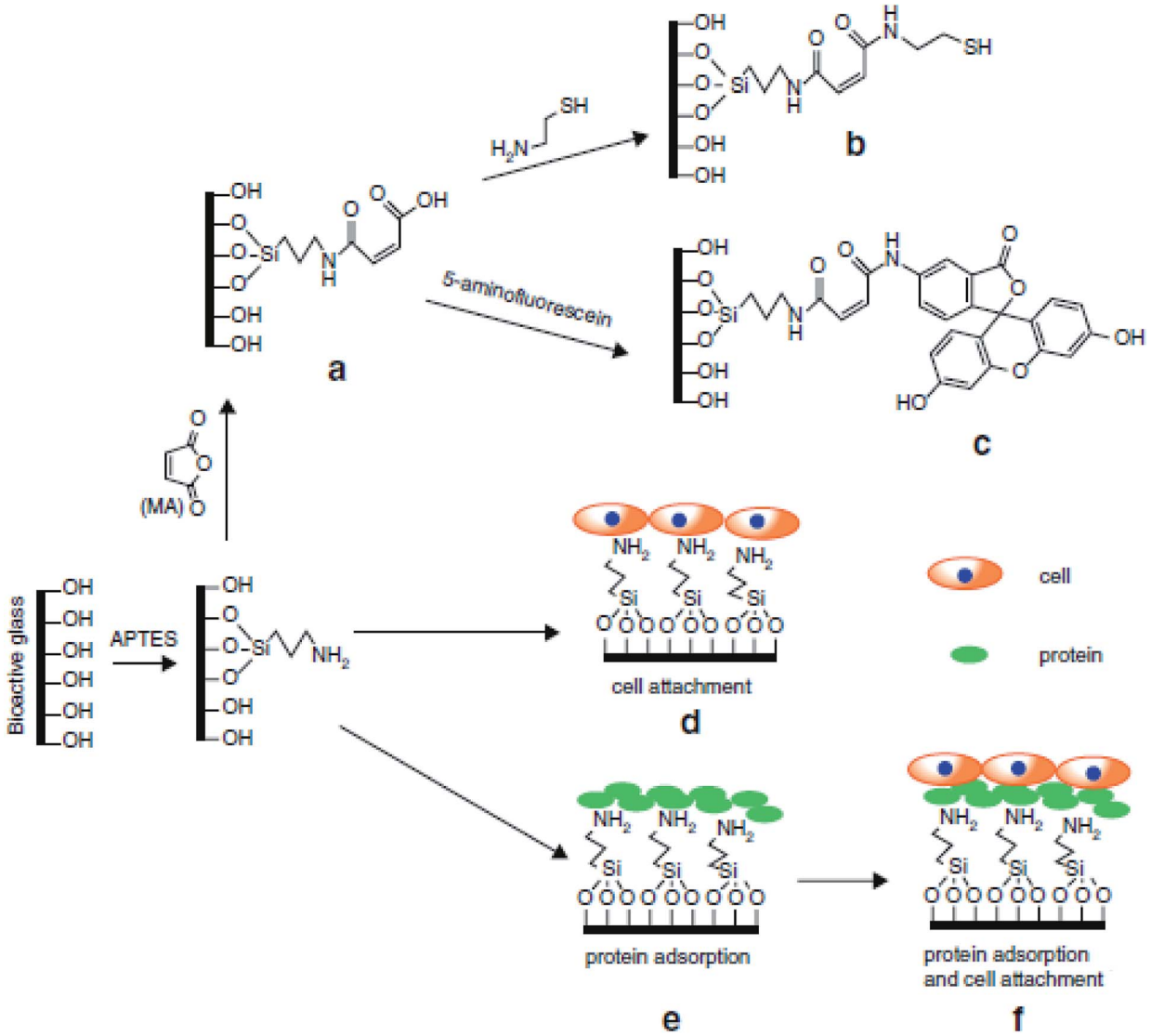

Fig. 20 (a) Procedure for preparation of APTES and MA functionalized bioactive glass. (b and c) Preparation of APTES and MA functionalized bioactive glass with cysteamine and 5-aminofluorescein conjugate. (d–f) Models for cell binding and protein absorption. Adapted from ref. 320. Copyright 2017, Springer.

Open Access Article. Published on 11 September 2020. Downloaded on 10/25/2025 7:46:44 PM.
This article is licensed under a Creative Commons Attribution-NonCommercial 3.0 Unported Licence.

Recent research has remained focused on the molecular interaction of bioactive glass-based ionic dissolution products with their physiological surroundings so as to understand such processes to formulate smart bioactive glasses with customized properties specifically for tissue engineering. Fig. 21 gives an outline of biological responses towards bioactive glass-based ionic dissolution products. In the context of tissue engineering, numerous literature evidence indicates the importance of ionic dissolution products in understanding the behavior of sol–gel derived bioactive glasses *in vivo* and *in vitro*. A large number of trace elements including Sr, Cu, Zn, Co *etc.*, present in a human body are well renowned for their growth-promoting effects in bone metabolism and play a major role in angiogenesis, growth and bone tissue mineralization.[46] Therefore, novel research avenues are being investigated for enhancing the glass bioactivity by introducing these therapeutic ions in different bioactive glasses resulting in the modification of their dissolution behavior and improved biological performance.[46] Furthermore, innovative methodologies have been suggested for advancing the fields of bioactive glass scaffolds by inducting active metal ions into the glass network for utilizing the therapeutic effects of such ions and to ameliorate the biological functioning of the materials as regards to the response of the specific host.[46] As stated earlier, Ca and P are the main component of the inorganic phase of the human bone, these ions play an integral part in bone formation and resorption. However, one should know the specific ECM concentration of these ions and their interaction mechanism with bone cells and exhilarating effect on bone formation.[46] This information can be useful in designing advanced scaffolds with controlled biological properties in a suitable physiological condition with tunable ion release kinetics.[46]

Bioactive glasses require specific dissolution rates in order to tune their *in vitro* and *in vivo* performances. The dissolution testing is generally performed by soaking the bioactive glasses in SBF, tris buffer solution (TBS), phosphate-buffered saline (PBS) and cell culture media.[369–371] If the dissolution rate is very slow, the ionic concentrations are insufficient to promote cell proliferation and differentiation. On the other hand, if the rate of dissolution is too quick, the ionic concentration might be beyond the effective level.[110,372] Moreover, the ionic concentration and the pH of SBF are the same as that of human blood plasma (HBP).[373] Therefore, SBF is the most common solution used for soaking bioactive glasses under static conditions. Besides, the soaking of bioactive glasses in SBF is a very simple, cost-effective and rapid method of assessing the probable bioactivity. In SBF, an *in vitro* test could be performed in a few minutes after immersion. Hence, this procedure has been widely adopted as a basis for assessing biomaterial for bone tissue regeneration. The first step in the bioactivity mechanism

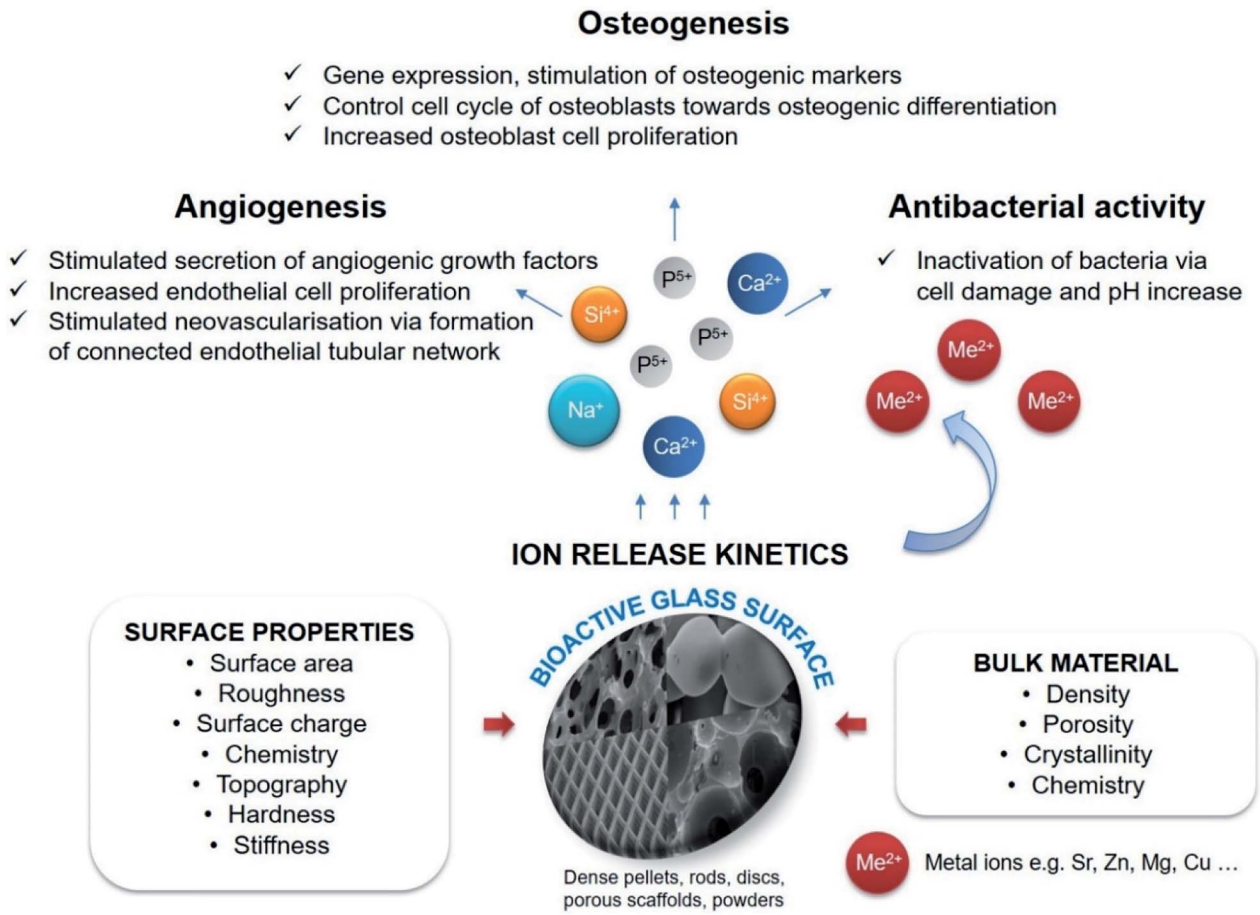

Fig. 21 Schematic outline of biological response to bioactive glass based ionic dissolution products.

Open Access Article. Published on 11 September 2020. Downloaded on 10/25/2025 7:46:44 PM.
This article is licensed under a Creative Commons Attribution-NonCommercial 3.0 Unported Licence.

is the resorption in which the bioactive material undergoes a rapid chemical reaction when in contact with physiological fluids. When soaked in SBF, the bioactive glasses exchange ions with SBF and form silanol groups on the surface thereby nucleating the HA layer.[374] The formation of the HA layer takes place *via* two steps namely (i) formation of dicalcium phosphate ($CaHPO_4$) by combining calcium and phosphorus ions in SBF and (ii) the conversion of $CaHPO_4$ into HA or TCP ($Ca_3(PO_4)_2$) *via* sequential reaction.[374] As reported, the higher concentrations of silanol groups result in a quicker dissolution or bioactive response and this valuable information can be useful in designing porous sol–gel glasses having a high surface area and high silanol concentrations.[93,375] It was shown that specific heat processing and relative proportions of CaO to SiO_2 are the decisive factors to obtain these porous glasses with prosperous bioactive behavior.[376] To date, several authors have reported the impromptu formation of the HA layer on bioactive glass surfaces comprising $CaO–SiO_2–P_2O_5$ ternary systems when contacted with the biological fluids.[377–379] The real developments came in regards to bioactivity kinetics with the developments of MBGs because of the high surface area and high mesoporosity, both features facilitate enhanced reaction degree between the glass and the biological fluids.[380] Fig. 22 compares the formation of a new apatite layer on the surface of the traditional sol–gel glass (left) and MBG (right) when in contact with the biological fluids.[381] Considering that both Ca and P are the major components of the apatite layer and the inorganic phase of human bone, it is accountable for profound bonding between bioactive glass and human bone.[118,381]

The chemical reactions occurring on the glass surface are derived from leaching, dissolution and precipitation.[110] Based on such interfacial reactions, the cellular reactions give rise to the development of a chemical bond between living tissues and the bioactive glass.[131] The first prompt reaction transpiring on the glass surface after implantation *in vivo* or soaking in SBF is the cation replacement of Ca^{2+}, Na^+ or K^+ with H^+ or H_3O^+ from the solution.[382] Simultaneously, the solution pH increases. The leaching reaction generates an alkaline microenvironment wherein the solution alkalinity is emerged due to breakage of –Si–O–Si– bonds mostly by hydroxyl ions. The dissolution takes place at the glass surface and leads to the establishment of silanol (Si–OH) groups at the interface between glass and the solution. The condensation and re-polymerization of hydrated silica groups occur with the silanol group resulting in the formation of SiO_2 rich layer (silica gel) on the surface. Such precipitations are promoted by the migration of Ca^{2+} and PO_4^{3-} ions to the surface within the SiO_2 rich layer to create an amorphous CaP layer at the top of the SiO_2 rich layer.[298] The amorphous CaP layer expands due to the inclusion of soluble CaP from the supersaturated solution.[131] Fig. 23 demonstrates different stages of surface reactions along with the generation of Si-rich and CaP layer at the bioactive glass surface.[382] The

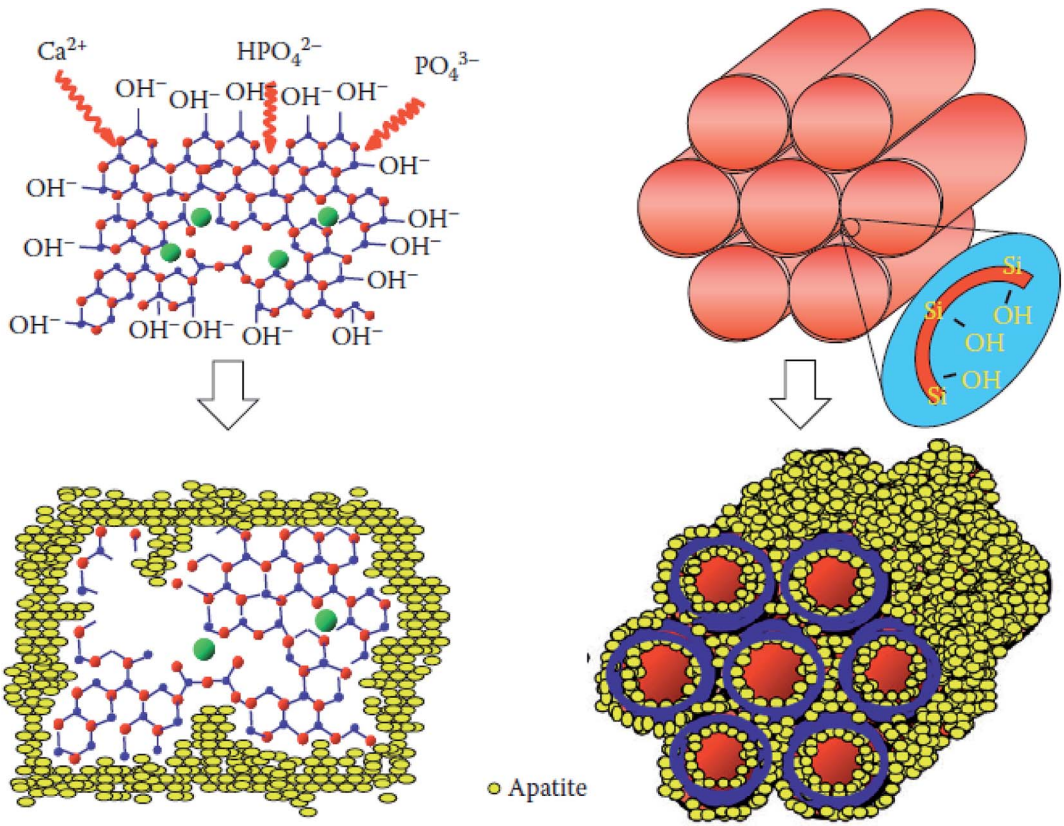

Fig. 22 Demonstration of the apatite layer formation on the surface of traditional sol–gel glass (left) and MBG (right) after contacting the biological fluids. Adapted from ref. 381. Copyright 2012, CRC Press.

Open Access Article. Published on 11 September 2020. Downloaded on 10/25/2025 7:46:44 PM.
This article is licensed under a Creative Commons Attribution-NonCommercial 3.0 Unported Licence.

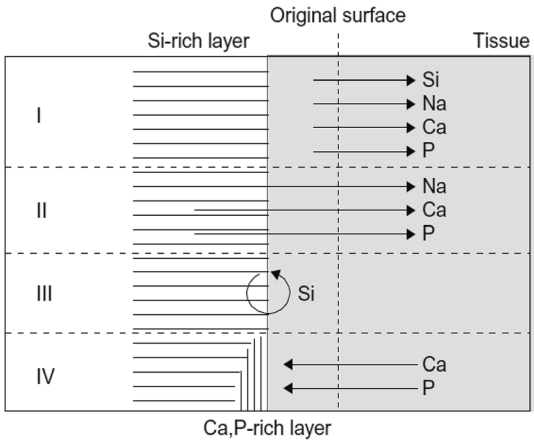

Fig. 23 Different stages of surface reactions and the development of Si-rich and CaP layer at the bioactive glass surface. (I) Initially, a glass layer with few micron thickness is dissolved. (II) Later, Na, Ca, P and Si are leached out from the glass surface. (III) Si-rich layer is developed *via* repolymerization. (IV) Ca and P from the solution are partly leached out from the glass precipitate on the Si-rich layer. Reproduced with permission from ref. 382. Copyright 2018, Elsevier.

thickness of the SiO_2 rich layer increases as a result of diffusion-controlled alkali ion interchange whereas the final thickness depends on its composition. The crystallization of the amorphous CaP layer takes place by the inclusion of OH^-, CO_3^{2-} or F^- anions from the solution to form the HCA or apatite layer substituted by fluoride ions (F-HCA) probably through similar reactions which facilitates the crystallization of Ca deficient apatite layer.[382] As the apatite crystals composition is analogous with the inorganic mineral phase of bone, such reaction steps are most often utilized for characterizing biomaterials which form interfacial tissue bond. In an ideal case, the reaction proceeds until the bioactive glasses are completely substituted by new tissue.[298]

There are several ways of investigating the dissolution rate of biomaterials and one of the simplest methods is the measurement of weight loss. The dissolution rate of biomaterials can also be evaluated by quantifying the released ions concentration and the pH shift within the solution. The pH variation is greatly reliant on the capability of the solution to buffer or the local environment *in vivo*.[370,371] As mentioned before, the dissolution reaction takes place at the interface between the surface of the bioactive glasses and the solution. Hence, the specific surface area is a critical parameter that can influence the degradation rate.[383] The high surface area is responsible for the high dissolution rate in sol–gel synthesized mesoporous glasses in comparison with the melt derived glasses which are relatively dense.[370] Furthermore, with an increase in pore size, the solution circulation within the pores becomes easy causing an enhanced reactivity.[383] The sol–gel derived glasses frequently undergo thermal treatment to eliminate the organic phase or to improve the stability and as a consequence, the porosity and the crystallinity of glass get affected.[114] Cacciotti *et al.*[384] evaluated the dissolution rate of sol–gel derived bioactive glasses heat-treated at different temperatures. The crystalline phases were observed when the glasses were heated at 1100 °C and very slow dissolution behavior was observed as compared with the glasses heated at 700 °C. These findings demonstrated a low degree of glass crystallinity when heated at low temperatures. Besides, the dissolution behavior of sol–gel based bioactive glasses is not only affected by the aforementioned conditions but also depends on the surrounding conditions namely solution temperature, pH and composition.[1] For example; the solution temperature substantially influences the degradation behavior of sol–gel synthesized silica glasses.[385] A similar trend was also observed in phosphate-based glass systems.[386] The solution pH also has an impact on the dissolution behavior of sol–gel derived glasses. For example; for silica glasses, the dissolution rate was enhanced with an increment in pH. This is because the Si–O–Si bonds are destroyed due to the nucleophilic attack of OH^- in water containing medium.[387] The dissolution rate is generally increased with an increase in pH from 2 to 8.5 because when pH > 8.5, ions which are more soluble ($SiO(OH)^{3-}$) are being developed.[388]

The composition is also an equally important factor that helps in determining the dissolution rate of the glass. For example; Ma *et al.*[60] reported that with partial substitution of MgO for CaO in the composition, the glass degradation rate decreases with the delay in HCA layer formation, which was ascribed to the effect of ionic field strength and diverse bonding configurations of glass. In another study, very rapid dissolution rates were observed for glasses without CaO in SBF.[389] However, the dissolution rate decreases as CaO content increases and P_2O_5 content decreases attributing to the soluble glass species such as Na^+, Ca^{2+} and HPO_4^{2-}. In TBS there are no Ca or P sources; therefore, the apatite layer is generated only by releasing the Ca and P ions from the glasses. On the contrary, in SBF or PBS, the generation of the HCA layer is expedited and further, dissolution is restrained as the number of Ca and P ions are accommodated in these solutions.[371] In addition, the biomolecules present in the solution also affect the dissolution of bioactive glasses. For example; Sepulveda *et al.*[370] performed a comparative assessment on the dissolution behavior of bioactive glasses in the SBF solution and the culture medium. From ICP mass spectroscopy studies, it was observed that the dissolution rate of bioactive glasses was faster in SBF solution than in culture medium due to positively charged serum proteins which can be adsorbed on the surface of the material and suppress the glass dissolution. Thus, the above discussion gives a consensus view that the biocompatibility of biomaterials in the physiological environment upon implantation should be investigated. However, the factor pertaining to the degradation of biomaterial itself is one of the aspects along with the equally important factors such as the influence of materials on its *in vivo* environment and bioactivity needs to be considered.[1]

4.6 Mechanical properties

Sol–gel derived bioactive glasses are often characterized by lower mechanical resistance to dense glasses of the same compositions due to their inherent highly porous structures.[1] For example; the flexural strength of TMOS based silica aerogels with 95% porosity was reported to be 0.02 MPa[390] which is about

Open Access Article. Published on 11 September 2020. Downloaded on 10/25/2025 7:46:44 PM.
This article is licensed under a Creative Commons Attribution-NonCommercial 3.0 Unported Licence.

0.0002% of the flexural strength of dense silica material.[391] The low mechanical strength is the key issue that is specifically serious when sol–gel derived glasses are processed as hierarchical porous scaffolds with multiscale porosity.[392] It is common knowledge that bone exhibit attractive mechanical properties due to its hierarchical structure and the sol–gel glass-ceramics exhibits lower toughness in comparison with the natural load-bearing bones. Therefore, it is essential to formulate new strategies for improving the mechanical behavior of sol–gel glasses to be used as coatings or in a bulk state for bone grafting. The bioactive sol–gel glass compositions need to be modified to yield improved mechanical properties. Studies have shown that the mechanical properties of sol–gel glasses can be substantially altered by varying few processing parameters such as the type of precursor, molar ratio of water to the precursor, pH and doping agents *etc.*,.[1] The type of precursors used for the sol–gel synthesis influences the sol–gel reactions and ultimately affects the mechanical properties of the final material. For example; it has been reported that TEOS and TMOS derived silica aerogels with the same porosity of about 50% exhibited different mechanical strength.[393] Hence, irrespective of the relatively higher strength or modulus, the brittleness issue limits the wider applications of sol–gel materials.

The doping agents or additives used during the sol–gel synthesis are also accountable for the mechanical properties of the final material. For example; substituting Si or O in the silica network with other elements can enhance the mechanical properties of sol–gel derived silica glasses.[1] For example; the effect of different additives such as MgO, TiO_2 or CaF_2 on the mechanical properties of sol–gel silica glasses was investigated by substituting Mg^{2+} and Ti^{4+} for Ca^{2+} or F^- for O^{2-}.[394] The ionic strength of Mg^{2+} is greater than the ionic strength of Ca^{2+} ions. Thus, the substitution of Mg^{2+} for Ca^{2+} strengthens the glass network owing to reduced bond lengths.[104] Likewise, the substitution of Ti^{4+} for Ca^{2+} ions enhances the glass strength by connecting with more O^{2-} ions (Ti^{4+} ions can connect with four O^{2-}).[395] Consequently, Ti^{4+} and Mg^{2+} substituted glasses demonstrated improved hardness, bending strength and fracture toughness as compared with Ti^{4+} and Mg^{2+} free glasses.[394] On the other hand, as a result of substituting CaO by CaF_2, the F^- ions disrupted the glass network and increases the crystallization tendency. Hence, CaF_2 incorporated sol–gel glasses do not possess advantageous mechanical properties.[1] Improved mechanical properties were reported by the incorporation of alumina, barium and calcium in the glass composition.[396–398] Barium ions exhibit a larger ionic radius than silicon ions which allows the formation of a denser network in the glass structure. Barium addition increases the flexural strength of sol–gel glasses.[397] The silicon and aluminum acted as a network forming elements in the sol–gel synthesis of bioactive glasses and improves compressive strength and Young's modulus respectively.[396,398] The mechanical resistances were decreased when silicon content was decreased.[397] Yang *et al.*[399] incorporated B_2O_3 in $CaO–SiO_2–P_2O_5$ bioactive glasses to improve the compressive and flexural strength of porous glass-ceramics. Ben Arfa *et al.*[400] reported mechanical properties of Cu^{2+} and La^{3+} doped silica sol–gel glass scaffolds with the composition 67% SiO_2–24% CaO–5% Na_2O–4% P_2O_5. The compressive strength values were reported for the sintered scaffolds of varied pore sizes (300, 400 and 500 μm). A small enhancement (7–18%) in the compressive strength of La^{3+} doped glass was observed as compared with undoped glass. On the other hand, considerably higher enhancement in the compressive strength up to 221% was noticed with the addition of Cu^{2+} ions as compared with the undoped silica glass. The high values of compressive strength for Cu^{2+} doped glasses as compared with La^{3+} doped glass is ascribed to their different ionic radius. The small ionic radius and low valence of Cu^{2+} in comparison to that of La^{3+} confer higher thermal diffusivity post sintering making Cu^{2+} serve as an efficacious sintering assistant resulting in enhanced densification and mechanical properties.[400] The maximum compressive strength value being reported is ~14 MPa which is around the upper limit registered for human cancellous bone (2–12 MPa).[401] The lower value of compressive strength was noted for the scaffolds with the largest pore size (500 μm) and the largest value of compressive strength was noted for the scaffolds with the smallest pore size (300 μm). In another investigation, an enhanced bulk, shear and Young's modulus were observed with increased CaO/P_2O_5 molar ratio in $SiO_2–CaO–Na_2O–P_2O_5$ glasses.[402]

The mechanical performance of sol–gel based glasses can also be improved by decreasing the pore size during the sintering process.[403] Nevertheless, there are two limitations, (i) high-temperature sintering can result in vanishing of mesopores due to densification thereby making material unsuited for drug delivery applications (ii) if the biomolecules are included into the material before sintering, then the temperature needs to be optimized at a certain level to preserve biological molecules from degradation and to prevent uncontrollable crystallization process.[1,233] The synthesis method also affects the mechanical properties. For example; sol–gel synthesis of bioactive glass foam delivers an enhanced porosity but a low compressive strength.[404] A maximum compressive strength exceeding 5 MPa was achieved recently for sol–gel glass foams by maintaining the interconnected porous network required for vascularized bone ingrowth.[403] This was achieved by optimizing the sintering process of the sol–gel foam. However, small changes in compressive strength were noticed after immersion of sol–gel glasses in SBF for several days. Jones *et al.*[405] noted an increase in the compressive strength of 70S30C sol–gel derived glasses with an increase in the sintering temperature *i.e.* the compressive strength of 0.36, 0.51, 2.26 and 2.25 MPa were obtained at sintering temperature of 600, 700, 800 and 1000 °C. The compressive strength of 2.26 MPa was obtained for the scaffolds which ascribed to the decrement in the textural porosity and thereby increasing the density of the macropore wall at the sintering temperature of 800 °C. With the increase in sintering temperature to 1000 °C, the compressive strength was found to be constant although the textural porosity was disappeared. This was attributed to the changes in the glass structure as the crystallization onset temperature was increased.[405]

Vallet Regi *et al.*[406] investigated the mechanical properties of glass-ceramics prepared from sol–gel glasses with

Open Access Article. Published on 11 September 2020. Downloaded on 10/25/2025 7:46:44 PM.
This article is licensed under a Creative Commons Attribution-NonCommercial 3.0 Unported Licence.

a composition of 55 mol% SiO_2 : 45 mol% CaO (55S45C). The mechanical properties of 55S45C were compared with the glass-ceramic containing the same amount of SiO_2 but with 4% content of P_2O_5 (55S41C4P). In addition, the samples were examined in order to ascertain the influence of the sintering process on the mechanical properties. It was observed that the flexural strength (*S*) and the Weibull (*m*) coefficient values are higher for the phosphorous free glasses. A significantly high value of *S* was observed for the glasses sintered at 1100 °C (55S45C-1100). Furthermore, the *S* values were increased with an increase in the temperature although the increase was not significant from the statistical point of view. However, in 55S41C4P glasses, a two-fold increase in *S* values with sintering temperature was observed even though these *S* values were lower than that obtained for 55S45C glasses. Li *et al.*[407] evaluated the mechanical properties of macroporous sol–gel bioactive glasses with the compositions of 58 wt% SiO_2–33 wt% CaO–9 wt% P_2O_5. These sol–gel glasses demonstrated compressive strengths higher than the human cancellous bone.[401] The high values of compressive strengths are beneficial in withstanding physiological stresses and minimizing stress shielding in the surrounding host bone.[408]

Sol–gel glasses together with organic polymers can enhance the mechanical strength and toughness of the resulting hybrid.[409,410] The integration of silica IPNs within the polymer matrix at the molecular level is anticipated to improve the mechanical properties of bioactive glasses. Recently, the mechanical properties of porous scaffolds based on bioactive silica–poly(γ-glutamic acid) (PGA) hybrids have been studied.[411] The authors hypothesized that by increasing the covalent coupling, the inherent mechanical properties such as compressive strength and toughness of hybrids can be improved. The elongation to failure was increased from 4.2% for the sol–gel glass to 27.5% for the hybrid monoliths. This indicates an improvement in the strain to failure and hence enhanced toughness. However, the compressive strength of the hybrids was low as compared to the sol–gel glass and to that of cortical bone.[412] Nevertheless, in the context of increased toughness, elongation and extended elastic behavior are highly promising. The elastic modulus, compressive strength and elongation to failure were also reported for the hybrids in response to increased covalent coupling. The lowest coupling showed the minimum compressive strength and elongation to failure. Further increasing the covalent coupling increases the compressive strength, elastic modulus and elongation to failure.[411] In another work, Li *et al.*[413] investigated the mechanical properties of PEG/SiO_2–CaO hybrids. The hybrids were prepared with IPNs of silica and PEG of two different molecular weights (PEG300 and PEG600) *via* the formation of Si–O–Si bonds. It was observed that the elongation to failure was greatly increased from 4.2% for sintered sol–gel glass monoliths (70S30C, 800 °C) to 35% for the hybrids. It was also noted that the mechanical properties were enhanced with an increase in inorganic ratio. Moreover, Young's modulus and compressive strength are found highest for the 50 : 50 compositions of the hybrids. The overall trend observed was 50 : 50 > 60 : 40 > 70 : 30 for hybrids containing both PEG300 and PEG600. Another aspect is that Young's modulus and compressive strength are greater for PEG600 hybrid as compared to PEG300 hybrid with the same composition. The PEG600 hybrids with 50 : 50 compositions were found to exhibit the best mechanical properties among other compositions tested. In another investigation, Bossard *et al.*[414] studied the mechanical properties of hybrids comprising PCL and SiO_2–CaO bioactive glasses. Adding PCL effectually introduced toughness to sol–gel glasses. However, the hybrids showed low stiffness as evident from their elastic modulus (0.49 ± 0.03 MPa) and yield strength of 0.036 ± 0.003 MPa. These values are significantly lower than that of trabecular bone with a similar porosity.[415,416] The low stiffness of the scaffolds can be assigned to the highly flexible PCL in comparison with other bio-resorbable polymers[417,418] and due to weak interaction between organic and inorganic phases.[62]

Sol–gel hybrids based on silica IPN and biodegradable polymeric materials can result in the combination of properties such as biological activities of glasses and the toughness of the polymer matrix. Recently, Valliant *et al.*[369] studied the mechanical properties of silica/γPGA sol–gel hybrids. Ca was incorporated into PGA by chelation while the Ca salt form of PGA (γCaPGA) was synthesized and used as calcium source as well as the biodegradable toughening component of the hybrids. The compressive strength greater than 300 MPa and the strain to failure of >26% was observed for the silica/PGA hybrids which is a considerable improvement as compared with the sol–gel glasses which were pretty brittle with the strain to failure of about 4% and the compressive strength of 66 MPa. It has been suggested that the incorporation of γPGA into the sol–gel process resulted in the elimination of brittleness of the resulting glasses. For the hybrids synthesized with γCaPGA, the maximum compressive strength was observed to be 540 MPa which is far greater than the compressive strength of cortical bone.[419] Young's modulus value of the same hybrid was found to be 1.9 GPa which is far lower than Young's modulus of cortical bone.[420] Chung *et al.*[421] reported mechanical properties of star-shaped methacrylate-based polymer–SiO_2 hybrids exhibiting the modulus of toughness 9.6 fold greater and Young's modulus 4.5 fold lower than the sol–gel based bioactive glasses. The main aim of this study was to ascertain the effect of polymer architecture on mechanical properties and its influence on bone cell attachment. Thus, all the aforementioned studies demonstrate the mechanical integrity of sol–gel based bioactive glasses as a potential biomaterial for bone tissue regeneration.

5. Sol–gel derived porous glasses for bone tissue regeneration

Tissue engineering has aroused tremendous interest as a prospective research field for repairing and regenerating tissues and organs which are damaged or lost due to trauma, injury or disease.[119] The main purpose of tissue engineering and regeneration of medicine is to regrow unhealthy or impaired tissue using a combination of cells, bioactive agents and biodegradable scaffolds.[380] The most common approach in

Open Access Article. Published on 11 September 2020. Downloaded on 10/25/2025 7:46:44 PM.
This article is licensed under a Creative Commons Attribution-NonCommercial 3.0 Unported Licence.

tissue engineering is to use the biomaterials based scaffold with a specific architecture which can serve as a provisional structure for cells and leads to their proliferation and differentiation into an appropriate tissue or organ.[119] Along with the cells, biomolecules such as growth factors can also be included in the scaffold to regulate the cellular functioning during tissue or organ regeneration.[422,423] Dramatic growth in the tissue engineering fields has been witnessed in the past two decades and this became possible only due to innovative design and synthesis of biomaterials and fabrication of scaffolds.[119] A scaffold is an essential constituent in tissue engineering for bone regeneration as it works as a template for cell interactions and the establishment of ECM of bone providing structural support to the newly formed tissue.[424] The scaffold is utilized to control growth factor and cell delivery in addition to providing the structural template to load the tissue lesion.[425] Preferably, the scaffold should assist in cell infiltration, cell attachment, matrix deposition and should be consists of osteoconductive mediums such as bone protein and HA providing load-bearing and initiating osteogenesis. Furthermore, the scaffolds created using biomaterials are formulated to meet the rigorous requirements which are imperative or desired for optimum tissue formation.[426] The scaffold architecture is also essential in furnishing the cells with an optimized microenvironment to develop new tissue and to grant flow or dissemination of nutrients within the cells and the surroundings.[426]

Bioactive glasses are one of the subsets of biomaterials that have a profound influence on tissue engineering especially for hard and soft tissue regeneration because they fit perfectly into this land space as materials for producing functional 3D scaffolds. Bone tissue engineering is among the most promising medical applications of bioactive glass and glass-ceramics due to their excellent osteoconductive and angiogenic properties, mechanical strength and good degradation rates.[427] By virtue of these properties, both bioactive glasses and glass-ceramics have been used in bone tissue regeneration applications over the past few decades.[428–430] Always, the spotlight is on the development of new bioactive glasses and converting them into scaffolds with necessary shape and architecture.[119] The tissue regeneration ability of bioactive glasses can be assessed based on their properties namely osteogenesis, osteoconductivity and osteoinductivity.[431] The osteogenic potential of bioactive glasses is evaluated on the basis of cells such as mesenchymal stem cells (MSCs), osteoblasts and osteocytes involved in bone formation. The osteoconductivity is the process where scaffolds or matrix excites growth of the bone cells on its surface and osteoinductive capability can be referred as the excitation of MSCs to distinguish preosteoblast, thus beginning the bone-constructing process.[431] Also, for bone tissue engineering, large interrelated pores and high porosity percentages are found imperative for attaching and growing bone-forming cells and further ingrowth of vascularized tissue.[432] The surface nanoporosity was also found to foster adhesion of cells to biomaterials[433] and bone ingrowth in bioactive glass scaffolds.[434] The most important requirements of fabricating scaffolds for bone tissue engineering that can be capable of inciting the tissue growth are;[62,96,432,435–437]

(i) Biocompatibility: the scaffold has to be biocompatible, bioactive and must assist in the attachment, proliferation and cell differentiation *in vivo* and must not deliver any toxic by-product or persuade any harmful inflammatory reactions.

(ii) Osteogenesis: the scaffold should have the potential to bond with the host bone (osteoconduction) as well as must prevent the encapsulation of fibrous tissue. The scaffold must recruit cells into the implantation site which can be further differentiated to create new bone.

(iii) Biodegradability: the scaffold needs to be degraded at the same rate at which the new tissue is formed at the implant site and ultimately must be remodeled by osteoblast action.

(iv) Mechanical strength: the mechanical strength of scaffolds should be equal to that of bone tissue to be replaced. The scaffold meant for regeneration should provide support at the time of degradation and tissue regeneration.

(v) Porous microstructure: an ideal scaffold should have high porosity (>80%) with interrelated pores. A hierarchical porosity with a minimum diameter of 100 μm is the requisites for cell penetration, tissue ingrowth and neovascularization.

(vi) Fabrication: the scaffold should be easily produced into irregular shapes that can mimic the bone defects of an individual patient.

(vii) Commercialization: the fabricated scaffold should possess the commercialization potential. The sterilization should be carried out by following the international norms and regulations for their use in biomedical devices.

Generally, the scaffolds for tissue engineering are fabricated using both synthetic and natural polymers which are biodegradable.[438,439] Biodegradable scaffolds facilitate primary structure and stability for forming a tissue but degrade as the tissue is formed. This provides a base for the deposition of matrix and tissue growth.[440,441] However, the main hurdle in designing scaffolds for tissue engineering is that the majority of the materials used for this purpose are usually bio-inert and the degradable materials are often mechanically weak. Therefore, the preparation of composites containing biodegradable polymer systems and the bioactive glass becomes a feasible alternative to accomplish the need for bioactivity, degradability and mechanical properties.[432] For instance; Bossard *et al.*[414] developed scaffolds from PCL/bioactive glass hybrids for bone tissue regeneration. The scaffolds obtained from PCL/SiO_2–CaO bioactive glass hybrids were highly flexible indicating that PCL has effectively introduced the toughness. The apatite formation was observed over 24 hours of soaking in SBF and the entire hybrid was changed steadily into bone-like minerals. The *in vivo* study confirmed the bioactivity, biodegradability and an appropriate degradation rate of the hybrid. Furthermore, efforts have also been undertaken to integrate biodegradable synthetic polymers in a biocompatible inorganic phase, for example, most frequently HA and TCP.[442,443] Chen *et al.*[444] studied the effect of Ca in the CaO–SiO_2–TiO_2 glass system modified by PDMS and obtained dense and homogeneous monoliths. In this study, Ca was found to excite apatite like phase on the surface of bioactive glasses when soaked in the SBF solution for about two days. These hybrids were structurally described as the network of silica–titania covalently bonded with PDMS where

Open Access Article. Published on 11 September 2020. Downloaded on 10/25/2025 7:46:44 PM.
This article is licensed under a Creative Commons Attribution-NonCommercial 3.0 Unported Licence.

Ca ions are bonded ionically. An increase in the mechanical properties of the hybrid was observed owing to the existence of PDMS while Ca promoted the generation of HCA layer by supplying physical sites for HCA nucleation resulting in an improved *in vitro* bioactivity. In another investigation,[445] a 3D porous scaffold comprising polylactide-*co*-glycolide (PLAGA) and bioactive glass composites has been developed. The PLAGA–bioactive glass composites were prepared as 3D porous scaffolds as well as thin films as shown in Fig. 24.[445] The scaffolds were found to be biodegradable, bioactive and suitable for bone tissue engineering. The soaking test was performed in SBF to assess the bioactivity of the composite where the CaP layer was formed within seven days. Moreover, it was found that the bioactive glass particles promoted the expressions of collagen (type I) by human osteoblast-like cells. The control PLAGA scaffold displayed 31% total porosity with a mean pore diameter of 116 μm while PLAGA–bioactive glass composite exhibits 43% total porosity with a mean pore diameter of 89 μm. Furthermore, the mechanical properties of the PLAGA–bioactive glass composite scaffold were investigated and an increase in the elastic modulus up to 51.336 ± 6.1 MPa was observed as compared with the elastic modulus (26.479 ± 3.4 MPa) of control PLAGA scaffold. All these findings point towards bioactive glasses as fascinating bioactive material to foster the bioactivity of polymer-based composites for prospective bone regeneration applications.

The significance of hierarchical scaffold porosity for bone tissue regeneration has been discussed by numerous researchers.[432,446] Porous structures having a total open porosity greater than 80% have proven to be efficient in promoting tissue ingrowth given that they allow cell migrations, proliferation and deposition of the matrix in the open spaces.[447] The existence of an interrelated pore network facilitates the invasion of blood vessels and the supply of nutrients.[446] Also, the average pore size can be instrumental in bone tissue engineering where small pores prevent migration of cells and restrict the diffusion of nutrients and elimination of waste products[448,449] while very wide pore restricts the cell attachment as a result of the decrease in the specific surface area.[450] MBGs display a highly ordered pore structure with a pore diameter in the range of 2–10 nm having a much-closed pore size distribution. The large architectural features and the existence of silanol groups are the main reason behind the quick *in vitro* bioactive response of certain compositions of MBGs.[451] Furthermore, MBGs are

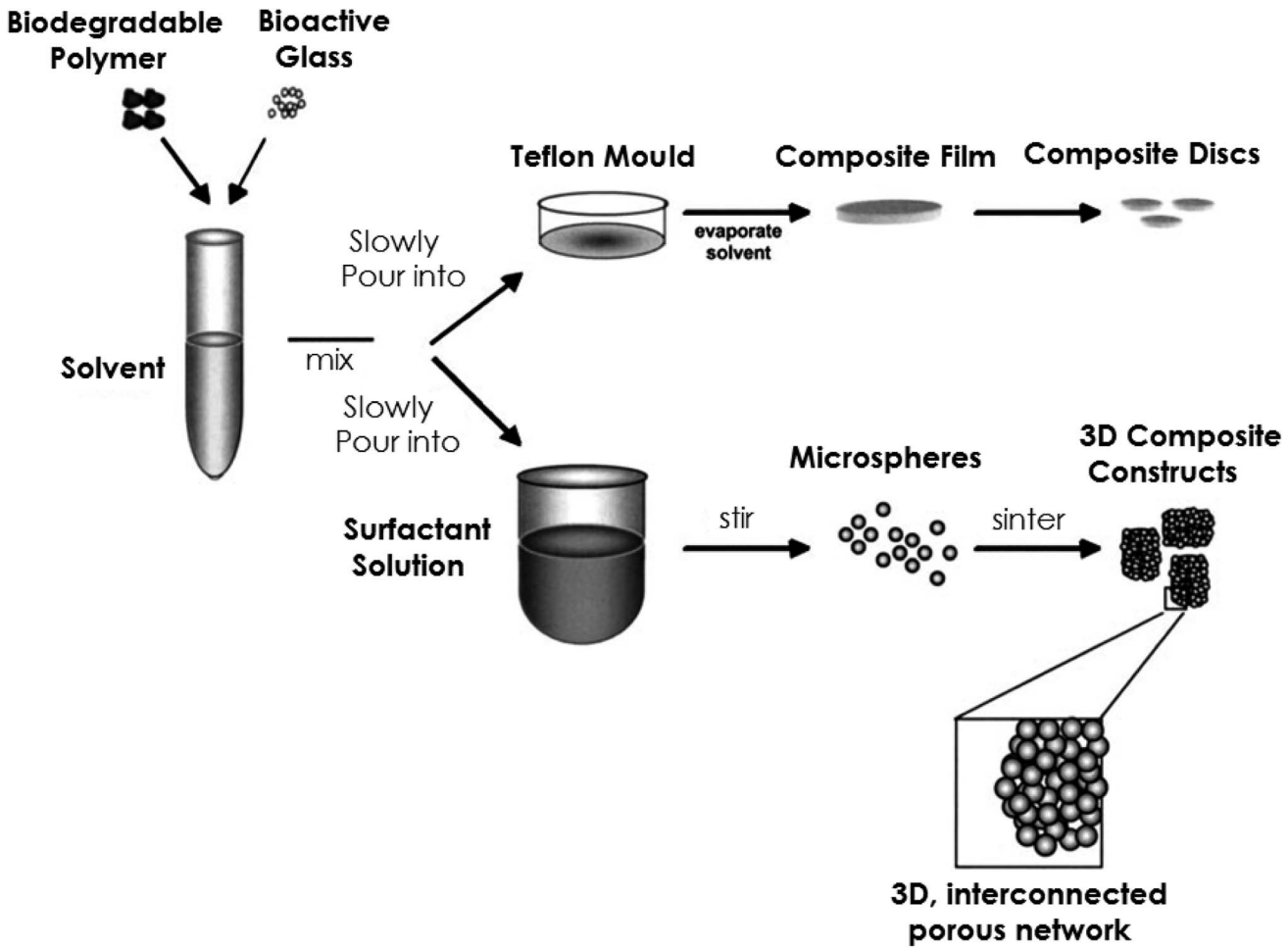

Fig. 24 A schematic representation of the fabrication process of PLAGA–bioactive glass composite scaffolds. Reproduced with permission from ref. 445. Copyright 2003, John Wiley & Sons.

Open Access Article. Published on 11 September 2020. Downloaded on 10/25/2025 7:46:44 PM.
This article is licensed under a Creative Commons Attribution-NonCommercial 3.0 Unported Licence.

accepted as a very appropriate vehicle for controlling drug release and growth factors which can be embedded inside the pores. Fig. 25 schematically represents the important features of MBGS which make them an ideal candidate for the synthesis of 3D mesoporous scaffold for bone tissue engineering, local drug delivery of biomolecules, drugs, therapeutic ions as well as for designing and developing stimuli-responsive systems.[382] Considering the properties of scaffolds for bone tissue regeneration, various strategies such as foaming, free drying, fiber bonding and rapid prototyping techniques have been proposed for designing mesoporous structure required for cell functions namely bone cell ingrowths, the supply of nutrients, vascularization and also for adhesion and growth of bone cells.[452] However, it is necessary to keep in mind that the powder processing of MBGs for scaffold preparation using the above-mentioned techniques should not affect the ordered mesoporosity and bioactivity.[453]

During the last ten years, MBGs have been widely explored for bone regeneration applications. Recently, Wu *et al.*[454] reported delivery of dimethyloxallyl glycine (DMOG) using the MBG scaffold to meliorate angiogenesis and osteogenesis of human bone marrow stromal cells (BMSCs). It has been observed that MBG scaffold can imitate a hypoxic microenvironment and thus elevate the angiogenic capacity of human BMSCs. Yun *et al.*[455] employed methylcellulose as a large pore porogen to prepare MBGs which demonstrated excellent apatite formation ability in SBF and assisted in the proliferation of MG-63 cells. In another study, Zhu *et al.*[456] demonstrated that the MBG scaffolds with 80Si15Ca5P composition exhibit the best apatite mineralization ability and assisted in the proliferation and differentiation of BMSCs. In another investigation, MBG powders were integrated into the PCL matrix to form composite scaffolds which displayed apatite mineralization in SBF.[457] The incorporation of MBG particles into PLAGA enhances the proliferation and ALP activities of human osteoblasts.[458] In another investigation, the authors reported the synthesis of silk modified MBG scaffolds with substantially enhanced attachment, proliferation, differentiation and osteogenic gene expression of BMSCs.[366] Moreover, various studies have shown that the integration of Fe, Sr, B, and Zr ions into MBG scaffolds can improve cell proliferation and osteogenic differentiation.[459–462] Wu *et al.*[463] in their excellent review highlights the potential of MBG particles, spheres, fibers and scaffolds as platforms for drug delivery and bone tissue regeneration. Besides, studies have also shown that both hydrophilic and hydrophobic drugs can also be effectively supplied using MBGs which are competent enough for substantially improving the proliferation, differentiation and osteogenic gene expression of human osteoblasts. These results deliver the paradigm change that osteoconductive drugs can be pre-installed in the MBG

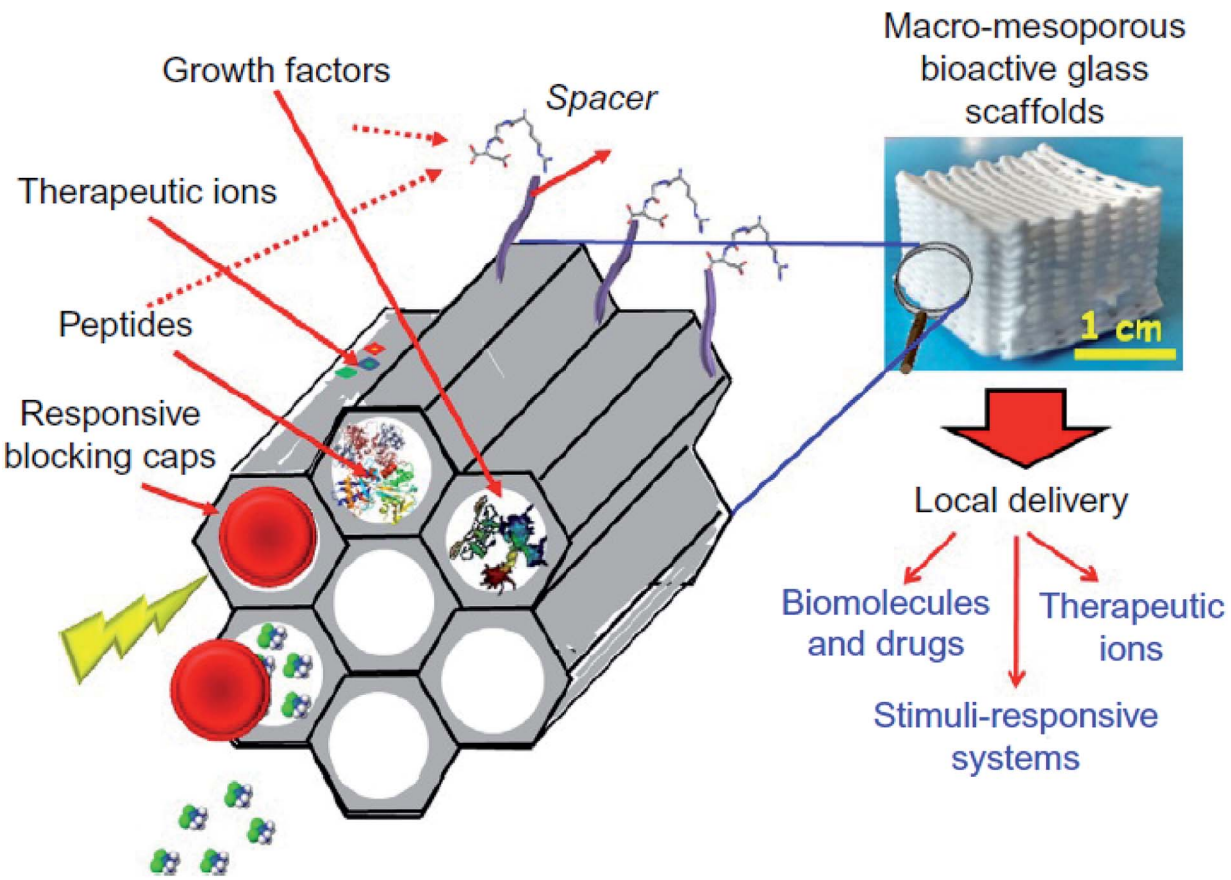

Fig. 25 Schematic presentation of ordered MBGs for bone tissue regeneration. Reproduced with permission from ref. 382. Copyright 2018, Elsevier.

Open Access Article. Published on 11 September 2020. Downloaded on 10/25/2025 7:46:44 PM.
This article is licensed under a Creative Commons Attribution-NonCommercial 3.0 Unported Licence.

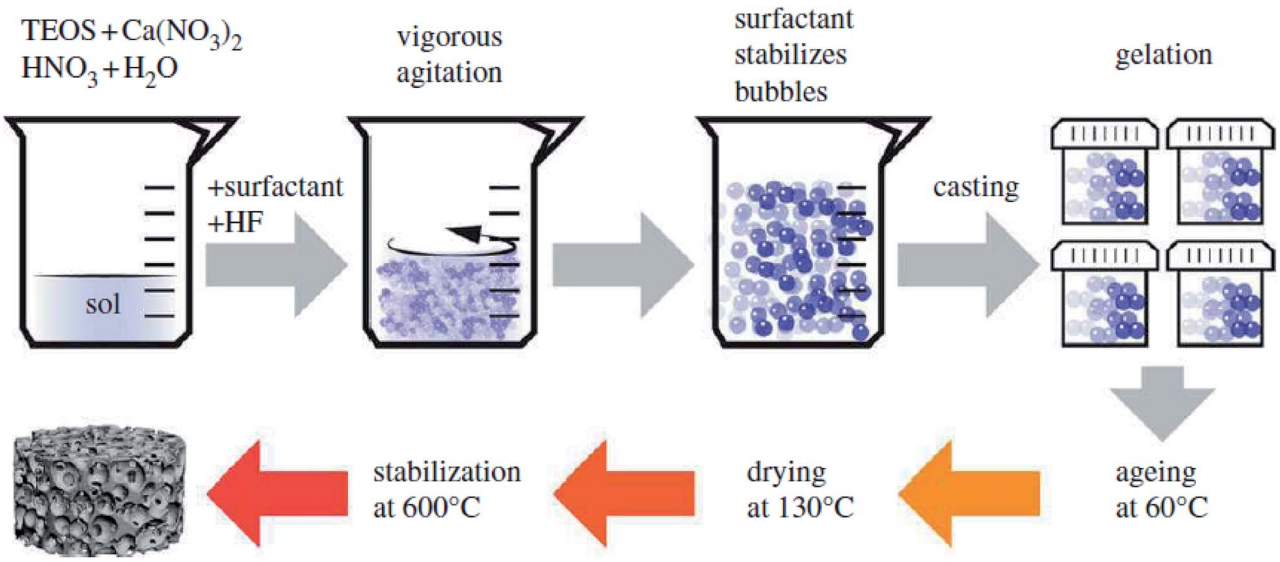

Fig. 26 Schematic representation of sol–gel foaming process. Adapted from ref. 465. Copyright 2012, the Royal Society of Chemistry.

scaffold to incite both *in vitro* and *in vivo* osteogenesis for bone tissue engineering.[463] Thus, achieving efficient drug delivery using the MBG scaffold is a fascinating prospect for bone tissue regeneration.

Recently, functionalized MBG scaffolds were synthesized for refined bone tissue regeneration.[336] To carry out functionalization, amino and carboxylic groups were effectively grafted on to the synthesized mesoporous glasses *via* a post grafting process. The osteogenic capabilities of both MBG and functionalized MBG scaffolds were comprehensively investigated *in vivo* as well as *in vitro* using rabbit BMSCs. It has been discovered that both types of scaffolds could dramatically improve the proliferation and osteogenic differentiation of BMSCs. Amino functional group grafted scaffolds showed the greatest *in vitro* osteogenic capability as compared with the other two scaffolds by virtue of its positively charged surface. Furthermore, *in vivo* test results demonstrated that scaffolds grafted with the amino-functional groups could promote a higher level of bone regeneration in comparison with the other two scaffolds. It was reported that the surface characteristics and the decreased degradation rate of the amino group functionalized scaffold played a vital role in promoting bone regeneration.

The interconnected porous structure is essential for creating an effective scaffold for the migration of cells into the pores and tissue growth throughout the scaffold template. 3D scaffolds with interconnected porous structures can be manufactured using the sol–gel foaming process. The first sol–gel foam process was demonstrated by Jones *et al.*[405,464] Fig. 26 schematically presents the steps involved in the sol–gel foaming process.[465] The hydrolyzed sol can be foamed by vigorous stirring in air and by including a surfactant.[118] The surfactant reduces the surface tension as it is composed of molecules

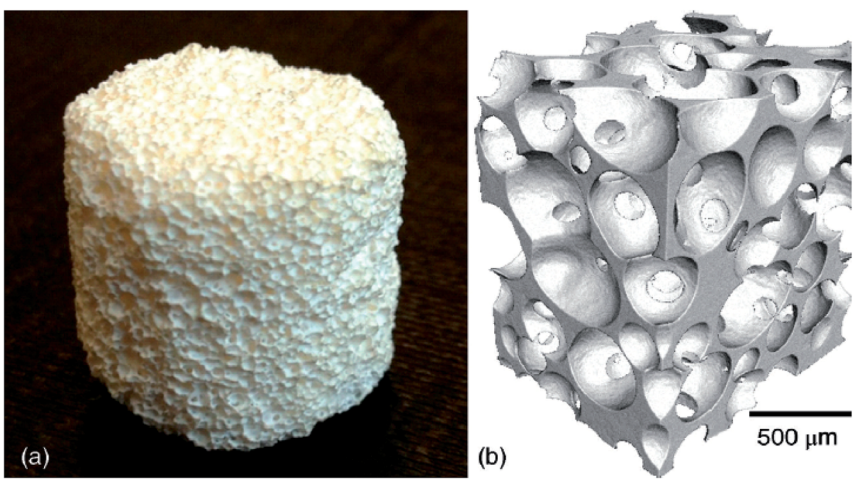

Fig. 27 (a) Photograph of bioactive glass foam scaffold and (b) X-ray micro CT image. Reproduced with permission from ref. 467. Copyright 2015, John Wiley & Sons.

Open Access Article. Published on 11 September 2020. Downloaded on 10/25/2025 7:46:44 PM.
This article is licensed under a Creative Commons Attribution-NonCommercial 3.0 Unported Licence.

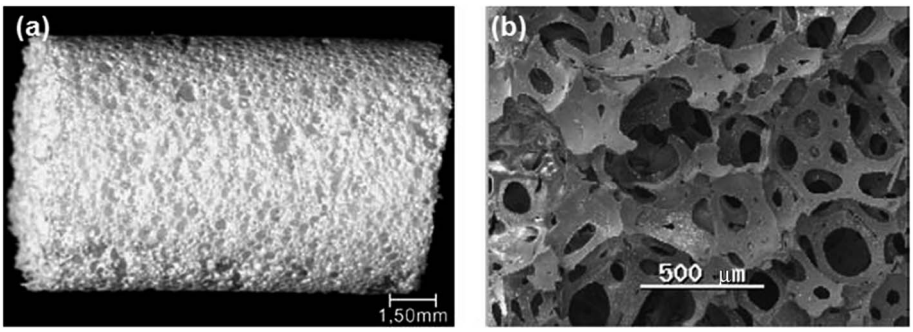

Fig. 28 (a) Representation of synthesized sol–gel glass foam. (b) SEM microstructure. Adapted from ref. 473. Copyright 2005, Springer Nature.

having polar (hydrophilic) and non-polar (hydrophobic) end groups and provides temporary stability to the foam. However, for the successful preparation of foam, it is necessary to expedite the gelation process. The gelation process can be expedited by adding HF acid so that the gelation takes place within minutes.[466] On gelation, a prompt viscosity increase helps in the foaming process where the air bubbles are stabilized as the condensation reactions form the silica network around them. The generation of Si–O–Si bonds leads to shrinkage of bubble walls which brings the neighboring bubbles into close contact with each other. During aging and drying, the liquid vents from the point of bubble contacts and additional shrinkage occurs resulting in the rupture of the liquid film at the points of bubble contacts and open up the interconnects between the macropores.[466] A hierarchical porous structure can be produced with interconnected macropores as shown in Fig. 27.[467] There are several factors namely glass composition, processing temperature, surfactant and gelling agent concentration, and the water usage in the surfactant that can affect the pore structure.[468,469] However, the most efficacious way of controlling the modal interconnect diameter is by changing the surfactant concentration while keeping all the other variables constant.[468]

Using the sol–gel foaming method, bioactive glass scaffolds were produced having macropores of diameter up to 600 μm linked with the pore windows of diameter up to 200 μm and modal diameter greater than 100 μm.[469,470] *In vitro* test utilizing primary human osteoblasts revealed that the foam stimulates the formation and mineralization of bone nodules within fourteen days of culture.[471] In another report, *in vivo* test demonstrated that foam scaffolds implanted in the rabbit crania promoted new bone growth at the same rate as that of the melt derived bioactive glass powder which is available commercially.[472] In another study, Valerio *et al.*[473] described the fabrication of sol–gel foam scaffolds with interrelated pores up to 500 μm, high porosity (88%) and specific surface area of 92 $m^2\ g^{-1}$. The photograph and SEM micrograph of the synthesized glass foam is depicted in Fig. 28 where highly interconnected pores with adequate pore size can be observed.[473] The macroporous glasses were examined in osteoblast cultures to assess adhesion, proliferation, collagen and ALP production. The osteoblast proliferation, as well as the collagen secretion, was reported to be higher in the presence of the foam as compared with the controlled sol–gel glass.[473] Besides, the viable osteoblasts have been observed throughout the foam implying that the synthesized porous glass foams are a prosperous material for bone repair considering that they provide a favorable environment for the adhesion and proliferation of osteoblast.[473] Moreover, the sol–gel foaming process has also been utilized to fabricate organic–inorganic hybrid scaffolds that can mimic the trabecular structure of bone.[411]

In a similar study, Jones *et al.*[474] utilized sol–gel derived bioactive silicate glasses of 70S30C (70 mol% SiO_2, 30 mol% CaO)

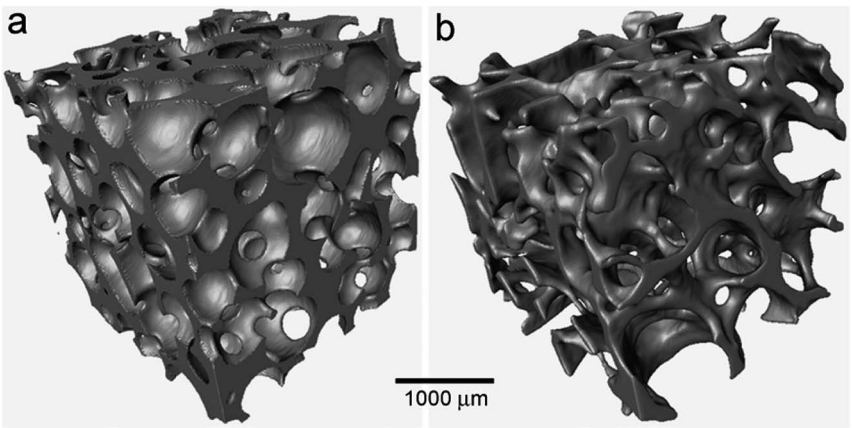

Fig. 29 μCT images of (a) 3D porous scaffold prepared from sol–gel derived bioactive silicate glass and (b) human trabecular bone. Reproduced with permission from ref. 474. Copyright 2007, Elsevier.

Open Access Article. Published on 11 September 2020. Downloaded on 10/25/2025 7:46:44 PM.
This article is licensed under a Creative Commons Attribution-NonCommercial 3.0 Unported Licence.

composition to prepare 3D porous foam scaffold having a hierarchical interconnected porous structure similar to the trabecular bone as depicted in Fig. 29. The bulk and true density of the fabricated scaffold was reported to be 0.25 g cm^{-3} and 2.71 g cm^{-3} respectively while the percent porosity of each scaffold was reported to be 91%.[474] The fabricated scaffold supported the osteoblast growth and stimulated changes within the culture period of three weeks, as evidenced by improved ALP enzymatic activity of human osteoblasts which were cultured on the glass foam. The formation of mineralized bone nodules was stimulated without adding any supplementary factors such as ascorbic acid (AA), β-glycerophosphate and dexamethasone in the medium. The deposition of ECM was also validated by the improved production of the ECM collagen type I protein. Finally, the authors concluded that the scaffolds satisfy most of the criteria of becoming an ideal scaffold material for bone tissue engineering without the requirement of phosphate in the glass composition for *in vitro* mineralization of ECM on porous foam scaffold.[474]

6. Concluding remarks and future perspectives

The sol–gel methods have become very popular during the last two decades because of the chemical homogeneity (molecular level mixing), low processing temperatures, possibility to control size, shape and morphology of the synthesized materials. The inherent advantages of the sol–gel technique and the chemical modification of the precursors allow tailoring the material properties to a great extent. A varied set of potential materials can be synthesized by a sol–gel method providing extraordinary matrices for a wide range of organic as well as inorganic compounds. The advantages of the sol–gel technique in biomedical fields are ascribed to the possibility of synthesizing mechanically robust and chemically inert porous materials with the high specific surface area. The sol–gel technique offers a unique opportunity to form porous glass-based materials with tunable porosity as long as the synthesis parameters that influence the hydrolysis and condensation reaction involving inorganic precursors as well as the thermal treatment are precisely controlled. The low-temperature sol–gel synthesis imparts an opportunity for the integration of materials which would otherwise get spoiled due to high temperatures. For example; the sol–gel method enables the integration of biomolecules and therapeutic agents such as drugs, growth factors and proteins during the synthesis process all of which can be released in a controlled way. The evolution of sol–gel based materials for the entanglement of biomolecules has led to an enhancement in the number of materials available for different applications and the types of biomolecules which have the ability to being entrapped in an active state. There are varied options available for selecting different materials and varying synthesis parameters during sol–gel processing for both industrial and biomedical applications. However, the economic viability of scaling up of the sol–gel derived material is one of the hurdles that need to be overcome. Furthermore, the sol–gel method is a continuous process and it is quite laborious. Hence, batch to batch discrepancies might appear.

The current research in the tissue engineering field is concentrated on the development of high-performance multifunctional biomaterials *i.e.* materials that are capable of stimulating bone regeneration and exhibiting drug delivery capabilities with significant mechanical stability. In the framework of this research, sol–gel derived bioactive glasses have been customized as the implantable materials for bone tissue regeneration owing to their unique features namely the ability to degrade at a controllable rate, conversion to HA-like material, ability to bind firmly with the living tissues, and improving the growth and proliferation of osteoblasts. These unique properties of bioactive glasses result from their special chemical compositions. Further benefits of bioactive glasses in bone tissue regeneration include the possibility to incorporate various doping materials which show improved bone regeneration capability. Besides, the improved antibacterial or angiogenesis activity of bioactive glasses set up a bacteria-free atmosphere in implanted sites during the healing and regeneration of the soft and hard tissue. Several types of bioactive glasses with different compositions have been examined for bone tissue regeneration. Furthermore, the incorporation of therapeutic elements namely Ag, Cu, Sr, Co, Zn or Ga into the bioactive glasses has demonstrated more promising therapeutic effects than the original or un-doped bioactive glasses. Recent studies have shown the proangiogenesis potential of bioactive glasses which are proved beneficial for soft tissue repair.

The important aspect of bioactive glasses is their surface functionalization which provides increased opportunity for designing, developing and controlling the surface properties. This, in turn, influences their biological properties (biocompatibility, reactivity, bone-bonding and cell-stimulating ability) making the material more versatile. Also, it has been demonstrated that the microstructural characteristics, nucleation and HCA growth rate can be influenced by introducing functional groups on the surfaces of bioactive glasses. Moreover, surface functionalization of bioactive glasses is reported to improve their efficiency towards the delivery of hydrophobic drugs. Several strategies and challenging approaches towards surface modifications such as biological functionalization have been explored for performance optimization of bioactive glasses. Thus, surface functionalization is the key for exploiting the surface reactivity of bioactive glasses to meet various biological requirements associated with their wide range of biomedical and clinical applications.

MBGs represent the most promising family of bioactive glasses and have been emerging as fascinating biomaterial owing to their well-ordered mesoporous structure, high specific surface area and pore volumes (two-fold greater than the conventional sol–gel glass) and superior bioactivity. The improved bioactivity is ascribed to the highly ordered arrangements of mesopores with uniform size. The improved bioactivity and controlled drug delivery capability of MBGs render them an excellent starting material for manufacturing 3D scaffolds for bone tissue regeneration. However, considerable emphasis needs to be devoted to the probability of covalent

Open Access Article. Published on 11 September 2020. Downloaded on 10/25/2025 7:46:44 PM.
This article is licensed under a Creative Commons Attribution-NonCommercial 3.0 Unported Licence.

grafting of osteoconductive agents (proteins, peptides, growth factors *etc.*) to the 3D scaffold surface which could serve as enticing signals for bone cells and assist in the bone regeneration process. In recent years, substantial progress is being made in developing MBGs with tailored architecture for desired applications other than bone tissue regeneration. Despite these advances in MBGs research, there remains scope for improving their bioactivity and controlled therapeutic delivery. Moreover, new research avenues are needed for viable vaccines, hormones, and therapeutic protein delivery in addition to the affirmation of growth factor and gene delivery. Also, in the future, MBGs should be examined in the form of a coating on the implants of other materials.

MBGs foams have shown the potential to be served as a scaffold material for bone tissue regeneration applications. These scaffolds should be degradable, bioactive and must possess compressive strength similar to porous bone. Also, they possess a hierarchical pore structure of interrelated macropores with intrinsic nanoporosity. However, fabricating bioactive glass foam scaffolds with the regulated structure for bone tissue engineering and drug delivery is still a challenge. Furthermore, the efficacious delivery of growth factors has always been a matter of concern. Therefore, polymer scaffolds were utilized for loading of growth factor with controlled release kinetics but they lack adequate osteoconductivity. Hence, polymer scaffolds are most commonly fabricated in the composites form using bioactive inorganic materials. Nevertheless, it is a challenge to match the degradation rates of the polymer matrix and the filler phase of the composite. The degradation rate of individual phases is different and does not match with the rate of new tissue formation which can result in the *in vivo* loss of mechanical properties. In an ideal case, both the phases ought to degrade at the rate which is suitable for the targeted application. The association of proficient drug delivery using MBGs scaffold is an enticing prospect for regenerative bone medicine.

Porous glass scaffolds show brittleness and exhibit inadequate fracture toughness, thereby restricting their utilization in load-carrying applications. To ameliorate the mechanical characteristics of scaffolds, numerous glass compositions which precipitate crystalline phases have been prepared and tested. The mechanical properties of bioactive glasses need to be explored extensively *in vivo* situations to strengthen their position as a promising biomaterial for bone tissue regeneration. Moreover, in future research on bioactive glasses, the degradation and bone ingrowth will play an important part as the mechanical properties of bioactive glasses can be significantly altered due to degradation with respect to time and with the bone-bonding, the behavior of the material can be modified drastically. Moreover, in the future, an attempt should be made in processing and designing innovative scaffolds with good mechanical properties especially for the load-bearing bones using bioactive glasses.

Conflicts of interest

The authors declare no conflict of interest.

Acknowledgements

This work has been supported by the Bavarian State Ministry of Economy and Media, Energy and Technology (Czech-Bavarian Cross-Border Cooperation Program, INTERREG V, EUS 2014–2020 Objective, MATEGRA-advanced porous biomaterials functionalized with stem cells for enhanced implant osseointegration, No. 201, co-funded by the ERDF and Ministry of Regional Development of the Czech Republic). Also, the authors would like to express their appreciation to the European Union for financial support provided through Mobility 3.0 project with Project No. CZ.02.2.69/0.0/0.0/16_027/0008370.

References

1 G. J. Owens, R. K. Singh, F. Foroutan, M. Alqaysi, C. M. Han, C. Mahapatra and H. W. Kim, Sol–gel based materials for biomedical applications, *Prog. Mater. Sci.*, 2016, **77**, 1–79.
2 S. N. Tan, W. Wang and L. Ge, 3.30 Biosensors based on sol–gel derived materials, *Compr. Biomater. II*, 2017, **3**, 657–689.
3 M. R. N. Monton, E. M. Forsberg and J. D. Brennan, Tailoring sol–gel derived silica materials for optical biosensing, *Chem. Mater.*, 2012, **24**, 796–811.
4 U. G. Akpan and B. H. Hameed, The advancement in sol–gel method of doped TiO_2 photocatalyst, *Appl. Catal., A*, 2010, **375**, 1–11.
5 D. Levy and M. Zayat, *The sol–gel handbook*, ed. D. Levy and M. Zayat, vol. 1–3, Wiley VCH, USA, 2015, pp. 1–1508.
6 J. M. Rosenholm, C. Sahlgren and M. Linden, Towards multifunctional, targeted drug delivery systems using mesoporous silica nanoparticles-opportunities & challenges, *Nanoscale*, 2010, **2**, 1870–1883.
7 P. Yang, S. Gai and J. Lin, Functionalized mesoporous silica materials for controlled drug delivery, *Chem. Soc. Rev.*, 2012, **41**, 3679–3698.
8 K. Sumida, K. Liang, J. Reboul, I. A. Ibara, S. Furukawa and P. Falcaro, Sol–gel processing of metal organic frameworks, *Chem. Mater.*, 2017, **29**, 2626–2645.
9 L. M. Muresan, Corrosion protective coatings for Ti and Ti alloys used for biomedical implants, in *Intelligent coatings for corrosion control*, ed. A. Tiwari, J. Rawlins and L. H. Hihara, 2015, pp. 585–602.
10 G. Kickelbick, Introduction to sol–gel nanocomposites, in *Sol–gel nanocomposites, Advances in sol–gel derived materials and technologies*, ed. M. Guglielmi, G. Kickelbick and A. Martucci, Springer-Verlag, New York, 2014, pp. 1–19.
11 D. Carta, D. M. Pickup, J. C. Knowles, M. E. Smith and R. J. Newport, Sol–gel synthesis of the P_2O_5–CaO–Na_2O–SiO_2 system as a novel bioresorbable glass, *J. Mater. Chem.*, 2005, **15**, 2134–2140.
12 S. Esposito, Traditional sol–gel chemistry as a powerful tool for the preparation of supported metal and metal oxide catalysts, *Materials*, 2019, **12**, 668.
13 T. Lopez, J. Manjarrez, D. Rembao, E. Vinogradova, A. Moreno and R. D. Gonzalez, An implantable sol–gel derived titania–silica carrier system for the controlled

Open Access Article. Published on 11 September 2020. Downloaded on 10/25/2025 7:46:44 PM.
This article is licensed under a Creative Commons Attribution-NonCommercial 3.0 Unported Licence.

release of anticonvulsants, *Mater. Lett.*, 2006, **60**, 2903–2908.

14 X. Chen, W. Zhang, Y. Lin, Y. Cai, M. Qiu and Y. Fan, Preparation of high-flux γ-alumina nanofiltration membranes by using a modified sol–gel method, *Microporous Mesoporous Mater.*, 2015, **214**, 195–203.

15 S. Priya, J. R. Jones, V. Sophie, B. Robert, S. J. Victoria, L. L. Hench and P. M. Julia, Binary CaO–SiO_2 gel-glasses for biomedical applications, *Biomed. Mater. Eng.*, 2004, **14**, 467–486.

16 M. Abbasian, B. Massoumi, R. Mohammad-Rezaei, H. Samadian and M. Jaymand, Scaffolding polymeric biomaterials: are naturally occurring biological macromolecules more appropriate for tissue engineering, *Int. J. Biol. Macromol.*, 2019, **134**, 673–694.

17 B. Massoumi, M. Hatamzadeh, N. Firouzi and M. Jaymand, Electrically conductive nanofibrous scaffold composed of poly(ethylene glycol)-modified polypyrrole and poly(ε-caprolactone) for tissue engineering applications, *Mater. Sci. Eng., C*, 2019, **98**, 300–310.

18 S. Vandhaanooni and M. Eskandani, Electrically conductive biomaterials based on natural polysaccharides: challenges and applications in tissue engineering, *Int. J. Biol. Macromol.*, 2019, **141**, 636–662.

19 H. Samadian, H. Maleki, Z. Allahyari and M. Jaymand, Natural polymers-based light-induced hydrogels: promising biomaterials for biomedical applications, *Coord. Chem. Rev.*, 2020, **420**, 213432.

20 M. P. Lutolf and J. A. Hubbel, Synthetic biomaterials as instructive extracellular microenvironments for morphogenesis in tissue engineering, *Nat. Biotechnol.*, 2005, **23**, 47–55.

21 L. S. Nair and C. T. Laurencin, Biodegradable polymers as biomaterials, *Prog. Polym. Sci.*, 2007, **32**, 762–798.

22 B. Toirac, A. Garcia-Casas, S. C. Cifuentes, J. J. Aguilera-Correa, J. Esteban, A. Mediero and A. Jimmez-Morales, Electrochemical characterization of coatings for local prevention of Candida infections on titanium based biomaterials, *Prog. Org. Coat.*, 2020, **146**, 105681.

23 J. J. Aguilera-Correa, A. Garcia-Casas, A. Mediero, D. Romera, F. Mulero, I. Cuevas-Lopez, A. Jimenez-Morales and J. Esteban, A new antibiotic loaded sol–gel can prevent bacterial prosthetic joint infections: from in vitro studies to an in vivo model, *Front. Microbiol.*, 2020, **10**, 2935.

24 L. Ming-Cheng, C. Chun-Cheng, W. I-Ting and D. Shinn-Jyh, Enhanced antibacterial activity of calcium silicate-based hybrid cements for bone repair, *Mater. Sci. Eng., C*, 2020, **110**, 110727.

25 M. Roozbahani, M. Alehosseini, M. Kharaziha and R. Emadi, Nano-calcium phosphate bone cement based on Si-stabilized α-tricalcium phosphate with improved mechanical properties, *Mater. Sci. Eng., C*, 2017, **81**, 532–541.

26 H. Li, J. Li, J. Jiang, F. Lv, J. Chang, S. Chen and C. Wu, An osteogenesis/angiogenesis-stimulation artificial ligament for anterior cruciate ligament reconstruction, *Acta Biomater.*, 2017, **54**, 399–410.

27 G. Wu, X. Deng, J. Song and F. Chen, Enhanced biological properties of biomimetic apatite fabricated polycaprolactone/chitosan nanofibrous bio-composite for tendon and ligament regeneration, *J. Photochem. Photobiol., B*, 2018, **178**, 27–32.

28 M. Catauro, F. bollino, F. Papale, C. Ferrara and P. Mustarelli, Silica–polyethylene glycol hybrids synthesized by sol–gel: biocompatibility improvement of titanium implants by coating, *Mater. Sci. Eng., C*, 2015, **55**, 118–125.

29 A. Cerqueira, F. Romero-Gavilan, N. Araujo-Gomes, I. Garcia-Arnez, C. Martinez-Ramos, S. Ozturan, M. Azkargota, F. Elortza, M. Gurruchanga, J. Suay and I. Goni, A possible use of melatonin in the dental field: protein adsorption and in vitro cell response on coated titanium, *Mater. Sci. Eng., C*, 2020, **116**, 111262.

30 W. D. Lee, R. Gawri, R. M. Pilliar, W. L. Stanford and R. A. Kandel, Sol–gel-derived hydroxyapatite films over porous calcium polyphosphate substrates for improved tissue engineering of osteochondral-like constructs, *Acta Biomater.*, 2017, **62**, 352–361.

31 M. Hu, J. Fang, Y. Zhang, X. Wang, W. Zhong and Z. Zhou, Design and evaluation a kind of functional biomaterial for bone tissue engineering: selenium/mesoporous bioactive glass nanospheres, *J. Colloid Interface Sci.*, 2020, **579**, 654–666.

32 S. Mondal, G. Hoang, P. Manivasagan, M. S. Moorthy, T. P. Nguyen, T. T. V. Phan, H. H. Kim, M. H. Kim, S. Y. Nam and J. Oh, Nano-hydroxyapatite bioactive glass composite scaffold with enhanced mechanical and biological performance for tissue engineering application, *Ceram. Int.*, 2018, **44**, 15735–15746.

33 X. Wang, Y. Zhang, C. Lin and W. Zhong, Sol–gel derived terbium-containing mesoporous bioactive glasses nanospheres: in vitro hydroxyapatite formation and drug delivery, *Colloids Surf., B*, 2017, **160**, 406–415.

34 S. Sebastiammal, A. S. L. Fathima, S. Devanesan, M. S. AlSalhi, J. Henry, M. Govindarajan and B. Vaseeharan, Curcumin-encased hydroxyapatite nanoparticles as novel biomaterials for antimicrobial, antioxidant and anticancer applications: a perspective of nano-based drug delivery, *J. Drug Delivery Sci. Technol.*, 2020, **57**, 101752.

35 C. Fa-Ming and L. Xiaohua, Advancing biomaterials of human origin for tissue engineering, *Prog. Polym. Sci.*, 2016, **53**, 86–168.

36 H. Yuan, J. D. De Bruijn, Y. Li, J. Feng, Z. Yang, K. De Groot and X. Zhang, Bone formation induced by calcium phosphate ceramics in soft tissue of dogs: a comparative study between porous α-TCP and β-TCP, *J. Mater. Sci.: Mater. Med.*, 2001, **12**, 7–13.

37 S. Areva, H. Paldan, T. Peltola, T. Narhi, M. Jokinen and M. Linden, Use of sol–gel-derived titania coating for direct soft tissue attachment, *J. Biomed. Mater. Res., Part A*, 2004, **70**, 169–178.

Open Access Article. Published on 11 September 2020. Downloaded on 10/25/2025 7:46:44 PM.
This article is licensed under a Creative Commons Attribution-NonCommercial 3.0 Unported Licence.

38 L. Meseguer-Olmo, M. J. Ros-Nicolas, V. Vincente-Ortega, M. Alcaraz-Banos, M. Clavel-Sainz, D. Arcos, C. V. Ragel, M. Vallet-Regi and C. I. Meseguer-Ortiz, A bioactive sol–gel glass implant for in vivo gentamicin release. Experimental model in rabbit, *J. Orthop. Res.*, 2006, **24**, 454–460.

39 R. Gupta and N. K. Chaudhary, Entrapment of biomolecules in sol–gel matrix for applications in biosensors: problems and future prospects, *Biosens. Bioelectron.*, 2007, **22**, 2387–2399.

40 M. S. Ahola, E. S. Sailynoja, M. H. Raitavno, M. H. Vaahtio, J. I. Salonen and A. U. O. Yli-Urpo, In vitro release of heparin from silica xerogels, *Biomaterials*, 2001, **22**, 2163–2170.

41 V. B. Kandimalla, V. S. Tripathi and H. Ju, Immobilization of biomolecules in sol–gels: biological and analytical applications, *Crit. Rev. Anal. Chem.*, 2006, **36**, 73–106.

42 S. Kargozar, N. Lotfibakshaiesh, J. Ai, A. Samadikuchaksaraie, R. G. Hill, P. A. Shah, P. B. Milan, M. Mozafari, M. Fathi and M. T. Joghataei, Synthesis, physico-chemical and biological characterization of strontium and cobalt substituted bioactive glasses for bone tissue engineering, *J. Non-Cryst. Solids*, 2016, **449**, 133–140.

43 S. Kargozar, F. Baino, S. Hamzehlou, R. G. Hill and M. Mozafari, Bioactive glasses: sprouting angiogenesis in tissue engineering, *Trends Biotechnol.*, 2018, **36**, 430–444.

44 S. Kargozar, M. Mozafari, S. J. Hashemian, P. B. Milan, S. Hamzehlou, M. Soleimani, M. T. Joghataei, M. Gholipourmalekabadi, A. Korourian, K. Mousavizadeh and A. M. Seifalian, Osteogenic potential of stem cells-seeded bioactive nanocomposite scaffolds: a comparative study between human mesenchymal stem cells derived from bone, umbilical cord Wharton's jelly, and adipose tissue, *J. Biomed. Mater. Res., Part B*, 2018, **106**, 61–72.

45 L. L. Hench, N. Roki and M. B. Fenn, Bioactive glass: importance of structure and properties in bone regeneration, *J. Mol. Struct.*, 2014, **1073**, 24–30.

46 A. Hoppe, N. S. Guldal and A. R. Boccaccini, A review of the biological response to ionic dissolution products from bioactive glass and glass-ceramics, *Biomaterials*, 2011, **32**, 2757–2774.

47 M. Vallet-Regi, I. Izquierdo-Barba and M. Colilla, Structure and functionalization of mesoporous bioceramics for bone tissue regeneration and local drug delivery, *Philos. Trans. R. Soc., A*, 2012, **370**, 1400–1421.

48 X. Yan, C. Yu, X. Zhou, J. Tang and D. Zhao, Highly ordered mesoporous bioactive glasses with superior in vitro bone-forming bioactivities, *Angew. Chem., Int. Ed.*, 2004, **43**, 5980–5984.

49 P. Chocolata, V. Kulda and V. Babuska, Fabrication of scaffolds for bone tissue regeneration, *Materials*, 2019, **12**, 568.

50 S. Ni, J. Chang and L. Chou, A novel bioactive porous $CaSiO_3$ scaffold for bone tissue engineering, *J. Biomed. Mater. Res., Part A*, 2006, **76**, 196–205.

51 A. J. El Haj, M. A. T. Wood, P. Homas and Y. Yang, Controlling cell biomechanics in orthopaedic tissue engineering and repair, *Pathol. Biol.*, 2005, **53**, 581–589.

52 M. Vallet-Regi, L. Ruiz-Gonzalez, I. Izquierdo-Barba and J. M. Gonzalez-Calbet, Revisiting silica based ordered mesoporous materials medical applications, *J. Mater. Chem.*, 2006, **16**, 26–31.

53 A. Hertz, V. FitzGerald, E. Pignotti, J. C. Knowles, T. Sen and I. J. Bruce, Preparation and characterization of porous silica and silica/titania monoliths for potential use in bone replacement, *Microporous Mesoporous Mater.*, 2012, **156**, 51–61.

54 I. Izquierdo-Barda, L. Ruiz-Gonzalez, J. M. Gonzalez-Calbet and M. Vallet-Regi, Tissue regeneration: a new property of mesoporous material, *Solid State Sci.*, 2005, **7**, 983–989.

55 T. Sen, G. J. T. Tiddy, J. L. Casci and M. W. Anderson, Meso-cellular silica foams, macro-cellular silica foams and mesoporous solids: a study of emulsion-mediated synthesis, *Microporous Mesoporous Mater.*, 2005, **78**, 255–263.

56 H. Sun and H. L. Yang, Calcium phosphate scaffolds combined with bone morphogenetic proteins or mesenchymal stem cells in bone tissue engineering, *Chin. Med. J.*, 2015, **128**, 1121–1127.

57 Q. Fu, E. Saiz, M. N. Rahaman and A. P. Tomsia, Bioactive glass scaffolds for bone tissue engineering: state of the art and future perspectives, *Mater. Sci. Eng., C*, 2011, **31**, 1245–1256.

58 H. M. Kim, Ceramic bioactivity and related biomimetic strategy, *Curr. Opin. Solid State Mater. Sci.*, 2003, **7**, 289–299.

59 J. P. Zhong and D. C. Greenspan, Processing and properties of sol–gel bioactive glasses, *J. Biomed. Mater. Res.*, 2000, **53**, 694–701.

60 J. Ma, C. Z. Chen, D. G. Wang, X. G. Meng and J. Z. Shi, In vitro degradability and bioactivity of mesoporous CaO–MgO–P_2O_5–SiO_2 glasses synthesized by sol–gel method, *J. Sol-Gel Sci. Technol.*, 2010, **54**, 69–76.

61 L. L. Hench, J. M. Polak, I. D. Xynos and L. D. K. Buttery, Bioactive materials to control cell cycle, *Mater. Res. Innovations*, 2000, **3**, 313–323.

62 K. Rezwan, Q. Z. Chen, J. J. Blaker and A. R. Boccaccini, Biodegradable and bioactive porous polymer/inorganic composite scaffolds for bone tissue engineering, *Biomaterials*, 2006, **27**, 3413–3431.

63 W. D. S. Roberto, M. M. Pereira and T. P. Ribiero de Campos, Analysis of bioactive glasses obtained by sol–gel processing for radioactive implants, *Mater. Res.*, 2003, **6**, 123–127.

64 A. H. Choi, R. C. Conway, S. Cazalbou and B. Ben-Nissan, Maxillofacial bioceramics in tissue engineering: production techniques, properties and applications, in *Fundamental Biomaterials: Ceramics*, S. Thomas, P. Balakrishnan and M. S. Sreekala, Woodhead Publishing, Elsevier, 2018, pp. 63–93.

65 M. A. Malik, M. Y. Wani and M. A. Hashim, Microemulsion method: a novel route to synthesize organic and inorganic

Open Access Article. Published on 11 September 2020. Downloaded on 10/25/2025 7:46:44 PM.
This article is licensed under a Creative Commons Attribution-NonCommercial 3.0 Unported Licence.

nanomaterials: 1st nano update, *Arabian J. Chem.*, 2012, **5**, 397–417.
66 K. Zheng and A. R. Boccaccini, Sol–gel processing of bioactive glass nanoparticles: a review, *Adv. Colloid Interface Sci.*, 2017, **249**, 363–373.
67 B. L. Cushing, V. L. Kolesnichenko and C. J. O'Connor, Recent advances in the liquid-phase syntheses of inorganic nanoparticles, *Chem. Rev.*, 2004, **104**, 3893–3946.
68 J. Eastoe, M. J. Hollamby and L. Hudson, Recent advances in nanoparticle synthesis with reversed micelles, *Adv. Colloid Interface Sci.*, 2006, **128–130**, 5–15.
69 C. Karagiozov and D. Momchilova, Synthesis of nanosized particles from metal carbonates by the method of reverse micelles, *Chem. Eng. Process.*, 2005, **44**, 115–119.
70 Y. Sun, G. Guo, D. Tao and Z. H. Wang, Reverse microemulsion directed synthesis of hydroxyapatite nanoparticles under hydrothermal conditions, *J. Phys. Chem. Solids*, 2007, **68**, 373–377.
71 A. Lukowiak, J. Lao, J. Lacroix and J. M. Nedelec, Bioactive glass nanoparticles obtained through sol–gel chemistry, *Chem. Commun.*, 2013, **49**, 6620–6622.
72 X. Li, X. Chen, G. Miao, H. Liu, C. Mao, G. Yuan, Q. Liang, X. Shen, C. Ning and X. Fu, Synthesis of radial mesoporous bioactive glass particles to deliver osteoactivin gene, *J. Mater. Chem. B*, 2014, **2**, 7045–7054.
73 Q. Liang, Q. Hu, G. Miao, B. Yuan and X. Chen, A facile synthesis of novel mesoporous bioactive glass nanoparticles with various morphologies and tunable mesostructure by sacrificial liquid template method, *Mater. Lett.*, 2015, **148**, 45–49.
74 T. H. Kim, R. K. Singh, M. S. Kang, J. H. Kim and H. W. Kim, Gene delivery nanocarriers of bioactive glass with unique potential to load BMP2 plasmid DNA and to internalize into mesenchymal stem cells for osteogenesis and bone regeneration, *Nanoscale*, 2016, **8**, 8300–8311.
75 T. H. Kim, R. K. Singh, M. S. Kang, J. H. Kim and H. W. Kim, Inhibition of osteoclstogenesis through siRNA delivery with tunable mesoporous bioactive nanocarriers, *Acta Biomater.*, 2016, **29**, 352–364.
76 Y. Wang and X. Chen, Facile synthesis of hollow mesoporous bioactive glasses with tunable shell thickness and good monodispersity by micro-emulsion, *Mater. Lett.*, 2017, **189**, 325–328.
77 K. Sinko, Influence of chemical conditions on the nanoporous structure of silicate aerogels, *Materials*, 2010, **3**, 704–740.
78 C. Vichery and J. M. Nedelc, Bioactive glass nanoparticles: from synthesis to material design for biomedical applications, *Materials*, 2016, **9**, 288–295.
79 Y. Wang, H. Pan and X. Chen, The preparation of hollow mesoporous bioglass nanoparticles with excellent drug delivery capacity for bone tissue regeneration, *Front. Chem.*, 2019, **7**, 283.
80 Q. Hu, Y. Li, N. Zhao, C. Ning and X. Chen, Facile synthesis of hollow mesoporous bioactive glass submicron spheres with a tunable cavity size, *Mater. Lett.*, 2014, **134**, 130–133.
81 H. Duan, J. Diao, N. Zhao and Y. Ma, Synthesis of hollow mesoporous bioactive glass microspheres with tunable shell thickness by hydrothermal assisted self transformation method, *Mater. Lett.*, 2016, **167**, 201–204.
82 J. Xiao, Y. Wan, F. Yao, Y. Huang, Y. Zhu, Z. Yang and H. Luo, Constructing 3D scaffold with 40 nm diameter hollow mesoporous bioactive glass nanofibres, *Mater. Lett.*, 2019, **248**, 201–203.
83 M. A. Fardad, Catalysts and the structure of SiO_2 sol–gel films, *J. Mater. Sci.*, 2000, **35**, 1835–1841.
84 A. A. Issa and A. S. Luyt, Kinetics of alkoxysilanes and organoalkoxysilanes polymerization: a review, *Polymers*, 2019, **11**, 537.
85 Q. Z. Chen, Y. Li, L. Y. Jin, J. M. W. Quinn and P. A. Komesaroff, A new sol–gel process for producing Na_2O-containing bioactive glass ceramics, *Acta Biomater.*, 2010, **6**, 4143–4153.
86 W. Xia and J. Chang, Preparation and characterization of nano-bioactive-glasses (NBG) by a quick alkali-mediated sol–gel method, *Mater. Lett.*, 2007, **61**, 3251–3253.
87 X. Chen, C. GuO and N. Zhao, Preparation and characterization of the sol–gel nano-bioactive glasses modified by the coupling agent gamma-aminopropyltriethoxysilane, *Appl. Surf. Sci.*, 2008, **255**, 466–468.
88 S. I. Roohani-Esfahani, S. Nouri-Khorasani, Z. F. F. Lu, R. C. Appleyard and H. Zreiqat, Effects of bioactive glass nanoparticles on the mechanical and biological behavior of composite coated scaffolds, *Acta Biomater.*, 2011, **7**, 1307–1318.
89 Z. Hong, G. M. Luz, P. J. Hampel, M. Jin, A. Liu, X. Chen and J. F. Mano, Mono-dispersed bioactive glass nanospheres: preparation and effects on biomechanics of mammalian cells, *J. Biomed. Mater. Res., Part A*, 2010, **95**, 747–754.
90 Z. Hong, R. L. Reis and J. F. Mano, Preparation and in vitro characterization of scaffolds of poly(L-lactic acid) containing bioactive glass ceramic nanoparticles, *Acta Biomater.*, 2008, **4**, 1297–1306.
91 G. M. Luz and J. F. Mano, Nanoengineering of bioactive glasses: hollow and dense nanospheres, *J. Nanopart. Res.*, 2013, **15**, 1457–1468.
92 S. Nagayama, K. Kajihara and K. Kanamura, Synthesis of nanocrystalline LaF_3 doped silica glasses by hydrofluoric acid catalyzed sol–gel process, *Mater. Sci. Eng., B*, 2012, **177**, 510–514.
93 R. Li, A. E. Clark and L. L. Hench, An investigation of bioactive glass powders by sol–gel processing, *J. Appl. Biomater.*, 1991, **2**, 231–239.
94 J. R. Jones, Bioactive glass, in *Bioceramics and their clinical applications*, ed. T. Kokubo, Woodhead Publishing Ltd., Cambridge UK, 2008, pp. 266–286.
95 J. R. Jones, New trends in bioactive scaffolds: the importance of nanostructure, *J. Eur. Ceram. Soc.*, 2009, **29**, 1275–1281.
96 J. R. Jones, Review of bioactive glass: from Hench to hybrids, *Acta Biomater.*, 2013, **9**, 4457–4486.

Open Access Article. Published on 11 September 2020. Downloaded on 10/25/2025 7:46:44 PM.
This article is licensed under a Creative Commons Attribution-NonCommercial 3.0 Unported Licence.

97 G. Kaur, G. Pickrell, S. Sriranganathan, V. Kumar and D. Homa, Review and the state of the art: sol–gel and melt quenched bioactive glasses for tissue engineering, *J. Biomed. Mater. Res., Part B*, 2016, **104**, 1248–1275.
98 A. J. Salinas and M. Vallet-Regi, Bioactive ceramics: from bone grafts to tissue engineering, *RSC Adv.*, 2013, **3**, 11116–11131.
99 D. S. Brauer, Bioactive glasses – structure and properties, *Angew. Chem., Int. Ed.*, 2015, **54**, 4160–4181.
100 L. Hupa and K. H. Karlsson, Tailoring of bioactive glasses, in *Bioactive glasses – fundamentals, technology and applications*, ed. A. R. Boccaccinni, D. S. Brauer and L. Hupa, The Royal Society of Chemistry, 2017, pp. 136–160.
101 J. E. Shelby, *Introduction to glass science and technology*, The Royal Society of Chemistry, 2nd edn, 2005.
102 L. Hupa, *Composition property relation of bioactive glasses; materials, properties and applications*, ed. H. Ylanen, Woodhand Publishing, 2018.
103 A. Pedone, G. Malavasi and M. C. Menziani, Computational insight into the effect of CaO/MgO substitution on the structural properties of phospho-silicate bioactive glasses, *J. Phys. Chem. C*, 2009, **113**, 15723–15730.
104 S. J. Watts, R. G. Hill, M. D. O'Donnell and R. V. Law, Influence of magnesia on the structure and properties of bioactive glasses, *J. Non-Cryst. Solids*, 2010, **356**, 517–524.
105 R. G. Hill and D. S. Brauer, Predicting the bioactivity of glasses using the network connectivity or split network models, *J. Non-Cryst. Solids*, 2011, **357**, 3884–3887.
106 A. Tilocca, Structural models of bioactive glasses from molecular dynamics simulations, *Proc. R. Soc. A*, 2009, **465**, 1003–1027.
107 M. W. G. Lockyer, D. Holland and R. Dupree, NMR investigation of the structure of some bioactive and related glasses, *J. Non-Cryst. Solids*, 1995, **188**, 207–219.
108 M. Eden, The split network analysis for exploring composition–structure correlations in multi-component glasses: I. Rationalizing bioactivity-composition trends of bioglasses, *J. Non-Cryst. Solids*, 2011, **357**, 1595–1602.
109 M. D. O'Donnell, Predicting bioactive glass properties from the molecular chemical composition: glass transition temperature, *Acta Biomater.*, 2011, **7**, 2264–2269.
110 M. Eden, NMR studies of oxide based glasses, *Annu. Rep. Prog. Chem., Sect. C: Phys. Chem.*, 2012, **108**, 177–221.
111 M. Vallet-Regi, Ceramics for medical applications, perspective article, *J. Chem. Soc., Dalton Trans.*, 2001, **2**, 97–108.
112 J. R. Jones, L. M. Ehrenfried, P. Sarapavan and L. L. Hench, Controlling ion release from bioactive glass foam scaffolds with antibacterial properties, *J. Mater. Sci.: Mater. Med.*, 2006, **17**, 989–996.
113 Y. Zhao, C. Ning and J. Chang, Sol–gel synthesis of Na_2CaSiO_4 and its in vitro biological behaviors, *J. Sol-Gel Sci. Technol.*, 2009, **52**, 69–74.
114 P. Saravapavan, J. R. Jones, R. S. Pryce and L. L. Hench, Bioactivity of gel–glass powders in the $CaO–SiO_2$ system: a comparison with ternary ($CaO–P_2P_5–SiO_2$) and quaternary glasses ($SiO_2–CaO–P_2O_5–Na_2O$), *J. Biomed. Mater. Res., Part A*, 2003, **66**, 110–119.
115 A. Tilocca and A. N. Cormack, Structural effects of phosphorus inclusion in bioactive silicate glasses, *J. Phys. Chem. B*, 2007, **111**, 14256–14264.
116 D. Arcos, D. C. Greenspan and M. Vallet-Regi, Influence of the stabilization temperature on textural and structural features and ion release in $SiO_2–CaO–P_2O_5$ sol–gel glasses, *Chem. Mater.*, 2002, **14**, 1515–1522.
117 F. Balas, D. Arcos, J. Perez-Pariente and M. Vallet-Regi, Textural properties of $SiO_2–CaO–P_2O_5$ glasses prepared by the sol–gel method, *J. Mater. Res.*, 2001, **16**, 1345–1348.
118 D. Arcos and M. Vallet-Regi, Sol–gel silica-based biomaterials and bone tissue regeneration, *Acta Biomater.*, 2010, **6**, 2874–2888.
119 M. N. Rahman, D. E. Day, D. S. Bal, Q. Fu, S. B. Jung, L. F. Bonewald and A. P. Tomsia, Bioactive glass in tissue engineering, *Acta Biomater.*, 2011, **7**, 2355–2373.
120 P. Kiran, V. Ramakrishna, M. Trebbin, N. K. Udayashankar and H. D. Shashikala, Effective role of CaO/P_2O_5 ratio on $SiO_2–CaO–P_2O_5$ glass system, *J. Adv. Res.*, 2017, **8**, 279–288.
121 P. Sepulveda, J. R. Jones and L. L. Hench, Characterization of melt-derived 45S5 and sol–gel-derived 58S bioactive glasses, *J. Biomed. Mater. Res.*, 2001, **58**, 734–740.
122 A. Oki, B. Parveen, S. Hossain, S. Adeniji and H. Donahue, Preparation and *in vitro* bioactivity of zinc containing sol–gel-derived bioglass materials, *J. Biomed. Mater. Res., Part A*, 2004, **69**, 216–221.
123 A. Moghanian, A. Sedghi, A. Ghorbanoghli and E. Salari, The effect of magnesium content on the in vitro bioactivity, biological behavior and antibacterial activity of sol–gel derived 58S bioactive glass, *Ceram. Int.*, 2018, **44**, 9422–9432.
124 X. Liu, W. Hunag, H. Fu, A. Yao, D. Wang, H. Pan, W. W. Lu, X. Jiang and X. Zhang, Bioactive borosilicate glass scaffolds: in vitro degradation and bioactivity behaviors, *J. Mater. Sci.: Mater. Med.*, 2009, **20**, 1237–1243.
125 J. Lao, J. M. Nedelec and E. Jallot, New strontium-based bioactive glasses: physicochemical reactivity and delivering capability of biologically active dissolution products, *J. Mater. Chem.*, 2009, **19**, 2940–2949.
126 V. G. Varansi, E. Siaz, P. M. Loomer, B. Ancheta, N. Uritani, A. P. Tomsia, S. J. Marshall and G. W. Marshall, Enhanced osteocalcin expression by osteoblast-like cells (MC3T3-E1) exposed to bioactive coating glass ($SiO_2–CaO–P_2O_5–MgO–K_2O–Na_2O$ system) ions, *Acta Biomater.*, 2009, **5**, 3536–3547.
127 L. L. Hench, Challenges for bioceramics in the 21st century, *Am. Ceram. Soc. Bull.*, 2005, **84**, 18–21.
128 H. Aguiar, J. Serra, P. Gonzalez and B. Leon, Influence of the stabilization temperature on the structure of bioactive sol–gel silicate glasses, *J. Am. Chem. Soc.*, 2010, **93**, 2286–2291.
129 G. Kaur, V. Kumar, F. Baino, J. C. Mauro, G. Pickrell, I. Evans and O. Breteano, Mechanical properties of bioactive glasses, ceramics and composites: state of the art review and future challenges, *Mater. Sci. Eng., C*, 2019, **104**, 109895.

Open Access Article. Published on 11 September 2020. Downloaded on 10/25/2025 7:46:44 PM.
This article is licensed under a Creative Commons Attribution-NonCommercial 3.0 Unported Licence.

130 R. F. Lenza, W. L. Vasconcelos, J. R. Jones and L. L. Hench, Surface-modified 3D scaffolds for tissue engineering, *J. Mater. Sci.: Mater. Med.*, 2002, **13**, 837–842.
131 L. L. Hench and J. M. Polak, Third-generation biomedical materials, *Science*, 2002, **295**, 1014–1017.
132 V. Kumar, G. Pickreu, S. G. Waldrop and N. Sriranganathan, Future perspectives of bioactive glasses for the clinical applications, in *Bioactive glasses: potential biomaterials for future therapy*, ed. G. Kaur, Springer Publication, 2017, p. 314.
133 M. Catauro, F. Bollino, R. A. Renella and F. Papale, Sol–gel synthesis of SiO_2–CaO–P_2O_5 glasses: influence of the heat treatment on their bioactivity and biocompatibility, *Ceram. Int.*, 2015, **73**, 12578–12588.
134 M. Dziadek, B. Zagrajczuk, E. Menassck, A. Wegrzynowicz, J. Pawlik and K. Cholewa-Kowalska, Gel derived SiO_2–CaO–P_2O_5 bioactive glasses and glass ceramics modified by SrO addition, *Ceram. Int.*, 2016, **42**, 5842–5857.
135 M. Vallet-Regi, D. Arcos and J. Perez-Pariente, Evolution of porosity during *in vitro* hydroxycarbonate apatite growth in sol–gel glasses, *J. Biomed. Mater. Res.*, 2000, **51**, 23–28.
136 M. Vallet-Regi, C. V. Ragel and A. J. Salinas, Glasses with medical applications, *Eur. J. Inorg. Chem.*, 2003, 1029–1042.
137 M. Hamadouche, A. Meunier, D. C. Greenspan, C. Blanchat, J. P. Zhong, G. P. La Torre and L. Sedel, Long-term *in vivo* bioactivity and degradability of bulk sol–gel bioactive glasses, *J. Biomed. Mater. Res.*, 2001, **54**, 560–566.
138 J. Gil-Albarova, R. Garrido-Lahiguera, A. J. Salinas, J. Roman, A. L. Bueno-Lozano, R. Gil-Albarova and M. Vallet-Regi, The in vivo performance of a sol–gel glass and glass ceramic in the treatment of limited bone defects, *Biomaterials*, 2004, **25**, 4639–4645.
139 I. A. Silver and M. Erecinska, Interactions of osteoblastic and other cells with bioactive glasses and silica in vitro and in vivo, *Materialwiss. Werkstofftech.*, 2003, **34**, 1069–1075.
140 C. Lin, C. Mao, J. Zhang, Y. Li and X. Chen, Healing effect of bioactive glass ointment on full thickness skin wounds, *Biomed. Mater.*, 2012, **7**, 045017.
141 W. H. Xie, X. F. Chen, G. H. Miao, J. Y. Tang and X. L. Fu, Regulation of cellular behaviors of fibroblasts related to wound healing by sol–gel derived bioactive glass particles, *J. Biomed. Mater. Res., Part A*, 2016, **104**, 2420–2429.
142 A. J. Salinas, A. I. Martin and M. Vallet-Regi, Bioactivity of three CaO–P_2O_5–SiO_2 sol–gel glasses, *J. Biomed. Mater. Res.*, 2002, **61**, 524–532.
143 J. Ma, C. Z. Chen, D. G. Wang, Y. Jiao and J. Z. Shi, Effect of magnesia on the degradability and bioactivity of sol–gel derived SiO_2–CaO–MgO–P_2O_5 system glasses, *Colloids Surf., B*, 2010, **81**, 87–95.
144 A. J. Salinas, J. Roman, M. Vallet-Regi, J. M. Oliveria, R. M. Correia and M. H. Fernandes, In vitro bioactivity of glass and glass-ceramics of the $3CaO \cdot P_2O_5$–$CaO \cdot SiO_2$–$CaO \cdot MgO \cdot 2SiO_2$ system, *Biomaterials*, 2000, **21**, 251–257.
145 J. Perez-Pariente, F. Balas and M. Vallet-Regi, Surface and chemical study of $SiO_2 \cdot P_2O_5 \cdot CaO \cdot (MgO)$ bioactive glasses, *Chem. Mater.*, 2000, **12**, 750–755.
146 A. Saboori, M. Rabiee, F. Mutarzadeh, M. Sheikhi, M. Tahiri and M. Karimi, Synthesis, characterizations and in vitro bioactivity of sol–gel derived SiO_2–CaO–P_2O_5–MgO bioglasses, *Mater. Sci. Eng., C*, 2009, **29**, 335–340.
147 M. Bellantone, N. J. Coleman and L. L. Hench, Bacteriostatic action of a novel four-component bioactive glass, *J. Biomed. Mater. Res.*, 2000, **51**, 484–490.
148 G. Hu, L. Xiao, P. Tong, D. Bi, H. Wang, H. Ma, G. Zhu and H. Liu, Antibacterial hemostatic dressings with nanoporous bioglass containing silver, *Int. J. Nanomed.*, 2012, **7**, 2613–2620.
149 J. Pratten, S. N. Nazhat, J. J. Blaker and A. R. Boccaccini, In vitro attachment of staphylococcus epidermidis to surgical sutures with and without Ag-containing bioactive glass coating, *J. Biomater. Appl.*, 2004, **19**, 47–57.
150 M. Catauro, M. G. Raucci, F. De Gaetano and A. Marotta, Antibacterial and bioactive silver-containing $Na_2O_xCaO_x2SiO_2$ glass prepared by sol–gel method, *J. Mater. Sci.: Mater. Med.*, 2004, **15**, 831–837.
151 A. Balamurugan, G. Balossier, S. Kannan, J. Michel, A. H. S. Rebelo and J. M. F. Fereira, Development and in vitro characterization of sol–gel derived CaO–P_2O_5–SiO_2–ZnO bioglass, *Acta Biomater.*, 2007, **3**, 255–262.
152 L. Courtheoux, J. Lao, J. M. Nedelec and E. Jallot, Controlled bioactivity in zinc-doped sol–gel-derived binary bioactive glasses, *J. Phys. Chem. C*, 2008, **112**, 13663–13667.
153 V. Aina, F. Banino, C. Morterra, M. Miola, C. L. Bianchi, G. Malavasi, M. Marchetti and V. Bolis, Influence of the chemical composition on nature and activity of the surface layer of Zn-substituted sol–gel (bioactive) glasses, *J. Phys. Chem. C*, 2011, **115**, 2196–2210.
154 V. Aina, G. Malavasi, A. F. Pla, L. Munaron and C. Morterra, Zinc-containing bioactive glasses: surface reactivity and behaviour towards endothelial cells, *Acta Biomater.*, 2009, **5**, 1211–1222.
155 J. Isaac, J. Nohra, J. Lao, E. Jallot, J. M. Nedelec, A. Berdal and J. M. Sautier, Effects of strontium doped bioactive glass on the differentiation of cultured osteogenic cells, *Eur. Cells Mater.*, 2011, **21**, 130–143.
156 A. J. Leite, A. I. Gonclaves, M. T. Rodrigues, M. E. Gomes and J. F. Mano, Strontium-doped bioactive glass nanoparticles in osteogenic commitment, *ACS Appl. Mater. Interfaces*, 2018, **10**, 23311–23320.
157 P. Naruphontjirakul, A. E. Porter and J. R. Jones, In vitro osteogenesis by intracellular uptake of strontium containing bioactive glass nanoparticles, *Acta Biomater.*, 2018, **66**, 67–80.
158 S. Herasaki, M. Alizadeh, H. Nazarian and D. Sharifi, Physico-chemical and in vitro biological evaluation of strontium/calcium silicophosphate glass, *J. Mater. Sci.: Mater. Med.*, 2010, **21**, 695–705.
159 K. L. Skelton, J. V. Glenn, S. A. Clarke, G. Georgiou, S. P. Valappil, J. C. Knowles, S. N. Nazhat and G. R. Jordan, Effect of ternary phosphate-based glass

Open Access Article. Published on 11 September 2020. Downloaded on 10/25/2025 7:46:44 PM.
This article is licensed under a Creative Commons Attribution-NonCommercial 3.0 Unported Licence.

compositions on osteoblast and osteoblast-like proliferation, differentiation and death in vitro, *Acta Biomater.*, 2007, **3**, 563–572.

160 R. K. Brow, Review: the structure of simple phosphate glasses, *J. Non-Cryst. Solids*, 2000, **263–264**, 1–28.

161 V. Rajendran, A. V. G. Devi, M. Azooz and F. H. El-Batal, Physicochemical studies of phosphate based P_2O_5–Na_2O–CaO–TiO_2 glasses for biomedical applications, *J. Non-Cryst. Solids*, 2006, **353**, 77–84.

162 E. A. Abou Neel, I. Ahmed, J. Pratten, S. N. Nazhat and J. C. Knowles, Characterisation of antibacterial copper releasing degradable phosphate glass fibres, *Biomaterials*, 2005, **26**, 2247–2254.

163 E. A. Abou Neel, L. A. O'Dell, M. E. Smith and J. C. Knowles, Processing, characterisation, and biocompatibility of zinc modified metaphosphate based glasses for biomedical applications, *J. Mater. Sci.: Mater. Med.*, 2008, **19**, 1669–1679.

164 I. Ahmed, C. A. Collins, M. P. Lewis, I. Olsen and J. C. Knowles, Processing, characterisation and biocompatibility of iron-phosphate glass fibres for tissue engineering, *Biomaterials*, 2004, **25**, 3223–3232.

165 R. Shah, A. C. M. Sinanam, J. C. Knowles, N. P. Hunt and M. P. Lewis, Craniofacial muscle engineering using a 3-dimensional phosphate glass fibre construct, *Biomaterials*, 2005, **26**, 1497–1505.

166 J. C. Knowles, Phosphate based glasses for biomedical applications, *J. Mater. Chem.*, 2003, **13**, 2395–2401.

167 D. Carta, J. C. Knowles, M. E. Smith and R. J. Newport, Synthesis and structural characterization of P2O5–CaO–Na_2O sol–gel materials, *J. Non-Cryst. Solids*, 2007, **353**, 1141–1149.

168 D. M. Pickup, P. Guerry, R. M. Moss, J. C. Knowles, M. E. Smith and R. J. Newport, New sol–gel synthesis of a $(CaO)_{0.3}(Na_2O)_{0.2}(P_2O_5)_{0.5}$ bioresorbable glass and its structural characterization, *J. Mater. Chem.*, 2007, **17**, 4777–4784.

169 D. M. Pickup, R. J. Speight, J. C. Knowles, M. E. Smith and R. J. Newport, Sol–gel synthesis and structural characterisation of binary TiO_2–P_2O_5 glasses, *Mater. Res. Bull.*, 2008, **43**, 333–342.

170 D. M. Pickup, R. J. Newport and J. C. Knowles, Sol–gel phosphate-based glass for drug delivery applications, *J. Biomater. Appl.*, 2012, **26**, 613–622.

171 E. A. Abou Neel, W. Chrzanowski, S. P. Vlappil, L. A. O'Dell, D. M. Pickup, M. E. Smith, R. J. Newport and J. C. Knowles, Doping of a high calcium oxide metaphosphate glass with titanium dioxide, *J. Non-Cryst. Solids*, 2009, **355**, 991–1000.

172 E. A. Abou Neel and J. C. Knowles, Physical and biocompatibility studies of novel titanium dioxide doped phosphate-based glasses for bone tissue engineering applications, *J. Mater. Sci.: Mater. Med.*, 2008, **19**, 377–386.

173 E. A. Abou Neel, T. Mizoguchi, M. Ito, M. Bitar, V. Salih and J. C. Knowles, In vitro bioactivity and gene expression by cells cultured on titanium dioxide doped phosphate-based glasses, *Biomaterials*, 2007, **28**, 2967–2977.

174 E. A. Abou Neel, A. M. Young, S. N. Nazhat and J. C. Knowles, A facile synthesis route to prepare microtubes from phosphate glass fibres, *Adv. Mater.*, 2007, **19**, 2856–2862.

175 J. C. Guedes, J. H. Park, N. J. Lakhkar, H. W. Kim, J. C. Knowles and I. B. Wall, TiO_2-doped phosphate glass microcarriers: a stable bioactive substrate for expansion of adherent mammalian cells, *J. Biomater. Appl.*, 2013, **28**, 3–11.

176 M. Bitar, V. Salih, J. C. Knowles and M. P. Lewis, Iron-phosphate glass fiber scaffolds for the hard–soft interface regeneration: the effect of fiber diameter and flow culture condition on cell survival and differentiation, *J. Biomed. Mater. Res., Part A*, 2008, **87**, 1017–1026.

177 C. Vitale-Brovarone, G. Novajra, J. Lousteau, D. Milanese, S. Raimondo and M. Fornaro, Phosphate glass fibres and their role in neuronal polarization and axonal growth direction, *Acta Biomater.*, 2012, **8**, 1125–1136.

178 E. A. Abou Neel, D. M. Pickup, S. P. Valappil, R. J. Newport and J. C. Knowles, Bioactive functional materials: a perspective on phosphate-based glasses, *J. Mater. Chem. B*, 2009, **19**, 690–701.

179 F. F. Sene, J. R. Martinelli and E. Okumo, Synthesis and characterization of phosphate glass microspheres for radiotherapy applications, *J. Non-Cryst. Solids*, 2008, **354**, 4887–4893.

180 S. N. Nazhat, E. A. Abou Neel, A. Kidane, I. Ahmed, C. Hope, M. Kershaw, P. D. Lee, E. Stride, N. Saffari, J. C. Knowles and R. A. Brown, Controlled microchannelling in dense collagen scaffolds by soluble phosphate glass fibers, *Biomacromol*, 2006, **8**, 543–551.

181 I. Ahmed, P. S. Cronin, E. A. Abou Neel, A. J. Parsons, J. C. Knowles and C. D. Rudd, Retention of mechanical properties and cytocompatibility of a phosphate-based glass fiber/polylactic acid composite, *J. Biomed. Mater. Res., Part B*, 2009, **89**, 18–27.

182 V. Salih, K. Franks, M. James, G. W. Hastings, J. C. Knowles and I. Olsen, Development of soluble glasses for biomedical use Part II: the biological response of human osteoblast cell lines to phosphate-based soluble glasses, *J. Mater. Sci.: Mater. Med.*, 2000, **11**, 615–620.

183 M. Bitar, V. Salih, V. Mudera, J. C. Knowles and M. P. Lewis, Soluble phosphate glasses: in vitro studies using human cells of hard and soft tissue origin, *Biomaterials*, 2004, **25**, 2283–2292.

184 J. E. Gough, P. Christian, C. A. Scotchford, C. D. Rudd and I. A. Jones, Synthesis, degradation, and *in vitro* cell responses of sodium phosphate glasses for craniofacial bone repair, *Biomed. Mater. Res.*, 2002, **59**, 481–489.

185 S. V. Dorozhkin and M. Epple, Biological and medical significance of calcium phosphates, *Angew. Chem.*, 2002, **41**, 3130–3146.

186 J. M. Bouler, R. Z. LeGeros and G. Daculsi, Biphasic calcium phosphates: influence of three synthesis parameters on the HA/β-TCP ratio, *J. Biomed. Mater. Res.*, 2000, **51**, 680–684.

 This journal is © The Royal Society of Chemistry 2020

Open Access Article. Published on 11 September 2020. Downloaded on 10/25/2025 7:46:44 PM.
This article is licensed under a Creative Commons Attribution-NonCommercial 3.0 Unported Licence.

187 M. Vallet-Regi and D. Arcos, Silicon substituted hydroxyapatites. A method to upgrade calcium phosphate based implants, *J. Mater. Chem.*, 2005, **15**, 1509–1516.
188 S. P. Valappil, D. M. Pickup, D. L. Carroll, C. K. Hope, J. Pratten, R. J. Newport, M. E. Smith, M. Wilson and J. C. Knowles, Effect of silver content on the structure and antibacterial activity of silver-doped phosphate-based glasses, *Antimicrob. Agents Chemother.*, 2007, **51**, 4453–4461.
189 J. K. Christie, R. I. Ainsworth and N. H. de Leeuw, Ab initio molecular dynamics simulations of structural changes associated with the incorporation of fluorine in bioactive phosphate glasses, *Biomaterials*, 2014, **35**, 6164–6171.
190 N. J. Lahkar, E. A. Abou Neel, V. Salih and J. C. Knowles, Strontium oxide doped quaternary glasses: effect on structure, degradation and cytocompatibility, *J. Mater. Sci.: Mater. Med.*, 2009, **20**, 1339–1346.
191 K. M. Z. Hussain, U. Patel, A. R. Kennedy, M. P. Laura, V. Sottile, D. M. Grant, B. E. Scammell and I. Ahmed, Porous calcium phosphate glass microspheres for orthobiologic applications, *Acta Biomater.*, 2018, **72**, 396–406.
192 S. Maeno, Y. Niki, H. Matsumoto, H. Morioka, T. Yatabe, A. Funayama, Y. Toyama, T. Taguchi and J. Tanaka, The effect of calcium ion concentration on osteoblast viability, proliferation and differentiation in monolayer and 3D culture, *Biomaterials*, 2005, **26**, 4847–4855.
193 S. Yoshizawa, A. Brown, A. Bachowsky and C. Sfeir, Role of magnesium ions on osteogenic response in bone marrow stromal cells, *Connect. Tissue Res.*, 2014, **55**, 155–159.
194 M. Julien, S. Khoshniat, A. Lacreusette, M. Gatius, A. Bozec, E. F. Wagner, Y. Wittrant, M. Masson, P. Weiss, L. Beck, D. Magne and J. Guicheux, Phosphate-dependent regulation of MGP in osteoblasts: role of ERK1/2 and Fra-1, *J. Bone Miner. Res.*, 2009, **24**, 1856–1868.
195 A. Michael-Titus, P. Revest and P. Shortland, Elements of cellular and molecular neurosciences, in *The nervous system*, 2nd Edition, 2010, pp. 31–46.
196 U. Patel, R. M. Moss, K. M. Z. Hossain, A. R. Kennedy, E. R. Barney, I. Ahmed and A. C. Hannon, Structural and physico-chemical analysis of calcium/strontium substituted, near-invert phosphate based glasses for biomedical applications, *Acta Biomater.*, 2017, **60**, 109–127.
197 I. Ahmed, E. A. Abou Neel, S. P. Valappil, S. N. Nazhat, D. M. Pickup, D. Carta, D. L. Carroll, R. J. Newport, M. E. Smith and J. C. Knowles, The structure and properties of silver-doped phosphate-based glasses, *J. Mater. Sci.*, 2007, **42**, 9827–9835.
198 I. Ahmed, D. Reddy, M. Wilson and J. C. Knowles, Antimicrobial effect of silver-doped phosphate-based glasses, *J. Biomed. Mater. Res., Part A*, 2006, **79**, 618–626.
199 V. Mourino, J. P. Cattalini and A. R. Boccaccini, Metallic ions as therapeutic agents in tissue engineering scaffolds: an overview of their biological applications and strategies for new developments, *J. R. Soc., Interface*, 2012, **9**, 401–419.
200 L. Weng, S. K. Boda, M. J. Teusink, F. D. Shuler, X. Li and J. Xie, Binary doping of strontium and copper enhancing osteogenesis and angiogenesis of bioactive glass nanofibers while suppressing osteoclast activity, *ACS Appl. Mater. Interfaces*, 2017, **9**, 24484–24496.
201 H. Zhu, Z. Pan, B. Chen, B. Lee, S. M. Mahurin, S. H. Overbury and S. Dai, Synthesis of ordered mixed titania and silica mesostructured monoliths for gold catalysts, *J. Phys. Chem. B*, 2004, **108**, 20038–20044.
202 J. Tang, J. Liu, J. Yang, Z. Feng, F. Fan and Q. Yang, Mesoporous titanosilicates with high loading of titanium synthesized in mild acidic buffer solution, *J. Colloid Interface Sci.*, 2009, **335**, 203–209.
203 W. I. Kim and I. K. J. Hong, Synthesis of monolithic titania–silica composite aerogels with supercritical drying process, *J. Ind. Eng. Chem.*, 2003, **9**, 728–734.
204 J. A. Melero, J. M. Arsuaga, P. de Frutos, J. Iglesias, J. Sainz and S. Blazquez, Direct synthesis of titanium-substituted mesostructured materials using non-ionic surfactants and titanocene dichloride, *Microporous Mesoporous Mater.*, 2005, **86**, 364–373.
205 O. Ruzimuradov, S. Nurmanov, Y. Kodani, R. Takahashi and I. Yamada, Morphology and dispersion control of titania–silica monolith with macro–meso pore system, *J. Sol-Gel Sci. Technol.*, 2012, **64**, 684–693.
206 W. H. Zhang, J. Lu, B. Han, M. Li, J. Xiu, P. Ying and C. Li, Direct synthesis and characterization of titanium-substituted mesoporous molecular sieve SBA-15, *Chem. Mater.*, 2002, **14**, 3413–3421.
207 G. Liu, Y. Liu, G. Yang, S. Li, Y. Zu, W. Zhang and M. Jia, Preparation of titania–silica mixed oxides by a sol–gel route in the presence of citric acid, *J. Phys. Chem. C*, 2009, **113**, 9345–9351.
208 H. J. Chen, L. Wang and W. Y. Chiu, Chelation and solvent effect on the preparation of titania colloids, *Mater. Chem. Phys.*, 2007, **101**, 12–19.
209 W. Rupp, N. Husing and U. Schubert, Preparation of silica–titania xerogels and aerogels by sol–gel processing of new single-source precursors, *J. Mater. Chem.*, 2002, **12**, 2594–2596.
210 R. F. Lenza and W. L. Vasconcelos, Synthesis of titania–silica materials by sol–gel, *Mater. Res.*, 2002, **5**, 497–502.
211 J. Konishi, K. Fujita, K. Nakanishi and K. Hirao, Monolithic TiO_2 with controlled multiscale porosity via a template-free sol–gel process accompanied by phase separation, *Chem. Mater.*, 2006, **18**, 6069–6074.
212 K. Nakanishi and N. Tanaka, Sol–gel with phase separation. Hierarchically porous materials optimized for high-performance liquid chromatography separations, *Acc. Chem. Res.*, 2007, **40**, 863–873.
213 O. N. Ruzimuradov, Formation of bimodal porous silica–titania monoliths by sol–gel route, *IOP Conf. Ser.: Mater. Sci. Eng.*, 2011, **18**, 032004.
214 K. Deshmukh, T. Kovarik, T. Krenek, T. Stitch and D. Docheva, Microstructural evaluation and thermal properties of sol–gel derived silica–titania based porous glasses, *J. Phys.: Conf. Ser.*, 2020, **1527**, 012031.
215 K. Nakanishi, Preparation of SiO_2–TiO_2 gels with controlled pore structure via sol–gel route, *Bull. Inst. Chem. Res., Kyoto Univ.*, 1992, **70**, 144–151.

Open Access Article. Published on 11 September 2020. Downloaded on 10/25/2025 7:46:44 PM.
This article is licensed under a Creative Commons Attribution-NonCommercial 3.0 Unported Licence.

216 S. Flaig, J. Akbarzadeh, P. Dolcet, S. Gross, H. Peterlik and N. Husing, Hierarchically organized silica–titania monoliths prepared under purely aqueous conditions, *Chem.–Eur. J.*, 2014, **20**, 17409–17419.

217 P. R. Aravind, P. Shjesh, P. Mukundan and K. G. K. Warrier, Silica–titania aerogel monoliths with large pore volume and surface area by ambient pressure drying, *J. Sol-Gel Sci. Technol.*, 2009, **52**, 328–334.

218 J. F. Destino, N. A. Dudukovic, M. A. Johnson, D. T. Nguyen, T. D. Yee, G. C. Egan, A. M. Sawvel, W. A. Steele, T. F. Baumann, E. B. Duoss, T. Suratwala and R. Dylla-Spears, 3D printed optical quality silica and silica–titania glasses from sol–gel feedstocks, *Adv. Mater. Technol.*, 2018, **3**, 1700323.

219 G. Scannell, A. Koike and L. Hunag, Structure and thermomechanical response of TiO_2–SiO_2 glasses to temperature, *J. Non-Cryst. Solids*, 2016, **447**, 238–247.

220 G. Brusatin, M. Guglielmi, P. Innocenzi, A. Martucci, G. Battaglin, S. Pelli and G. Righini, Microstructural and optical properties of sol–gel silica–titania waveguides, *J. Non-Cryst. Solids*, 1997, **220**, 202–209.

221 K. Shingyouchi and S. Konishi, Gradient-index doped silica rod lenses produced by a sol gel method, *Appl. Opt.*, 1990, **29**, 4061–4063.

222 Z. Deng, J. Wang, Y. Zhang, Z. Weng, Z. Zhang, B. Zhou, J. Shen and L. Chen, Preparation and photocatalytic activity of TiO_2–SiO_2 binary aerogels, *Nanostruct. Mater.*, 1999, **11**, 1313–1318.

223 D. C. M. Dutoit, M. Schneider and A. Baiker, Titania-silica mixed oxides: I. Influence of sol–gel and drying conditions on structural properties, *J. Catal.*, 1995, **153**, 165–176.

224 Z. Xu, Y. Jia, Z. Hao, M. Liu and L. Chen, Preparation and characterization of silica–titania aerogel-like balls by ambient pressure drying, *J. Sol-Gel Sci. Technol.*, 2007, **41**, 203–207.

225 B. Malinowska, J. Walendziewski, D. Robert, J. V. Weber and M. Stolarski, The study of photocatalytic activities of titania and titania–silica aerogels, *Appl. Catal., B*, 2003, **46**, 441–451.

226 Z. Deng, E. Breval and C. G. Pantano, Colloidal sol/gel processing of ultra-low expansion TiO_2/SiO_2 glasses, *J. Non-Cryst. Solids*, 1988, **100**, 364–370.

227 S. Satoh, K. Susa and I. Matsuyama, Sol–gel derived binary silica glasses with high refractive index, *J. Non-Cryst. Solids*, 1992, **146**, 121–128.

228 S. M. El-Bashir, Physical properties Nd^{3+} doped (SiO_2–TiO_2) monolithic glass for photoresistor applications, *Mater. Res. Express*, 2017, **4**, 115203.

229 L. Guangwu and L. Yangang, Preparation and characterization of silica–titania aerogel monoliths by sol gel method, *IEEE 16th International Conference on Nanotechnology (IEEE-NANO), Sendai, Japan, August 22–25*, 2016, pp. 85–88.

230 S. Pandey and S. B. Mishra, Sol–gel derived organic–inorganic hybrid materials: synthesis, characterizations and applications, *J. Sol-Gel Sci. Technol.*, 2011, **59**, 73–94.

231 S. H. Mir, L. A. Nagahara, T. Thundat, P. Mokarian-Tabari, H. Furukawa and A. Khosla, Review – organic–inorganic hybrid functional materials: an integrated platform for applied technologies, *J. Electrochem. Soc.*, 2018, **165**, B3137–B3156.

232 G. Kickelbick, Introduction to hybrid materials, in *Hybrid materials: synthesis, characterization and applications*, ed. G. Kickelbick, Wiley-VCH Verlag, GmbH & Co KGaA, Weinheim, 2007, pp. 1–48.

233 F. Baino, E. Fiume, M. Miola and E. Verne, Bioactive sol–gel glasses: processing, properties, and applications, *Int. J. Appl. Ceram. Technol.*, 2018, **15**, 841–860.

234 I. Gill, Bio-doped nanocomposite polymers: sol–gel bioencapsulates, *Chem. Mater.*, 2001, **13**, 3404–3421.

235 E. M. Vallient and J. R. Jones, Softening bioactive glass for bone regeneration: sol–gel hybrid materials, *Soft Matter*, 2011, **7**, 5083–5095.

236 I. Crouzet and D. Leclercq, Polyphosphazene–metal oxide hybrids by nonhydrolytic sol–gel processes, *J. Mater. Chem.*, 2000, **10**, 1195–1201.

237 R. Tamaki, K. Naka and Y. Chujo, Synthesis of poly(*N*,*N*-dimethylacrylamide)/silica gel polymer hybrids by *in situ* polymerization method, *Polym. J.*, 1998, **30**, 60–65.

238 M. Toki, T. Y. Chow, T. Ohnaka, H. Samura and T. Saegusa, Structure of poly(vinylpyrrolidone)–silica hybrid, *Polym. Bull.*, 1992, **29**, 653–660.

239 K. Landfester, Miniemulsion polymerization and the structure of polymer and hybrid nanoparticles, *Angew. Chem.*, 2009, **48**, 4488–4507.

240 F. Yang and G. L. Nelson, PMMA/silica nanocomposite studies: synthesis and properties, *J. Appl. Polym. Sci.*, 2004, **91**, 3844–3850.

241 K. A. Mauritz and C. K. Jones, Novel poly (*n*-butyl methacrylate)/titanium oxide alloys produced by sol–gel process for titanium alkoxides, *J. Appl. Polym. Sci.*, 1990, **40**, 1401–1420.

242 X. Zhao, Y. Wu, Y. Du, X. Chen, B. Lei, Y. Xue and P. X. Ma, A highly bioactive and biodegradable poly(glycerolsebacate)–silica glass hybrid elastomer with tailored mechanical properties for bone tissue regeneration, *J. Mater. Chem. B*, 2015, **3**, 3222–3233.

243 M. Kamitakahara, M. Kawashita, N. Miyata, T. Kokubo and T. Nakamura, Bioactivity and mechanical properties of polydimethylsiloxane (PDMS)–CaO–SiO_2 hybrids with different calcium contents, *J. Mater. Sci.: Mater. Med.*, 2002, **13**, 1015–1020.

244 D. Sanchez-Tellez, L. Tellez-Jurado and L. M. Rodriguez-Lorenzo, Optimization of the CaO and P_2O_5 contents on PDMS–SiO_2–CaO–P_2O_5 hybrids intended for bone regeneration, *J. Mater. Sci.*, 2015, **50**, 5993–6006.

245 A. P. V. Pereira, W. L. Vasconcelos and R. L. Orefice, Novel multicomponent silicate–poly(vinyl alcohol) hybrids with controlled reactivity, *J. Non-Cryst. Solids*, 2000, **273**, 180–185.

246 A. I. Martin, A. J. Salinas and M. Vallet-Regi, Bioactive and degradable organic–inorganic hybrids, *J. Eur. Ceram. Soc.*, 2005, **25**, 3533–3538.

 This journal is © The Royal Society of Chemistry 2020

Open Access Article. Published on 11 September 2020. Downloaded on 10/25/2025 7:46:44 PM.
This article is licensed under a Creative Commons Attribution-NonCommercial 3.0 Unported Licence.

247 M. Catauro, F. Bollino, F. Papale, M. Gallicchio and S. Pacifico, Influence of the polymer amount on bioactivity and biocompatibility of SiO_2/PEG hybrid materials synthesized by sol–gel technique, *Mater. Sci. Eng., C*, 2015, **48**, 548–555.
248 J. H. Song, B. H. Yoon, H. E. Kim and H. W. Kim, Bioactive and degradable hybridized nanofibers of gelatin–siloxane for bone regeneration, *J. Biomed. Mater. Res., Part A*, 2008, **84**, 875–884.
249 E. J. Lee, S. H. Jun, H. E. Kim, H. W. Kim, Y. H. Koh and J. H. Jang, Silica xerogel–chitosan nano-hybrids for use as drug eluting bone replacement, *J. Mater. Sci.: Mater. Med.*, 2010, **21**, 207–214.
250 E. J. Lee, D. S. Shin, H. E. Kim, H. W. Kim, Y. H. Koh and J. H. Jang, Membrane of hybrid chitosan–silica xerogel for guided bone regeneration, *Biomaterials*, 2009, **30**, 743–750.
251 E. J. Lee, S. H. Teng, T. S. Jang, P. Wang, S. W. Yook, H. E. Kim and Y. H. Koh, Nanostructured poly(ε-caprolactone)–silica xerogel fibrous membrane for guided bone regeneration, *Acta Biomater.*, 2010, **6**, 3557–3565.
252 M. Catauro, F. Bollino, F. Papale, S. Marciano and S. Pacifico, TiO_2/PCL hybrid materials synthesized via sol–gel technique for biomedical applications, *Mater. Sci. Eng., C*, 2015, **47**, 135–141.
253 M. Catauro, F. Bollino, F. Papale, P. Mozetic, A. Rainer and M. Trombetta, Biological response of human mesenchymal stromal cells to titanium grade 4 implants coated with PCL/ZrO_2 hybrid materials synthesized by sol–gel route: in vitro evaluation, *Mater. Sci. Eng., C*, 2014, **45**, 395–401.
254 L. Ren, K. Tsuru, S. Hayakawa and A. Osaka, Sol–gel preparation and in vitro deposition of apatite on porous gelatin–siloxane hybrids, *J. Non-Cryst. Solids*, 2001, **285**, 116–122.
255 L. Ren, K. Tsuru, S. Hayakawa and A. Osaka, Novel approach to fabricate porous gelatin–siloxane hybrids for bone tissue engineering, *Biomaterials*, 2002, **23**, 4765–4773.
256 S. S. Silva, R. A. S. Ferreira, L. Fu, L. D. Carlos, J. F. Mano, R. L. Reis and J. Rocha, Functional nanostructured chitosan–siloxane hybrids, *J. Mater. Chem.*, 2005, **15**, 3952–3961.
257 C. Ohtsuki, T. Miyazaki and M. Tanihara, Development of bioactive organic–inorganic hybrid for bone substitutes, *Mater. Sci. Eng., C*, 2002, **22**, 27–34.
258 R. Gupta and A. Kumar, Bioactive materials for biomedical applications using sol–gel technology, *Biomed. Mater.*, 2008, **3**, 034005.
259 B. Szczesniak, J. Choma and M. Joroniec, Major advances in the development of ordered mesoporous materials, *Chem. Commun.*, 2020, **56**, 7836–7848.
260 M. Thommes, K. Kaneko, A. V. Neimark, J. P. Olivier, F. Rodriguez-Reinoso, J. Rouquerol and K. S. W. Sing, Physisorption of gases, with special reference to the evaluation of surface area and pore size distribution (IUPAC Technical Report), *Pure Appl. Chem.*, 2015, **87**, 1051–1069.
261 J. R. Jones, P. D. Lee and L. L. Hench, Hierarchical porous materials for tissue engineering, *Philos. Trans. R. Soc., A*, 2006, **364**, 263–281.
262 N. Pal and A. Bhaumik, Soft templating strategies for the synthesis of mesoporous materials: inorganic, organic–inorganic hybrids and purely organic solids, *Adv. Colloid Interface Sci.*, 2013, **189–190**, 21–41.
263 D. Arcos and M. Vallet-Regi, Bioceramics for drug delivery, *Acta Mater.*, 2013, **61**, 890–911.
264 C. Wu and J. Chang, Mesoporous bioactive glasses: structure characteristics, drug/growth factor delivery and bone regeneration application, *Interface Focus*, 2012, **2**, 292–306.
265 P. Horcajada, A. Ramila, J. Perez-Pariente and M. Vallet-Regi, Influence of pore size of MCM-41 matrices on drug delivery rate, *Microporous Mesoporous Mater.*, 2004, **68**, 105–109.
266 Y. Li, B. P. Bastakoti and Y. Yamauchi, Smart soft-templating synthesis of hollow mesoporous bioactive glass spheres, *Chem.–Eur. J.*, 2015, **21**, 8038–8042.
267 G. S. Pappas, P. Liatsi, I. A. Kartsonakis, I. Danilidis and G. Kordas, Synthesis and characterization of new SiO_2–CaO hollow nanospheres by sol–gel method: bioactivity of the new system, *J. Non-Cryst. Solids*, 2008, **354**, 755–760.
268 K. Zheng, J. A. Bortuzzo, Y. Liu, W. Li, M. Pischetsrieder, J. Roether, M. Lu and A. R. Boccaccini, Bio-templated bioactive glass particles with hierarchical macro–nano porous structure and drug delivery capability, *Colloids Surf., B*, 2015, **135**, 825–832.
269 X. Li, M. Guohou, C. Xiaofeng, Y. Guang, L. Hui, M. Cong, S. Xiongjun and N. Chengyun, Investigation of radial mesoporous bioactive glass particles as drug carriers for inhibition of tumor cells, *Sci. Adv. Mater.*, 2017, **9**, 562–570.
270 D. Arcos, A. Lopez-Noriega, E. Ruiz-Hernandez, O. Terasaki and M. Vallet-Regi, Ordered mesoporous microspheres for bone grafting and drug delivery, *Chem. Mater.*, 2009, **21**, 1000–1009.
271 K. Zheng, M. Lu, B. Rutkowski, X. Dai, Y. Yang, N. Taccardi, U. Stachewicz, A. Czyrska-Filemonowicz, N. Huser and A. R. Boccaccini, ZnO quantum dots modified bioactive glass nanoparticles with pH-sensitive release of Zn ions, fluorescence, antibacterial and osteogenic properties, *J. Mater. Chem. B*, 2016, **4**, 7936–7949.
272 O. Tsigkou, S. Labbaf, M. M. Stevens, A. E. Porter and J. R. Jones, Monodispersed bioactive glass submicron particles and their effect on bone marrow and adipose tissue-derived stem cells, *Adv. Healthcare Mater.*, 2014, **3**, 115–125.
273 Q. Hu, Y. Li, G. Miao, N. Zhao and X. Chen, Size control and biological properties of monodispersed mesoporous bioactive glass sub-micron spheres, *RSC Adv.*, 2014, **4**, 22678–22687.
274 P. Kolhar, A. C. Anselmo, V. Gupta, K. Pant, B. Prabhakarpandian, E. Ruoslahti and S. Mitragotri, Using shape effects to target antibody-coated nanoparticles to lung and brain endothelium, *Proc. Natl. Acad. Sci. U. S. A.*, 2013, **110**, 10753–10758.

Open Access Article. Published on 11 September 2020. Downloaded on 10/25/2025 7:46:44 PM.
This article is licensed under a Creative Commons Attribution-NonCommercial 3.0 Unported Licence.

275 R. Colquhoun and K. E. Tanner, Mechanical behaviour of degradable phosphate glass fibres and composites: a review, *Biomed. Mater.*, 2015, **11**, 14105.
276 Y. Li, X. Chen, C. Ning, B. Yuan and Q. Hu, Facile synthesis of mesoporous bioactive glasses with controlled shapes, *Mater. Lett.*, 2015, **161**, 605–608.
277 E. El-Meliegy, M. Mabrouk, S. A. M. El-Sayed, B. M. Abd El-Hady, M. R. Shehata and W. M. Hosny, Novel Fe_2O_3-doped glass/chitosan scaffolds for bone tissue replacement, *Ceram. Int.*, 2018, **44**, 9140–9151.
278 S. A. M. El-Sayed, M. Mabrouk, M. E. Khallaf, B. M. Abd El-Hady, E. El-Meliegy and M. R. Shehata, Antibacterial, drug delivery, and osteoinduction abilities of bioglass/chitosan scaffolds for dental applications, *J. Drug Delivery Sci. Technol.*, 2020, **57**, 101757.
279 F. Baino, E. Fiume, M. Miola, F. Leone, B. Onida and E. Verne, Fe-doped bioactive glass-derived scaffolds produced by sol–gel foaming, *Mater. Lett.*, 2019, **235**, 207–211.
280 T. Charoensuk, C. Sirisathitkul, U. Boonyang, I. J. Macha, J. Santos, D. Grossin and B. Ben-Nissan, In vitro bioactivity and stem cells attachment of three-dimensionally ordered macroporous bioactive glass incorporating iron oxides, *J. Non-Cryst. Solids*, 2016, **452**, 62–73.
281 J. Mesquita-Guimarães, L. Ramos, R. Detsch, B. Henriques, M. C. Fredel, F. S. Silva and A. R. Boccaccini, Evaluation of in vitro properties of 3D micro–macro porous zirconia scaffolds coated with 58S bioactive glass using MG-63 osteoblast-like cells, *J. Eur. Ceram. Soc.*, 2019, **39**, 2545–2558.
282 S. Ni, X. Li, P. Yang, S. Ni, F. Hong and T. J. Webster, Enhanced apatite-forming ability and antibacterial activity of porous anodic alumina embedded with CaO–SiO_2–Ag_2O bioactive materials, *Mater. Sci. Eng., C*, 2016, **58**, 700–708.
283 M. Yazdimamaghani, D. Vashae, S. Assefa, K. J. Walker, S. V. Madihally, G. A. Kohler and L. Tayebi, Hybrid macroporous gelatin/bioactive-glass/nanosilver scaffolds with controlled degradation behavior and antimicrobial activity for bone tissue engineering, *J. Biomed. Nanotechnol.*, 2014, **10**(6), 911–931.
284 F. Sharifianjazi, N. Parvin and M. Tahriri, Synthesis and characteristics of sol–gel bioactive SiO_2–P_2O_5–CaO–Ag_2O glasses, *J. Non-Cryst. Solids*, 2017, **476**, 108–113.
285 S. Z. Jalise, N. Baheiraei and F. Bagheri, The effects of strontium incorporation on a novel gelatin/bioactive glass bone graft: in vitro and in vivo characterization, *Ceram. Int.*, 2018, **44**, 14217–14227.
286 M. Shaltooki, G. Dini and M. Mehdikhani, Fabrication of chitosan-coated porous polycaprolactone/strontium-substituted bioactive glass nanocomposite scaffold for bone tissue engineering, *Mater. Sci. Eng., C*, 2019, **105**, 110138.
287 S. Amudha, J. R. Ramya, K. T. Arul, A. Deepika, P. Sathiamurthi, B. Mohana, K. Asokan, C. L. Dong and S. N. Kalkura, Enhanced mechanical and biocompatible properties of strontium ions doped mesoporous bioactive glass, *Composites, Part B*, 2020, **196**, 108099.
288 D. Zamani, F. Moztarzadeh and D. Bizari, Alginate-bioactive glass containing Zn and Mg composite scaffolds for bone tissue engineering, *Int. J. Biol. Macromol.*, 2019, **137**, 1256–1267.
289 Y. Hong, X. Chen, X. Jing, H. Fan, Z. Gu and X. Zhang, Fabrication and drug delivery of ultrathin mesoporous bioactive glass hollow fibers, *Adv. Funct. Mater.*, 2010, **20**, 1503–1510.
290 G. Poologasundarampillai, D. Wang, S. Li, J. Nakamura, R. Bradley, P. D. Lee, M. M. Stevens, D. S. McPhail, T. Kasuga and J. R. Jones, Cotton–wool-like bioactive glasses for bone regeneration, *Acta Biomater.*, 2014, **10**, 3733–3746.
291 F. Baino, G. Novajra, V. Miguez-Pacheco, A. R. Boccaccini and C. Vitale-Bovarone, Bioactive glasses: special applications outside the skeletal system, *J. Non-Cryst. Solids*, 2016, **432**, 15–30.
292 S. M. Rabie, N. Nazparvar, M. Azizian, D. Vashaee and L. Tayebi, Effect of ion substitution on properties of bioactive glasses: a review, *Ceram. Int.*, 2015, **41**, 7241–7251.
293 J. Faure, R. Drevet, A. Lemelle, N. B. Jaber, A. Tara, H. El Btaouri and H. Benhayoune, A new sol–gel synthesis of 45S5 bioactive glass using an organic acid as catalyst, *Mater. Sci. Eng., C*, 2015, **47**, 407–412.
294 J. H. Lopes, O. M. V. M. Bueno, I. O. Mazali and C. A. Bertran, Investigation of citric acid-assisted sol–gel synthesis coupled to the self-propagating combustion method for preparing bioactive glass with high structural homogeneity, *Mater. Sci. Eng., C*, 2019, **97**, 669–678.
295 M. H. Thibault, C. Comeau, G. Vienneau, J. Robichaud, D. Brown, R. Bruening, L. J. Martin and Y. Djaoued, Assessing the potential of boronic acid/chitosan/bioglass composite, *Mater. Sci. Eng., C*, 2020, **110**, 110674.
296 L. L. Hench, The story of bioglass, *J. Mater. Sci.: Mater. Med.*, 2006, **17**, 967–978.
297 F. Baino, Bioactive glass – when glass science and technology meet regenerative medicine, *Ceram. Int.*, 2018, **44**, 14953–14966.
298 L. Hupa, Composition–property relations of bioactive silicate glasses, in *Bioactive glasses: materials properties and applications*, ed. H. Ylanen, Woodhead Publishing, 2nd edn, 2018, pp. 1–36.
299 A. M. Deliormanli, X. Liu and M. N. Rahaman, Evaluation of borate bioactive glass scaffolds with different pore sizes in a rat subcutaneous implantation model, *J. Biomater. Appl.*, 2014, **28**, 643–653.
300 F. A. Shah, D. S. Brauer, N. Desai, R. G. Hill and K. A. Hing, Fluoride-containing bioactive glasses and Bioglass® 45S5 form apatite in low pH cell culture medium, *Mater. Lett.*, 2014, **119**, 96–99.
301 O. H. Andersson, G. Liu, K. H. Karlsson, L. Niemi, J. Miettinen and J. Juhanoja, In vivo behaviour of glasses in the SiO_2–Na_2O–CaO–P_2O_5–Al_2O_3–B_2O_3 system, *J. Mater. Sci.: Mater. Med.*, 1990, **1**, 219–227.

Open Access Article. Published on 11 September 2020. Downloaded on 10/25/2025 7:46:44 PM.
This article is licensed under a Creative Commons Attribution-NonCommercial 3.0 Unported Licence.

302 M. Brink, T. Turunen, R. P. Happonen and A. Yli-Urpo, Compositional dependence of bioactivity of glasses in the system Na_2O–K_2O–MgO–CaO–B_2O_3–P_2O_5–SiO_2, *J. Biomed. Mater. Res.*, 1997, **37**, 114–121.

303 G. Lusvardi, G. Malavasi, L. Menabue and M. C. Menziani, Synthesis, characterization, and molecular dynamics simulation of Na_2O–CaO–SiO_2–ZnO glasses, *J. Phys. Chem. B*, 2002, **106**, 9753–9760.

304 A. W. Wren, A. Coughlan, C. M. Smith, S. P. Hudson, F. R. Laffir and M. R. Towler, Investigating the solubility and cytocompatibility of CaO–Na_2O–SiO_2/TiO_2 bioactive glasses, *J. Biomed. Mater. Res., Part A*, 2015, **103**, 709–720.

305 S. Pourshahrestani, E. Zeimaran, N. A. Kadri, N. Gargiulo, S. Samuel, S. V. Naveen, T. Kamarul and M. R. Towler, Gallium-containing mesoporous bioactive glass with potent hemostatic activity and antibacterial efficacy, *J. Mater. Chem. B*, 2016, **4**, 71–86.

306 G. Kaur, O. P. Pandey, K. Singh, D. Homa, B. Scott and G. Pickrell, A review of bioactive glasses: their structure, properties, fabrication and apatite formation, *J. Biomed. Mater. Res., Part A*, 2014, **102**, 254–274.

307 O. M. Goudouri, E. Kontonasaki, U. Lohbauer and A. R. Boccaccini, Antibacterial properties of metal and metalloid ions in chronic periodontitis and peri-implantitis therapy, *Acta Biomater.*, 2014, **10**, 3795–3810.

308 X. Li, X. Wang, D. He and J. Shi, Synthesis and characterization of mesoporous CaO–MO–SiO_2–P_2O_5 (M = Mg, Zn, Cu) bioactive glasses/composites, *J. Mater. Chem.*, 2008, **18**, 4103–4109.

309 E. Verne, S. D. Nunzio, M. Bosetti, P. Appendino, C. V. Brovarone, G. Maina and M. Cannas, Surface characterization of silver-doped bioactive glass, *Biomaterials*, 2005, **26**, 5111–5119.

310 M. Yamaguchi, Role of zinc in bone metabolism and preventive effect on bone disorder, *Biomed. Res. Trace Elem.*, 2007, **18**, 346–366.

311 D. Boyd, O. M. Clarkin, A. W. Wren and M. R. Towler, Zinc-based glass polyalkenoate cements with improved setting times and mechanical properties, *Acta Biomater.*, 2008, **4**, 425–431.

312 H. Zreqat, S. M. Valenzuela, B. B. Nissan, R. Roest, C. Knabe, R. J. Radlanski, H. Renz and P. J. Evans, The effect of surface chemistry modification of titanium alloy on signalling pathways in human osteoblasts, *J. Biomed. Mater. Res.*, 2002, **62**, 175–184.

313 Y. Arima and H. Iwata, Effect of wettability and surface functional groups on protein adsorption and cell adhesion using well-defined mixed self-assembled monolayers, *Biomaterials*, 2007, **28**, 4079–4087.

314 A. Hasan, S. K. Pattanayek and L. M. Pandey, Effect of functional groups of self assembled monolayers on protein adsorption and initial cell adhesion, *ACS Biomater. Sci. Eng.*, 2018, **4**, 3224–3233.

315 K. Duan and R. Z. Wang, Surface modifications of bone implants through wet chemistry, *J. Mater. Chem.*, 2006, **16**, 2309–2321.

316 J. Chang and Y. L. Zhou, Surface modification of bioactive glasses, in *Bioactive glasses: materials properties and applications*, ed. H. Ylanen, Woodhead Publishing, 2017, pp. 119–143.

317 S. Kargozar, F. Kermani, S. M. Beidokhti, S. Hamzehlou, E. Verne, S. Ferraris and F. Baino, Functionalization and surface modification of bioactive glasses (BGs): tailoring the biological response working on the outermost surface layer, *Materials*, 2019, **12**, 3696.

318 S. Ferraris and E. Verne, Surface functionalization of bioactive glasses: reactive groups, biomolecules, and drugs on bioactive surfaces for smart and functional biomaterials, in *Bioactive glasses: fundamentals, technology and applications*, ed. A. R. Boccaccini, D. S. Brauer and L. Hupa, The Royal Society of Chemistry, 2018, pp. 221–235.

319 Z. Y. Qiu, C. Chen, X. M. Wang and I. S. Lee, Advances in the surface modification techniques of bone-related implants for last 10 years, *Regener. Biomater.*, 2014, **1**, 67–79.

320 V. Stanic, Variation in properties of bioactive glasses after surface modification, in *Clinical applications of biomaterials*, ed. G. Kaur, Springer International Publishing AG, 2017, pp. 35–63.

321 G. K. Towarfe, R. J. Composto and I. M. Shapiro, Nucleation and growth of calcium phosphate on amine-, carboxyl- and hydroxyl-silane self-assembled monolayers, *Biomaterials*, 2006, **27**, 631–642.

322 P. Zucca and E. Sanjust, Inorganic materials as supports for covalent enzyme immobilization: methods and mechanisms, *Molecules*, 2014, **19**, 14139–14194.

323 V. Aina, C. Magistris, G. Cerrato, G. Martra, G. Viscardi, G. Lusvardi, G. Malavasi and L. Menabue, New formulation of functionalized bioactive glasses to be used as carriers for the development of pH-stimuli responsive biomaterials for bone diseases, *Langmuir*, 2014, **30**, 4703–4715.

324 E. Verne, C. Vitale-Brovarone, E. Bui, C. L. Bianchi and A. R. Boccaccini, Surface functionalization of bioactive glasses, *J. Biomed. Mater. Res., Part A*, 2009, **90**(4), 981–992.

325 S. Ferraris, C. Vitale-Brovarone, O. Bretcanu, C. Cassinelli and E. Verne, Surface functionalization of 3D glass-ceramic porous scaffolds for enhanced mineralization in vitro, *Appl. Surf. Sci.*, 2013, **271**, 412–420.

326 Q. Z. Chen, K. Rezwan, V. Francon, D. Armitage, S. N. Nazhat, F. H. Jones and A. R. Boccaccini, Surface functionalization of Bioglass®-derived porous scaffolds, *Acta Biomater.*, 2007, **3**, 551–562.

327 A. Lopez-Noriega, D. Arcos and M. Vallet-Regi, Functionalizing mesoporous bioglasses for long-term anti-osteoporotic drug delivery, *Chem.–Eur. J.*, 2010, **16**, 10879–10886.

328 A. El-Fiqi, J. H. Lee, E. J. Lee and H. W. Kim, Collagen hydrogels incorporated with surface-aminated mesoporous nanobioactive glass: improvement of physicochemical stability and mechanical properties is effective for hard tissue engineering, *Acta Biomater.*, 2013, **9**, 9503–9521.

Open Access Article. Published on 11 September 2020. Downloaded on 10/25/2025 7:46:44 PM.
This article is licensed under a Creative Commons Attribution-NonCommercial 3.0 Unported Licence.

329 E. Verne, S. Ferraris, C. Vitale-Brovarone, S. Spriano, C. L. Bianchi, A. Naldoni, M. Morra and C. Cassinelli, Alkaline phosphatase grafting on bioactive glasses and glass ceramics, *Acta Biomater.*, 2010, **6**, 229–240.
330 G. Lusvardi, G. Malavasi, L. Menabue and S. Shruti, Gallium-containing phosphosilicate glasses: functionalization and in vitro bioactivity, *Mater. Sci. Eng., C*, 2013, **33**, 3190–3196.
331 Q. Z. Chen, K. Rezwan, D. Armitage, S. N. Nazhat and A. R. Boccaccini, The surface functionalization of 45S5 Bioglass®-based glass–ceramic scaffolds and its impact on bioactivity, *J. Mater. Sci.: Mater. Med.*, 2006, **17**, 979–987.
332 Q. Z. Chen, I. Ahmed, J. C. Knowles, S. N. Nazhat, A. R. Boccaccini and K. Rezwan, Collagen release kinetics of surface functionalized 45S5 Bioglass®-based porous scaffolds, *J. Biomed. Mater. Res., Part A*, 2008, **86**, 987–995.
333 C. Gruian, E. Vanea, S. Simon and V. Simon, FTIR and XPS studies of protein adsorption onto functionalized bioactive glass, *Biochim. Biophys. Acta*, 2012, **1824**, 873–881.
334 V. Ainar, G. Malavasi, C. Magistris, G. Cerrato, G. Martra, G. Viscardi, L. Menabue and G. Lusvardi, Conjugation of amino-bioactive glasses with 5-aminofluorescein as probe molecule for the development of pH sensitive stimuli-responsive biomaterials, *J. Mater. Sci.: Mater. Med.*, 2014, **25**, 2243–2253.
335 J. Sun, Y. Li, L. Li, W. Zhao, L. Li, J. Gao, M. Ruan and J. Shi, Functionalization and bioactivity in vitro of mesoporous bioactive glasses, *J. Non-Cryst. Solids*, 2008, **354**, 3799–3805.
336 X. Zhang, D. Zeng, N. Li, J. Wen, X. Jiang, C. Liu and Y. Li, Functionalized mesoporous bioactive glass scaffolds for enhanced bone tissue regeneration, *Sci. Rep.*, 2016, **6**, 19361.
337 S. K. Misra, D. Mohn, T. J. Brunner, W. J. Stark, S. E. Philip, I. Roy, V. Salih, J. C. Knowles and A. R. Boccaccini, Comparison of nanoscale and microscale bioactive glass on the properties of P(3HB)/Bioglass® composites, *Biomaterials*, 2008, **25**, 1750–1761.
338 V. Maquet, A. R. Boccaccini, L. Pravata, I. Notingher and R. Jerome, Porous poly(α-hydroxyacid)/Bioglass® composite scaffolds for bone tissue engineering. I: preparation and in vitro characterization, *Biomaterials*, 2004, **25**, 4185–4194.
339 G. Jiang, M. E. Evans, I. A. Jones, C. D. Rudd, C. A. Scotchford and G. S. Walker, Preparation of poly(ε-caprolactone)/continuous bioglass fibre composite using monomer transfer moulding for bone implant, *Biomaterials*, 2005, **26**, 2281–2288.
340 G. A. Silva, F. J. Costa, O. P. Coutinho, S. Radin, P. Ducheyne and R. L. Reis, Synthesis and evaluation of novel bioactive composite starch/bioactive glass microparticles, *J. Biomed. Mater. Res., Part A*, 2004, **70**, 442–449.
341 J. A. Roether, A. R. Boccaccini, L. L. Hench, V. Maquet, S. Gautier and R. Jerome, Development and in vitro characterisation of novel bioresorbable and bioactive composite materials based on polylactide foams and Bioglass® for tissue engineering applications, *Biomaterials*, 2002, **23**, 3871–3878.
342 Z. Zhou, L. Liu, Q. Liu, Q. Yi, W. Zeng and Y. Zhao, Effect of surface modification of bioactive glass on properties of poly-L-lactide composite materials, *J. Macromol. Sci., Part B: Phys.*, 2012, **51**, 1637–1646.
343 R. E. Ducker, M. T. Montague and G. J. Leggett, A comparative investigation of methods for protein immobilization on self-assembled monolayers using glutaraldehyde, carbodiimide, and anhydride reagents, *Biointerphases*, 2008, **3**, 59–65.
344 C. Gruian, A. Vulpoi, H. J. Steinhoff and S. Simon, Structural changes of methemoglobin after adsorption on bioactive glass, as a function of surface functionalization and salt concentration, *J. Mol. Struct.*, 2012, **1015**, 20–26.
345 C. Gruian, A. Vulpoi, E. Vanea, B. Oprea, H. J. Steinhoff and S. Simon, The attachment affinity of hemoglobin toward silver-containing bioactive glass functionalized with glutaraldehyde, *J. Phys. Chem. B*, 2013, **117**, 16558–16564.
346 K. Wang, C. Zhou, Y. Hong and X. Zhang, A review of protein adsorption on bioceramics, *Interface Focus*, 2012, **2**, 259–277.
347 Q. Long, Z. Da-Li, X. Zhang and Z. Jia-Bei, Surface modification of apatite–wollastonite glass ceramic by synthetic coupling agent, *Front. Mater. Sci.*, 2014, **8**, 157–164.
348 V. Aina, T. Marchis, E. Laurenti, E. Diana, G. Lusvardi, G. Malavasi, L. Menabue, G. Cerrato and C. Morterra, Functionalization of sol gel bioactive glasses carrying Au nanoparticles: selective Au affinity for amino and thiol ligand groups, *Langmuir*, 2010, **26**, 18600–18605.
349 I. B. Leonor, C. M. Alves, H. S. Azevedo and R. L. Reis, Effects of protein incorporation on calcium phosphate coating, *Mater. Sci. Eng., C*, 2009, **29**, 913–918.
350 M. Zhu, J. Zhang, C. Tao, X. He and Y. Zhu, Design of mesoporous bioactive glass/hydroxyapatite composites for controllable co-delivery of chemotherapeutic drugs and proteins, *Mater. Lett.*, 2014, **115**, 194–197.
351 K. Schickle, K. Zurlinden, C. Bergmann, M. Lindner, A. Kirsten, M. Laub, R. Telle, H. Jennissen and H. Fischer, Synthesis of novel tricalcium phosphate–bioactive glass composite and functionalization with rhBMP-2, *J. Mater. Sci.: Mater. Med.*, 2011, **22**, 763.
352 S. Hattar, A. Asselin, D. Greenspan, M. Oboeuf, A. Berdal and J. M. Sautier, Potential of biomimetic surfaces to promote in vitro osteoblast-like cell differentiation, *Biomaterials*, 2005, **26**, 839–848.
353 R. F. S. Lenza, J. R. Jones, W. L. Vasconcelos and L. L. Hench, *In vitro* release kinetics of proteins from bioactive foams, *J. Biomed. Mater. Res., Part A*, 2003, **67**, 121–129.
354 W. Xia and J. Chang, Preparation, in vitro bioactivity and drug release property of well-ordered mesoporous 58S bioactive glass, *J. Non-Cryst. Solids*, 2008, **354**, 1338–1341.
355 W. Xia and J. Chang, Well-ordered mesoporous bioactive glasses (MBG): a promising bioactive drug delivery system, *J. Controlled Release*, 2006, **110**, 522–530.

 This journal is © The Royal Society of Chemistry 2020

Open Access Article. Published on 11 September 2020. Downloaded on 10/25/2025 7:46:44 PM.
This article is licensed under a Creative Commons Attribution-NonCommercial 3.0 Unported Licence.

356 L. Zhao, X. Yan, L. Zhou, H. Wang, J. Tang and C. Yu, Mesoporous bioactive glasses for controlled drug release, *Microporous Mesoporous Mater.*, 2008, **109**, 210–215.
357 F. Baino, S. Fiorilli, R. Mortera, B. Onida, E. Saino, L. Visai, E. Verne and C. Vitale-Brovarone, Mesoporous bioactive glass as a multifunctional system for bone regeneration and controlled drug release, *J. Appl. Biomater. Funct. Mater.*, 2012, **10**, 12–21.
358 E. Verne, M. Miola, S. Ferraris, C. L. Bianchi, A. Naldoni, G. Maina and O. Bretcanu, Surface activation of a ferrimagnetic glass-ceramic for antineoplastic drugs grafting, *Adv. Biomater.*, 2010, **12**, B309–B319.
359 E. Boanini, S. Panseri, F. Arroyo, M. Montesi, K. Rubini, A. Tampieri, C. Covarrubias and A. Bigi, Alendronate functionalized mesoporous bioactive glass nanospheres, *Materials*, 2016, **9**, 135.
360 G. Malavasi, E. Ferrari, L. Gigliola, A. Valentina, F. Francesca, M. Claudio, P. Francesca, S. Monica and M. Ledi, The role of coordination chemistry in the development of innovative gallium-based bioceramics: the case of curcumin, *J. Mater. Chem.*, 2011, **21**, 5027–5037.
361 X. Zhang, S. Ferraris, E. Prenesti and E. Verne, Surface functionalization of bioactive glasses with natural molecules of biological significance, Part I: gallic acid as model molecule, *Appl. Surf. Sci.*, 2013, **287**, 329–340.
362 S. Ferraris, X. Zhang, E. Prenesti, I. Corazzari, F. Turci, M. Tomatis and E. Verne, Gallic acid grafting to a ferrimagnetic bioactive glass-ceramic, *J. Non-Cryst. Solids*, 2016, **432**, 167–175.
363 S. Zhao, J. Zhang, M. Zhu, Y. Zhang, Z. Liu, Y. Ma, Y. Zhu and C. Zhang, Effects of functional groups on the structure, physicochemical and biological properties of mesoporous bioactive glass scaffolds, *J. Mater. Chem. B*, 2015, **3**, 1612–1623.
364 N. Olmo, A. I. Marti, A. J. Salinas, J. Turnay, M. Vallet-Regi and M. A. Lizarbe, Bioactive sol–gel glasses with and without a hydroxycarbonate apatite layer as substrates for osteoblast cell adhesion and proliferation, *Biomaterials*, 2003, **24**, 3383–3393.
365 J. A. Sanz-Herrera and A. R. Boccaccini, Modelling bioactivity and degradation of bioactive glass based tissue engineering scaffolds, *Int. J. Solids Struct.*, 2011, **48**, 257–268.
366 C. Wu, Y. Zhang, Y. Zhu, T. Friis and Y. Xiao, Structure–property relationships of silk-modified mesoporous bioglass scaffolds, *Biomaterials*, 2010, **31**, 3429–3438.
367 A. R. Amini, J. S. Wallace and S. P. Nukavarapu, Short-term and long-term effects of orthopedic biodegradable implants, *J. Long-Term Eff. Med. Implants*, 2011, **21**, 93–122.
368 S. Solgi, M. Khakbiz, M. Shahrezaee, A. Zamanian, M. Tahriri, S. Keshtkari, M. Raz, K. Khoshroo, S. Moghadas and A. Rajabnejad, Synthesis, characterization and in vitro biological evaluation of sol–gel derived Sr-containing nano bioactive glass, *Silicon*, 2017, **9**, 535–542.
369 E. M. Valliant, F. Romer, D. Wang, D. S. McPhail, M. E. Smith, J. V. Hanna and J. R. Jones, Bioactivity in silica/poly(γ-glutamic acid) sol–gel hybrids through calcium chelation, *Acta Biomater.*, 2013, **9**, 7662–7671.
370 P. Sepulveda, J. R. Jones and L. L. Hench, *In vitro* dissolution of melt-derived 45S5 and sol–gel derived 58S bioactive glasses, *J. Biomed. Mater. Res.*, 2002, **61**, 301–311.
371 L. Varila, S. Fagerlund, T. Lehtonen, J. Tuominen and L. Hupa, Surface reactions of bioactive glasses in buffered solutions, *J. Eur. Ceram. Soc.*, 2012, **32**, 2757–2763.
372 H. R. Fernandes, A. Gaddam, A. Rebelo, D. Brazete, G. E. Stan and J. M. F. Ferreira, Bioactive glasses and glass ceramics for healthcare applications in bone regeneration and tissue engineering, *Materials*, 2018, **11**, 2530.
373 T. Kokubo and H. Takadama, How useful is SBF in predicting in vivo bone bioactivity?, *Biomaterials*, 2006, **27**, 2907–2915.
374 G. M. Luz and J. F. Mano, Preparation and characterization of bioactive glass nanoparticles prepared by sol–gel for biomedical applications, *Nanotechnology*, 2011, **22**, 494014–494025.
375 C. Turdean-Ionescu, B. Stevensson, I. Izquierdo-Barba, A. Garcia, D. Arcos, M. Vallet-Regi and M. Eden, Surface reactions of mesoporous bioactive glasses monitored by solid state NMR: concentration effects in simulated body fluid, *J. Phys. Chem. C*, 2016, **120**, 4961–4974.
376 M. Vallet-Regi, A. J. Salinas, A. Martinez, I. Izquierdo-Barba and J. Perez-Pariente, Textural properties of CaO–SiO_2 glasses for use in implants, *Solid State Ionics*, 2004, **172**, 441–444.
377 A. A. R. De Oliveira, A. A. De Souza, L. L. S. Dias, S. M. De Carvalho, H. S. Mansur and M. D. M. Pereira, Synthesis, characterization and cytocompatibility of spherical bioactive glass nanoparticles for potential hard tissue engineering applications, *Biomed. Mater.*, 2011, **8**, 025011.
378 T. Kokubo, Design of bioactive bone substitutes based on biomineralization process, *Mater. Sci. Eng., C*, 2005, **25**, 97–104.
379 C. Vitale-Brovarone, F. Baino, F. Tallia, C. Gervasio and E. Verne, Bioactive glass-derived trabecular coating: a smart solution for enhancing osteointegration of prosthetic elements, *J. Mater. Sci.: Mater. Med.*, 2012, **23**, 2369–2380.
380 A. D. Lopez-Noriego, D. Arcos, I. Izquierdo-Barba, Y. Sakamoto, O. Terasaki and M. Vallet-Regi, Ordered mesoporous bioactive glasses for bone tissue regeneration, *Chem. Mater.*, 2006, **18**, 3137–3144.
381 M. Vallet-Regi, M. M. Garcia and M. Colilla, Biocompatible and bioactive mesoporous ceramics, in *Biomedical applications of mesoporous ceramics: drug delivery, smart materials and bone tissue engineering*, CRC Press, Boca Raton, FL, USA, 2012, p. 40.
382 A. J. Salinas, M. Vallet-Regi and J. Heikkila, Use of bioactive glasses as bone substitutes in orthopedics and traumatology, in *Bioactive glasses: materials, properties and applications*, ed. H. Ylanen, 2018, pp. 337–364.

Open Access Article. Published on 11 September 2020. Downloaded on 10/25/2025 7:46:44 PM.
This article is licensed under a Creative Commons Attribution-NonCommercial 3.0 Unported Licence.

383 M. M. Pereira and L. L. Hench, Mechanisms of hydroxyapatite formation on porous gel-silica substrates, *J. Sol-Gel Sci. Technol.*, 1996, **7**, 59–68.
384 I. Cacciotti, M. Lombardi, A. Bianco, A. Ravaglioli and L. Montanaro, Sol–gel derived 45S5 bioglass: synthesis, microstructural evolution and thermal behaviour, *J. Mater. Sci.: Mater. Med.*, 2012, **23**, 1849–1866.
385 B. C. Bunker, Molecular mechanisms for corrosion of silica and silicate glasses, *J. Non-Cryst. Solids*, 1994, **179**, 300–308.
386 B. C. Bunker, G. W. Arnold and J. A. Wilder, Phosphate glass dissolution in aqueous solutions, *J. Non-Cryst. Solids*, 1984, **64**, 291–316.
387 J. L. Paris, M. Colilla, I. Izquierdo-Barba, M. Manzano and M. Vallet-Regi, Tuning mesoporous silica dissolution in physiological environment: a review, *J. Mater. Sci.*, 2017, **52**, 8761–8771.
388 M. Etou, Y. Tsuji, K. Somiya, Y. Okaue and T. Yokoyama, The dissolution of amorphous silica in the presence of tropolone under acidic conditions, *Clays Clay Miner.*, 2014, **62**, 235–242.
389 M. Uo, M. Mizuno, Y. Kuboki, A. Makishima and F. Watari, Properties and cytotoxicity of water soluble Na_2O–CaO–P_2O_5 glass, *Biomaterials*, 1998, **19**, 2277–2284.
390 T. Woignier and J. Phalippou, Mechanical strength of silica aerogels, *J. Non-Cryst. Solids*, 1988, **100**, 404–408.
391 S. Calas, F. Despetis, T. Woignier and J. Phalippou, Mechanical strength evaluation from aerogel to silica glass, *J. Porous Mater.*, 1997, **4**, 211–217.
392 F. Baino and C. Vitale-Brovarone, Three-dimensional glass-derived scaffolds for bone tissue engineering: current trends and forecasts for the future, *J. Biomed. Mater. Res., Part A*, 2011, **97**, 514–535.
393 L. C. Klein, *Sol–gel optics: processing and applications*, Springer Science and Business Media, New York, 1994.
394 H. C. Li, D. G. Wang, J. H. Hu and C. Z. Chen, Effect of various additives on microstructure, mechanical properties and invitro bioactivity of sodium oxide–calcium oxide–silica–phosphorous pentoxide glass ceramics, *J. Colloid Interface Sci.*, 2013, **405**, 296–304.
395 R. A. Martin, R. M. Moss, N. J. Lakar, J. C. Knowles, G. J. Cuello, M. E. Smith, J. V. Hanna and R. J. Newport, Structural characterization of titanium doped bioglass using isotopic substitution neutron diffraction, *Phys. Chem. Chem. Phys.*, 2012, **14**, 15807–15815.
396 S. M. Rabie, R. Ravarian, M. Mehmanchi, P. Khoshakhlagh and M. Azizian, Effect of alumina on microstructure and compressive strength of a porous silicate hydroxyapatite, *J. Appl. Biomater. Funct. Mater.*, 2012, **12**, 102–106.
397 S. K. Arepalli, H. Tripathi, V. K. Vyas, S. Jain, S. K. Suman, R. Pyare and S. P. Singh, Influence of barium substitution on bioactivity, thermal and physio-mechanical properties of bioactive glass, *Mater. Sci. Eng., C*, 2015, **49**, 549–559.
398 O. Castano, N. Sachot, E. Xuriguera, E. Engel, J. A. Planell, J. H. Park, G. Z. Jin, T. H. Kim, J. H. Kim and H. W. Kim, Angiogenesis in bone regeneration: tailored calcium release in hybrid fibrous scaffolds, *ACS Appl. Mater. Interfaces*, 2014, **6**, 7512–7522.
399 X. Yang, L. Zhang, X. Chen, X. Sun, G. Yang, X. GuO, H. Yang, C. Gao and Z. GuO, Incorporation of B_2O_3 in CaO–SiO_2–P_2O_5 bioactive glass system for improving strength of low temperature co-fired porous glass ceramics, *J. Non-Cryst. Solids*, 2012, **358**, 1171–1179.
400 B. A. E. Ben Arfa, S. Neto, I. M. M. Salvado, R. C. Pullar and J. M. F. Ferreira, Robocasting of Cu^{2+} & La^{3+} doped sol–gel glass scaffolds with greatly enhanced mechanical properties: compressive strength up to 14 MPa, *Acta Biomater.*, 2019, **87**, 265–272.
401 D. R. Carter, G. H. Schwab and D. M. Spengler, Tensile fracture of cancellous bone, *Acta Orthop. Scand.*, 1980, **51**, 733–741.
402 C. C. Lin, S. F. Chen, K. S. Leung and P. Shen, Effects of CaO/P_2O_5 ratio on the structure and elastic properties of SiO_2–CaO–Na_2O–P_2O_5 bioglass, *J. Mater. Sci.: Mater. Med.*, 2012, **23**, 245–258.
403 G. Poologasundarampillai, P. D. Lee, C. Lam, A. M. Kourkouta and J. R. Jones, Compressive strength of bioactive sol–gel glass foam scaffolds, *Int. J. Appl. Glass Sci.*, 2016, **7**, 229–237.
404 Q. Chen and G. A. Thouas, Fabrication and characterization of sol–gel derived 45S5 bioglass ceramic scaffolds, *Acta Biomater.*, 2011, **7**, 3616–3626.
405 J. R. Jones, L. M. Ehrenfried and L. L. Hench, Optimising bioactive glass scaffolds for bone tissue engineering, *Biomaterials*, 2006, **27**, 964–973.
406 M. Vallet-Regi, J. Roman, S. Padilla, J. C. Doadrio and F. J. Gil, Bioactivity and mechanical properties of SiO_2–CaO–P_2O_5 glass ceramics, *J. Mater. Chem.*, 2005, **15**, 1353–1359.
407 N. Li, C. Wang, S. Zhu, Q. Li and R. Wang, Preparation and evaluation of macroporous sol–gel bioglass with high mechanical strength, *Key Eng. Mater.*, 2005, **280–283**, 1585–1588.
408 J. M. Karp, P. D. Dalton and M. S. Shoichet, Scaffolds for tissue engineering, *MRS Bull.*, 2003, **28**, 301–306.
409 A. R. Boccaccini, J. J. Blaker, V. Maquet, R. M. Day and R. Jerome, Preparation and characterisation of poly(lactide-*co*-glycolide) (PLGA) and PLGA/Bioglass® composite tubular foam scaffolds for tissue engineering applications, *Mater. Sci. Eng., C*, 2005, **25**, 23–31.
410 K. Zhang, Y. Wang, M. A. Hillmyer and L. F. Francis, Processing and properties of porous poly(L-lactide)/bioactive glass composites, *Biomaterials*, 2004, **25**, 2489–2500.
411 G. Poologasundarampillai, B. Yu, O. Tsigkou, E. Valliant, S. Yue, P. D. Lee, R. W. Hamilton, M. M. Stevens, T. Kasuga and J. R. Jones, Bioactive silica–poly(γ-glutamic acid) hybrids for bone regeneration: effect of covalent coupling on dissolution and mechanical properties and fabrication of porous scaffolds, *Soft Matter*, 2012, **8**, 4822–4832.
412 L. L. Hench and J. K. West, Biological applications of bioactive glasses, *Life Chem. Rep.*, 1996, **13**, 187–241.
413 A. Li, H. Shen, H. Ren, D. Wu, R. A. Martin and D. Qiu, Bioactive organic/inorganic hybrids with improved

Open Access Article. Published on 11 September 2020. Downloaded on 10/25/2025 7:46:44 PM. This article is licensed under a Creative Commons Attribution-NonCommercial 3.0 Unported Licence.

mechanical performance, *J. Mater. Chem. B*, 2015, **3**, 1379–1390.

414 C. Bossard, H. Granel, Y. Wittrant, E. Jallot, J. Lao, C. Vial and H. Tiainen, Polycaprolactone/bioactive glass hybrid scaffolds for bone regeneration, *Biomed. Glas.*, 2018, **4**(1), 108–122.

415 L. J. Gibson, Biomechanics of cellular solids, *J. Biomech.*, 2005, **38**, 377–399.

416 D. L. Kopperdahl and T. M. Keaveny, Yield strain behavior of trabecular bone, *J. Biomech.*, 1998, **31**, 601–608.

417 I. Engelberg and J. Kohn, Physico-mechanical properties of degradable polymers used in medical applications: a comparative study, *Biomaterials*, 1991, **12**, 292–304.

418 K. Vandel de Velde and P. Kiekens, Biopolymers: overview of several properties and consequences on their applications, *Polym. Test.*, 2002, **21**, 433–442.

419 J. D. Currey, Ontogenetic changes in compact bone material properties, in *Bone mechanics handbook*, ed. S. C. Cowin, Boca Raton, FL, Informa Healthcare, CRC Press, 2001, ch. 19, pp. 5–9.

420 X. E. Guo, Mechanical properties of cortical bone and cancellous bone tissue, in *Bone mechanics handbook*, ed. S. C. Cowin, Informa Healthcare, CRC Press, Boca Raton, FL, 2001, ch. 10, pp. 4–11.

421 J. J. Chung, S. Li, M. M. Stevens, T. K. Georgiou and J. R. Jones, Tailoring mechanical properties of sol–gel hybrids for bone regeneration through polymer structure, *Chem. Mater.*, 2016, **28**, 6127–6135.

422 J. E. Babensee, L. V. McIntire and A. G. Mikos, Growth factor delivery for tissue engineering, *Pharm. Res.*, 2000, **17**, 497–504.

423 M. J. Mahoney and W. M. Saltzman, Transplantation of brain cells assembled around a programmable synthetic microenvironment, *Nat. Biotechnol.*, 2001, **19**, 934–939.

424 S. Pina, V. P. Ribeiro, C. F. Marques, F. R. Maia, T. H. Silva, R. L. Reis and J. M. Oliveira, Scaffolding strategies for tissue engineering and regenerative medicine applications, *Materials*, 2019, **12**, 1824.

425 S. Yang, K. F. Leong, Z. Du and C. K. Chua, The design of scaffolds for use in tissue engineering. Part I. Traditional factors, *Tissue Eng.*, 2001, **7**, 679–689.

426 D. W. Hutmacher, Scaffold design and fabrication technologies for engineering tissues – state of the art and future perspectives, *J. Biomater. Sci., Polym. Ed.*, 2001, **12**, 107–124.

427 V. Miguez-Pacheco, L. L. Hench and A. R. Boccaccini, Bioactive glass beyond bone and teeth: emerging applications in contact with soft tissues, *Acta Biomater.*, 2015, **13**, 1–15.

428 *Handbook of bioactive ceramics*, ed. T. Yamamuro, L. L. Hench and J. Wilson, CRC Press, Boca Raton, FL, 1990, vol. 1 and 2.

429 M. N. Rahaman, R. F. Brown, B. S. Bal and D. E. Day, Bioactive glasses for nonbearing applications in total joint replacement, *Semin. Arthroplasty*, 2007, **17**, 102–112.

430 S. Kargozar, S. Hamsehlou and F. Baino, Can bioactive glasses be useful to accelerate the healing of epithelial tissues?, *Mater. Sci. Eng., C*, 2019, **97**, 1009–1020.

431 T. Albrektsson and C. Johansson, Osteoinduction, osteoconduction and osteointegration, *Eur. Spine J.*, 2001, **10**, S96–S101.

432 V. Karageorgiou and D. Kaplan, Porosity of 3D biomaterial scaffolds and osteogenesis, *Biomaterials*, 2005, **26**, 5474–5491.

433 K. Anselme, P. Davidson, A. M. Popa, M. Giazzon, M. Liley and L. Ploux, The interaction of cells and bacteria with surfaces structured at the nanometre scale, *Acta Biomater.*, 2010, **6**, 3824–3846.

434 S. Wang, T. J. Kowal, M. K. Marei, M. M. Falk and H. Jain, Nanoporosity significantly enhances the biological performance of engineered glass tissue scaffolds, *Tissue Eng., Part A*, 2013, **9**, 1632–1640.

435 D. W. Hutmacher, Scaffolds in tissue engineering bone and cartilage, *Biomaterials*, 2000, **21**, 2529–2543.

436 J. R. Jones and A. R. Boccaccini, Cellular ceramics in biomedical applications: tissue engineering, in *Cellular ceramics: structure, manufacturing, processing and applications*, ed. M. Scheffler and P. Colombo, Wiley-VCH Verlag GmbH & Co., Wenheim, 2005, pp. 550–573.

437 R. G. Ribbas, V. M. Schatkoksi, T. L. D. A. Montanheiro, B. R. C. de Menezes, C. Stegemann, D. M. G. Leite and G. P. Thim, Current advances in bone tissue engineering concerning ceramic and bioglass scaffolds: a review, *Ceram. Int.*, 2019, **45**, 21051–21061.

438 L. G. Griffith, Polymeric biomaterials, *Acta Mater.*, 2000, **48**, 263–277.

439 K. Y. Lee and D. J. Mooney, Hydrogels for tissue engineering, *Chem. Rev.*, 2001, **101**, 1869–1880.

440 B. D. Porter, J. B. Oldham, S. L. He, M. E. Zobitz, R. G. Payne, K. N. An, B. L. Currier, A. G. Mikos and M. J. Yaszemski, Mechanical properties of a biodegradable bone regeneration scaffold, *J. Biomech. Eng.*, 2000, **122**, 286–288.

441 H. Yu, H. W. Mathew, P. H. Wooley and S. Y. Yang, Effect of porosity and pore size on microstructures and mechanical properties of poly-ε-caprolactone–hydroxyapatite composites, *J. Biomed. Mater. Res., Part B*, 2008, **86**, 541–547.

442 R. C. Thomson, M. J. Yaszemski, J. M. Powers and A. G. Mikos, Hydroxyapatite fiber reinforced poly(α-hydroxy ester) foams for bone regeneration, *Biomaterials*, 1998, **19**, 1935–1943.

443 S. S. Kim, K. M. Ahn, M. S. Park, J. H. Lee, C. Y. Choi and B. S. Kim, A poly(lactide-*co*-glycolide)/hydroxyapatite composite scaffold with enhanced osteoconductivity, *J. Biomed. Mater. Res., Part A*, 2007, **80**, 206–215.

444 Q. Chen, N. Miyata, T. Kokubo and T. Nakamura, Bioactivity and mechanical properties of PDMS-modified $CaO–SiO_2–TiO_2$ hybrids prepared by sol–gel process, *J. Biomed. Mater. Res.*, 2000, **51**, 605–611.

445 H. H. Lu, S. F. El-Amin, K. D. Scott and C. T. Laurencrin, Three-dimensional, bioactive, biodegradable, polymer–

Open Access Article. Published on 11 September 2020. Downloaded on 10/25/2025 7:46:44 PM.
This article is licensed under a Creative Commons Attribution-NonCommercial 3.0 Unported Licence.

bioactive glass composite scaffolds with improved mechanical properties support collagen synthesis and mineralization of human osteoblast-like cells *in vitro*, *J. Biomed. Mater. Res., Part A*, 2003, **64**, 465–474.

446 F. Baino, S. Fiorilli and C. Vitale-Brovone, Bioactive glass based materials with hierarchical porosity for medical applications: review of recent advances, *Acta Biomater.*, 2016, **42**, 18–32.

447 O. M. Goudourni, C. Vogel, A. Grunewald, R. Detsch, E. Kontonasaki and A. R. Boccaccini, Sol–gel processing of novel bioactive Mg-containing silicate scaffolds for alveolar bone regeneration, *J. Biomater. Appl.*, 2016, **30**, 740–749.

448 C. M. Murphy and F. J. Obrien, Understanding the effect of mean pore size on cell activity in collagen–glycosaminoglycan scaffolds, *Cell Adhes. Migr.*, 2010, **4**, 377–381.

449 F. J. Obrien, B. A. Harley, M. A. Waller, I. V. Yannas, L. J. Gibson and P. J. Prendergast, The effect of pore size on permeability and cell attachment in collagen scaffolds for tissue engineering, *Technol. Health Care*, 2007, **15**, 3–17.

450 I. V. Yannas, Tissue regeneration by use of collagen–glycosaminoglycan copolymers, *Clin. Mater.*, 1992, **9**, 179–187.

451 I. Izquierdo-Barba, D. Arcos, Y. Sakamoto, O. Terasaki, A. Lopez-Noriega and M. Vallet-Regi, High-performance mesoporous bioceramics mimicking bone mineralization, *Chem. Mater.*, 2008, **20**, 3191–3198.

452 A. J. Salgado, O. P. Coutinho and R. L. Reis, Bone tissue engineering: state of the art and future trends, *Macromol. Biosci.*, 2004, **4**, 743–765.

453 A. J. Salinas and M. Vallet-Regi, Glasses in bone regeneration: a multiscale issue, *J. Non-Cryst. Solids*, 2016, **432**, 9–14.

454 C. Wu, Y. Zhou, J. Chang and Y. Xiao, Delivery of dimethyloxallyl glycine in mesoporous bioactive glass scaffolds to improve angiogenesis and osteogenesis of human bone marrow stromal cells, *Acta Biomater.*, 2013, **9**, 9159–9168.

455 H. Yun, S. E. Kim, Y. T. Hyun, S. J. Heo and J. W. Shin, Hierarchically mesoporous–macroporous bioactive glasses scaffolds for bone tissue regeneration, *J. Biomed. Mater. Res., Part B*, 2008, **87**, 374–380.

456 Y. Zhu, C. Wu, Y. Ramaswamy, E. Kockrick, P. Simon, S. Kaskel and H. Zreiqat, Preparation, characterization and in vitro bioactivity of mesoporous bioactive glasses (MBGs) scaffolds for bone tissue engineering, *Microporous Mesoporous Mater.*, 2008, **112**, 494–503.

457 X. Li, J. Shi, X. Dong, L. Zhang and H. Zeng, A mesoporous bioactive glass/polycaprolactone composite scaffold and its bioactivity behavior, *J. Biomed. Mater. Res., Part A*, 2008, **84**, 84–91.

458 C. Wu, Y. Ramaswamy, Y. Zhu, R. Zheng, R. Appleyard, A. Howard and H. Zreiqat, The effect of mesoporous bioactive glass on the physiochemical, biological and drug-release properties of poly(DL-lactide-*co*-glycolide) films, *Biomaterials*, 2009, **30**, 2199–2208.

459 Y. Zhu, Y. Zhang, C. Wu, Y. Fang, J. Yang and S. Wang, The effect of zirconium incorporation on the physiochemical and biological properties of mesoporous bioactive glasses scaffolds, *Microporous Mesoporous Mater.*, 2011, **143**, 311–319.

460 C. Wu, R. Miron, A. Sculean, S. Kaskel, T. Doert, R. Schulze and Y. Zhang, Proliferation, differentiation and gene expression of osteoblasts in boron-containing associated with dexamethasone deliver from mesoporous bioactive glass scaffolds, *Biomaterials*, 2011, **32**, 7068–7078.

461 C. Wu, W. Fan, M. Gelinsky, Y. Xiao, P. Simon, R. Schulze, T. Doert, Y. Luo and G. Cuniberti, Bioactive SrO–SiO_2 glass with well-ordered mesopores: characterization, physiochemistry and biological properties, *Acta Biomater.*, 2011, **7**, 1797–1806.

462 C. Wu, W. Fan, Y. Zhu, M. Gelinsky, J. Chang, G. Cuniberti, V. Albrecht, T. Friis and Y. Xiao, Multifunctional magnetic mesoporous bioactive glass scaffolds with a hierarchical pore structure, *Acta Biomater.*, 2011, **7**, 3563–3572.

463 C. Wu, J. Chang and Y. Xiao, Mesoporous bioactive glasses as drug delivery and bone tissue engineering platforms, *Ther. Delivery*, 2011, **2**, 1189–1198.

464 J. R. Jones, G. Poologasundarampillai, R. C. Atwood, D. Bernard and P. D. Lee, Non-destructive quantitative 3D analysis for the optimisation of tissue scaffolds, *Biomaterials*, 2007, **28**, 1404–1413.

465 R. A. Martin, S. Yue, J. V. Hanna, P. D. Lee, R. J. Newport, M. E. Smith and J. R. Jones, Characterizing the hierarchical structures of bioactive sol–gel silicate glass and hybrid scaffolds for bone regeneration, *Philos. Trans. R. Soc., A*, 2012, **370**, 1422–1443.

466 J. R. Jones, S. Lin and S. Yue, Bioactive glass scaffolds for bone regeneration and their hierarchical characterization, *Proc. Inst. Mech. Eng., Part H*, 2010, **224**, 1373–1387.

467 J. R. Jones, Sol–gel materials for biomedical applications, in *The sol–gel handbook: synthesis, characterization and application*, ed. L. David and Z. Marcos., Wiley-VCH Verlag GmbH, 1st edn, 2015, pp. 1345–1369.

468 J. R. Jones and L. L. Hench, Effect of surfactant concentration and composition on the structure and properties of sol–gel-derived bioactive glass foam scaffolds for tissue engineering, *J. Mater. Sci.*, 2003, **38**, 3783–3790.

469 J. R. Jones and L. L. Hench, Factors affecting the structure and properties of bioactive foam scaffolds for tissue engineering, *J. Biomed. Mater. Res., Part B*, 2004, **68**, 36–44.

470 P. Sepulveda, J. R. Jones and L. L. Hench, Bioactive sol–gel foams for tissue repair, *J. Biomed. Mater. Res.*, 2002, **59**, 340–348.

471 J. E. Gough, J. R. Jones and L. L. Hench, Nodule formation and mineralization of human primary osteoblasts cultured on a porous bioactive glass scaffold, *Biomaterials*, 2004, **25**, 2039–2046.

472 R. J. Crook, 58S sol–gel bioglass: a study of osteoproductive interfacial and handling properties using new microscopic techniques, PhD thesis, University of London, 2013.

Open Access Article. Published on 11 September 2020. Downloaded on 10/25/2025 7:46:44 PM.
This article is licensed under a Creative Commons Attribution-NonCommercial 3.0 Unported Licence.

473 P. Valerio, M. H. R. Guimaraes, M. M. Pereira, M. F. Leite and A. M. Goes, Primary osteoblast cell response to sol–gel derived bioactive glass foams, *J. Mater. Sci.: Mater. Med.*, 2005, **16**, 851–856.

474 J. R. Jones, O. Tsigkou, E. E. Coates, M. M. Steven, J. M. Polak and L. L. Hench, Extracellular matrix formation and mineralization on a phosphate free porous bioactive glass scaffold using primary human osteoblasts (HOB) cells, *Biomaterials*, 2007, **28**, 1653–1663.